UNIVERSITAT DE BARCELONA

Chitin deposition in the apical extracellular matrices of *Drosophila melanogaster*: a focus on Expansion, Rebuf and Chitin Synthases

Ettore De Giorgio

Aquesta tesi doctoral està subjecta a la llicència ***Reconeixement- NoComercial – CompartirIgual 4.0. Espanya de Creative Commons***.

Esta tesis doctoral está sujeta a la licencia ***Reconocimiento - NoComercial – CompartirIgual 4.0. España de Creative* Commons**.

This doctoral thesis is licensed under the ***Creative Commons Attribution-NonCommercial-ShareAlike 4.0. Spain License***.

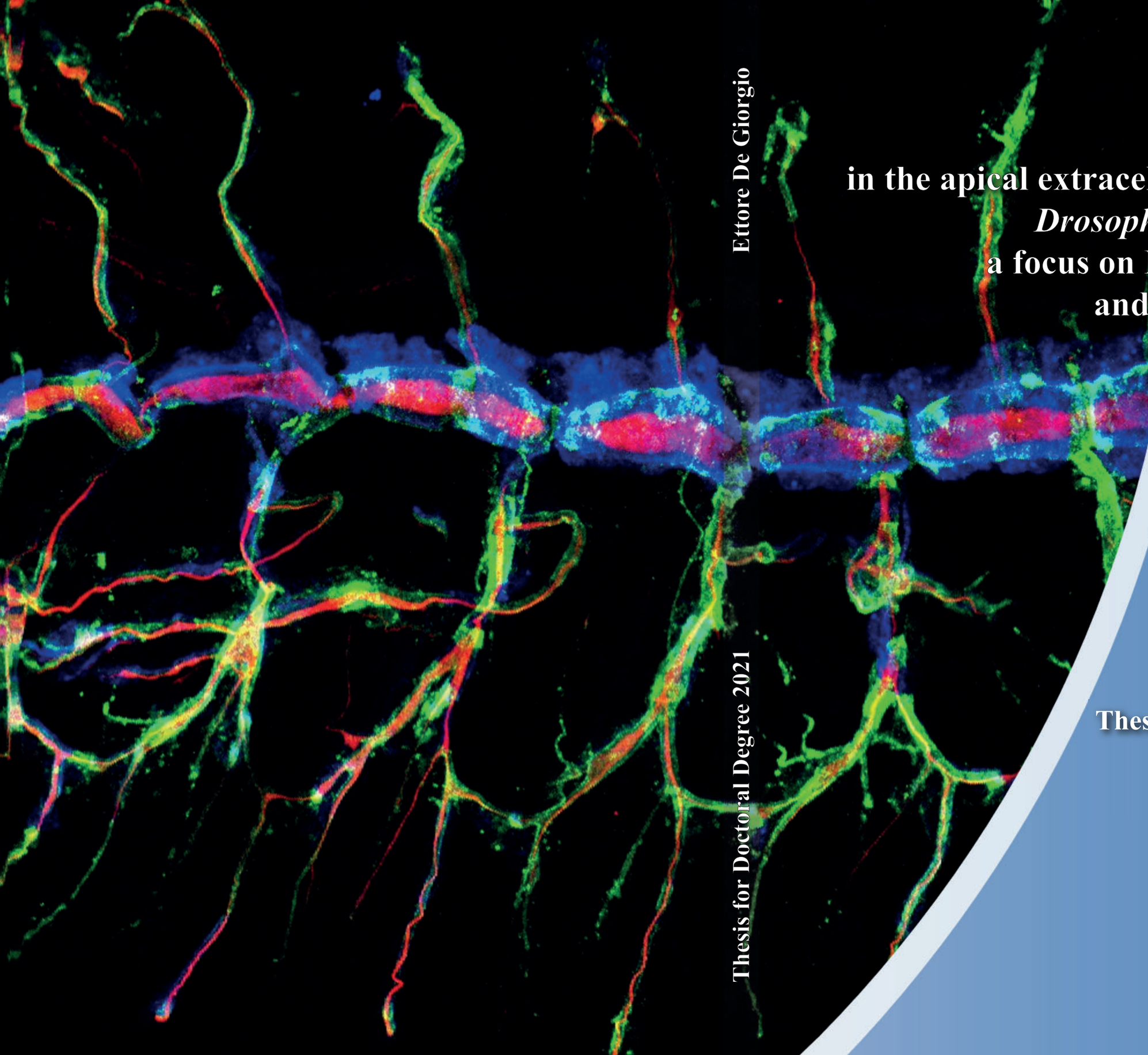

Ettore De Giorgio

Thesis for Doctoral Degree 2021

Chitin deposition in the apical extracellular matrices of *Drosophila melanogaster*: a focus on Expansion, Rebuf and Chitin Synthases

Thesis for Doctoral degree

Ettore De Giorgio

December, 2021

Departamento de Genética, Microbiología y Estadística

Programa de Doctorado de Genética (HDK0S)

Facultad de Biología

Universidad de Barcelona (UB)

Chitin deposition in the apical extracellular matrices of *Drosophila melanogaster*: a focus on Expansion, Rebuf and Chitin Synthases

Memoria presentada por

Ettore De Giorgio

Para optar al grado de

Doctor por la Universidad de Barcelona

Tesis dirigida por

Marta Llimargas Casanova

En el Instituto de Biología Molecular de Barcelona (IBMB)

Consejo Superior de Investigación Científicas (CSIC)

Marta Llimargas Casanova
Directora

Ettore De Giorgio
Autor

Sofia J. Araújo
Tutora

Acknowledgements

Finally, this moment has come! I would like to thank all the people that have been with me during this important time of my work life and personal life, without them this period would not have been the same.

First, I want to thank my director Marta Llimargas to give me the opportunity to work in this amazing lab and to make me increase the passion for science, for our fruitfly, for genetics and developmental biology and to make me grow professionally.

Luego no puedo que agradecer el equipo del desayuno. Anni, per essere stata come una sorella maggiore nel lab, aiutandomi nella vita scientifica e personale, per essere di supporto nei momenti di stress e per esserci anche nei momenti di divertimento (mi raccomando, "*e leggilo tutto!"* anche se ho già parlato di te). He de agradecer a Nico que me ha enseñado todo lo que sé de biología molecular y de castellano, que nos hace más ligero el día con sus chistes y que está siempre disponible para echarte una mano y para animarte. A Natalia, que te preparas las cosas antes que tú te des cuenta de que las necesites, que nos hace la vida más fácil en el lab y que está siempre lista para ayudarte y para darte buenos consejos. Aunque hayan pasados ya unos años, de este equipo hacen parte también Ivette y Esther, os echamos mucho de menos por aquí. He de agradecer a las super nuevas incorporaciones del lab: a Lluisa, para enriquecer el laboratorio con una visión más bioquímica de nuestros experimentos y para sus risas contagiosas, y a Fleur, que ha encajado perfectamente en nuestro grupo, estoy seguro de que tu tesis te irá genial.

Tengo que agradecer a todos los miembros del laboratorio de Jordi Casanova: a Jordi por sus consejos dentro y fuera de los lab meetings, a Marc por las horas pasadas juntos en la sala de mosca, a Panos por su sabiduría (el curso en Oeiras es uno de mis recuerdos favoritos del doctorado), a Delia por su felicidad y su pasión para este trabajo, y a Bea que nos es solo una compañera de trabajo pero también una maravillosa compañera de piso y amiga, la primera en Barcelona (una presencia constante 24h al día, vaya).

A mi tutora Sofia, a Silvia y Pablo del PCB, a toda la gente que está y que ha pasado por los grupos de Marco Milán (especialmente Elena y Daniela), de Gerardo Jiménez, de

Sebastian Pons y de Joan Roig. A mis antiguas compañera de piso Teresa, Marina y Vanesa y a mis nuevos compañeros Joaquín y Silvia.

I thank all the friends of the “Thursday meetings” to be the funny and light (but very important) part of Barcelona: Kevin, Abed, Harry, Omar L, Omar M and Tomasz.

Gli amici di Bologna Silvia, Alessia, Anna, Giulia e Anna Rita; è incredibile come solo due anni della nostra vita siano stati così importanti e fondamentali per me. Nonostante le distanze, il tempo non sembra essere passato, con voi mi faccio sempre le risate migliori e so sempre che su di voi posso contare in qualsiasi momento; uno dei miei più grandi desideri è tornare a vivere insieme nella stessa città, sarebbe stupendo.

I miei primi migliori amici Nicoletta e Nicola, quando ci rivediamo sembra sempre di ritornare all’adolescenza, con la stessa intesa e allegria.

Tutta la mia famiglia, i miei genitori per essere sempre di supporto, per appoggiare sempre tutte le mie scelte ed essere sempre di aiuto; i miei fratelli, le cognate e le nipotine, non potevamo essere più fortunati a stare insieme; gli zii e cugini, che rendete le vacanze natalizie ed estive più belle e speciali.

To Ali to make me believe again that good people exist, for all his support, for all his jokes, for all his kindness, for his salads and for all the good moments we have passed together, I really hope this will never end… أنا أحبك كثيرا

Per zia Maria, zio Mariano e la Nonna

Abstract

Chitin has a recognised importance in physiology but also as a biomaterial. In insects, it is the principal component of the apical extracellular matrix of epidermis, tracheae, foregut and hindgut. In these compartments, chitin is synthesised by the family A of Chitin Synthases (ChS), which in *Drosophila* is encoded by the gene *kkv*. Chitin is also the main constituent of the peritrophic matrix that lines the inner surface of the midgut. In this case, the polymer is synthesized by the family B of Chitin Synthases, encoded by *ChS2* in *Drosophila*. Kkv alone is not sufficient to deposit chitin, and two interchangeable MH2-containing proteins, namely Expansion (Exp) and Rebuf (Reb), are equally required for chitin deposition. Kkv and Exp/Reb constitute the minimal genetic program necessary and sufficient for chitin deposition.

The aim of this work is to gain further insights into chitin deposition in apical extracellular matrices of *Drosophila melanogaster*. In particular, through a structure-function analysis approach, we aimed to investigate the molecular mechanisms of activity of Exp, Reb and Kkv in the tracheal system, focusing our attention on domains that we speculated could be involved in putative protein-protein interactions between these factors. Furthermore, we aimed to produce extracellular chitin in cell culture and to investigate how the differences between Kkv and ChS2, the two Chitin Synthases in *Drosophila*, correlate with chitin deposition and with the functional requirement of Exp/Reb.

We found that the Nα-MH2 domain of Exp and Reb, the only domain recognisable in these proteins, is necessary for the extracellular chitin deposition, but it is not involved in the subcellular localisation of the chitin machinery. By the comparison of amino acid sequences of homolog proteins to Exp, we identified a new highly conserved region. This conserved motif does not seem to be involved in chitin deposition but it may be relevant for Exp/Reb localisation. On the other hand, our results suggest that Exp/Reb proteins appear to regulate the organised distribution of Kkv at the apical membrane.

We found Kkv, or Kkv complex, assembles at the level of Golgi, then it is translocated to the membrane where the synthesis of chitin starts. Later, Kkv is endocytosed and recycled. From the structure-function analysis of Kkv, we found out that the conserved motif WGTRE is involved in Kkv subcellular localisation and that mis-localised Kkv is

not able to deposit chitin, indicating that the localisation of the protein is important for its function. Instead, the coiled-coil domain of Kkv is dispensable for the chitin deposition activity of Kkv, but more experiments are necessary to determine a role for this domain.

It is possible to synthesise chitin *in vitro* in cell culture of S2 cells transfected with Kkv and Exp/Reb; however, the chitin machinery is not localised at the membrane and the chitin produced is present in intracellular particles. The analysis of chitin synthesis *in vitro* revealed that the cells need to be polarised to properly localise the chitin machinery and that polarised cells with Kkv and Exp/Reb activity produce less intracellular chitin particles than non-polarised cells with the same activity. We speculate that most of the chitin particles are extruded to the extracellular compartment.

Finally, we confirmed that ChS2 cannot exert the function of Kkv and that, in the embryo, ChS2 does not localise at the membrane. Furthermore, we found that ChS2 is not able to act in concert of Exp and Reb to deposit chitin.

Index

1. Introduction

1. Introduction

1.1 Chitin: a historical overview

Aristotle (384–322 BC), in his main work about animal biology *Historia animalium*, named χιτών (kithon), which means 'sheath' in Greek, the casted case of the larvae of a moth he found in clothes. However, the term χιτών does not seem to specifically assign the insect cuticle in Aristotle's work but is rather defining any structure that surrounds an insect (Moussian, 2019). Only in 1823, the term chitin was used again by the French naturalist Auguste Odier to denote a substance he extracted from the cuticle of the scarab beetle (Odier, 1823). He mentioned that chitin contains carbon, but only very little nitrogen as compared to other animal substances, like hairs and horn. Henri Braconnot, in 1811, extracted a substance, probably chitin, from the cell wall of fungi that he had termed fungine (Braconnot, 1811), describing that it is composed of carbon, nitrogen, hydrogen and acetate. Later, it was proposed that chitin from crabs is a carbohydrate (Städeler, 1859), and the monomers of chitin were identified as a sweet sugar that can be consumed by yeast as an energy source (Ledderhose, 1876). Subsequently, chitin was defined as poly- or oligosaccharide containing nitrogen and acetic acid. In the late nineteenth century, the polysaccharide in fungi was named Pilzcellulose (Winterstein, 1893–95; Moussian, 2019) and it was soon discovered that Pilzcellulose and the arthropod chitin are the same molecule (Hoppe-Seyler, 1894; Moussian, 2019). In 1901, Fränkel and Kelly determined the composition of chitin demonstrating that it consists of an acetylated chitosamine (glucosamine) with the acetyl group bond to a nitrogen yielding N-acetyl-chitosamine and they demonstrated for the first time that chitin is a polysaccharide (Fränkel and Kelly, 1901). Gonell, Meyer and Pankow proposed an organisation with antiparallel chitin fibres, named α-chitin (Gonell, 1926; Meyer and Pankow, 1935). Besides α-chitin, two other types of chitin organisation were described, namely β-chitin with parallel running chitin fibres (Lotmar and Picken, 1950) and γ-chitin with alternating parallel and antiparallel aligned chitin fibres (Rudall, 1963) (**Fig. 1 B**). Discovery of chitin in different phyla occurred at different dates and was often under debate. A part from arthropods and fungi, presence of chitin has been found in sponges

(Ehrlich *et al.*, 2007; Brunner *et al.*, 2009), in mollusc shells (Peters, 1972), in nematodes (Wharton, 1980; Zhang *et al.*, 2005) and in the gut of fish (Tang *et al.*, 2015). Finally, chitin oligosaccharides are found in vertebrates where they are involved in the production of hyaluronic acid, a polysaccharide related to chitin (Semino *et al.*, 1996; Semino and Allende, 2000). Commonly, chitin is found exclusively in the extracellular space as a protective and supporting component of complex extracellular matrices like the cell wall of fungi, the shell of molluscs or the cuticle of arthropods. Correlating with its requirement in different contexts, chitin organisation varies. Besides in nature, chitin and its derivative chitosan, the deacetylated form of chitin, are used in biomedicine and biotechnology (Crini *et al.*, 2007).

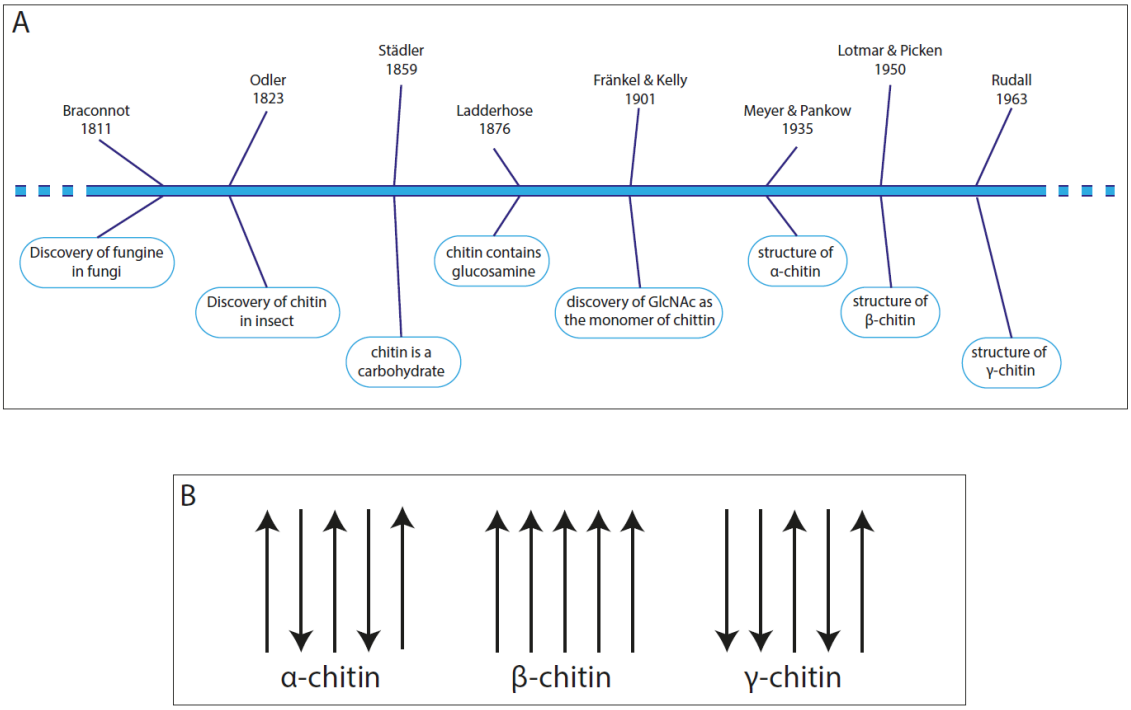

Fig. 1. History of chitin and Model of chitin organization (adapted from Moussian, 2019). (**A**) Main steps of chitin discovery. (**B**) Scheme of α-, β- and γ-chitin.

1.2 Chitin synthesis

Chitin, one of the three major biopolymers found in nature along with cellulose and hyaluronan, is a linear polymer composed of monomers of β-1,4-linked N-acetylglucosamine (GlcNAc). The monomer is produced in the cytoplasm by the Leloir pathway (Merzendorfer and Zimoch, 2003; Araújo *et al.*, 2005; Moussian, 2013) and it is polymerized by the cytoplasmic catalytic domain of Chitin Synthases (ChS). It has been proposed that, while it is polymerized, the nascent chitin is translocated across the plasma membrane and released into the extracellular space through the pore formed by the transmembrane helices of the ChS; afterwards, in the extracellular space, chitin chains assemble spontaneously into crystalline chitin microfibrils (Merzendorfer, 2006).

Nonsense and missense mutations in chitin synthase coding genes cause a chitin-less cuticle in the fruit fly *Drosophila melanogaster* (Moussian *et al.*, 2005) and downregulation of chitin synthase transcripts by RNA interference provokes a reduction in cuticular chitin in various insects. The cuticle without or with reduced chitin is, in all cases, lethal (Arakane *et al.*, 2005, 2008; Zhang *et al.*, 2010).

1.2.1 Chitin Synthases

Chitin Synthases (ChS) belong to the large family of glycosyltransferases, a ubiquitous group of enzymes that catalyze the transfer of sugar moieties from activated sugar donors to specific acceptors, thereby forming a glycosidic bond. Based on sequence homologies, chitin synthases have been grouped into family 2 of glycosyltransferases (GTF2), containing sequences from bacteria, fungi, plants and animals. Apart from chitin synthases, this family includes other important enzymes such as cellulose synthases or hyaluronan synthases. Phylogenetic analysis indicates that GTF2 enzymes have diverged from a common ancestral molecule. Although between these enzymes the overall amino acid similarity is rather limited, regions within the catalytic domain are remarkably conserved (Coutinho *et al.*, 2003; Merzendorfer, 2006).

ChSs present multiple transmembrane domains and, as signature motifs, they have several consensus sequences including EDR, Q(Q/R)XRW and (S/T)WGT(K/R). Some of the conserved residues in these motifs have been implicated to be essential for the catalytic

mechanism or in the translocation process of nascent chitin polymers across the membrane (Zhu *et al.*, 2002; Moussian *et al.*, 2005; Merzendorfer, 2006).

In most insect species, two ChS types have been identified based on their differences in the cDNA sequences and tissue-specific expressions: the group of ChS-A is involved in the synthesis of chitin in epidermis, trachea, foregut and hindgut and the group of ChS-B synthesizes chitin in midgut, as principal component of the Peritrophic Matrix (PM) (Liu *et al.*, 2019). The general domain architectures of the two types of ChS proteins are nearly the same with some notable differences (**Fig. 2**). In the C-terminal domain, both families of ChS enzymes have a similar number and organization of transmembrane segments (TMSs), but a predicted coiled coil domain is present in ChS-A enzymes and it is absent in ChS-B enzymes. Some sequence differences, such as the coiled-coil region or some other unidentified difference between ChS-A and -B, may determine their oligomerization and/or interaction with other proteins and, hence, the assembly of the chitin products: in fact, the products of ChS-A are organized into hydrophobic chitin laminae (α-form) but the products of ChS-B are hydrophilic and consist of multiple concentric lamellae of chitin (presumably β-form), (Muthukrishnan *et al.*, 2019).

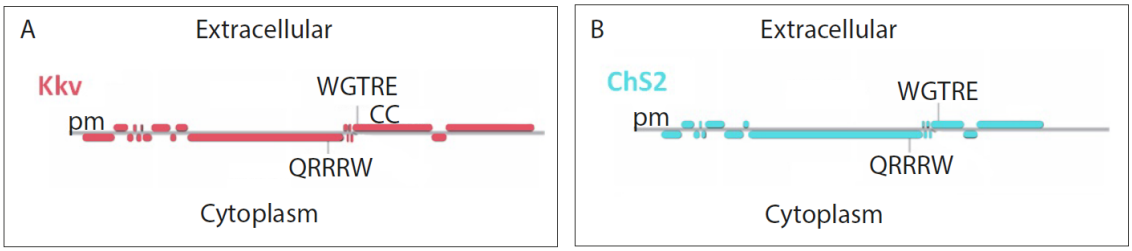

Fig. 2. Structures of Chitin Synthases (adapted from Moussian, 2013). Scheme of *Drosophila melanogaster* ChS-A (Kkv) and ChS-B (ChS2). (**A**) The chitin synthase Kkv presents several transmembrane domains, the catalytic domain QRRRW, the conserved motif WGTRE and a coiled coil domain (CC). (**B**) Chitin Synthase 2 differs mainly from Kkv for the absence of the coiled coil domain (Moussian, 2013). Abbreviations: coiled coil domain (CC), plasma membrane (pm).

1.2.2 Chitin Synthase oligomers: a model from Cellulose Synthase

Although chitin is a linear chain of β-1,4-linked GlcNAc residues, every single sugar is rotated by 180° with respect to its neighboring sugars. In order to facilitate simultaneous polymerization, the inverse orientation of the sugar moieties may require two active sites in close proximity, one for each sugar orientation. The formation of the active site(s) for chitin synthesis could depend on oligomerization of different chitin synthase molecules (Merzendorfer, 2006). There is evidence that chitin synthases are di/oligomeric complexes that assemble on cell membranes. In *Manduca sexta*, ChS2 appears to be present as an oligomer, presumably a trimer, in the midgut (Maue *et al.*, 2009). Using bimolecular fluorescence complementation techniques, Gohlke *et al.* demonstrated that yeast ChS3 subunits formed oligomers at the bud neck and lateral plasma membrane (Gohlke *et al.*, 2017). These oligomers presumably form even in the ER indicating oligomerization prior to their final transport to the Golgi, bud neck, or plasma membrane. Oligomerization of yeast ChS3 appeared to occur through interactions involving the N-terminal domain and several proteins of the vesicular transport pathway (Sacristan *et al.*, 2013).

It is conceivable that like cellulose synthase, larger assemblies of ChS are involved in the coordinated synthesis of chitin fibrils. By the comparison between Chitin Synthases and the closely related Cellulose Synthases, it has been proposed that Chitin Synthase oligomers could be organized at the plasma membrane forming rosettes. Chitin synthases and Cellulose Synthases enzymes belong to GTF2, they produce polymers with similar molecular structure (they differ only for a substitution of the 2-hydroxyl group with an acetyl amino group on each monomer) and several motifs in the amino acids structure are conserved, among them the catalytic domain QxxRW and several transmembrane domains (Merzendorfer, 2006; Bi *et al.*, 2015). Cellulose Synthases seem to be organized as hexagonal structures with sixfold symmetries (rosettes) which are assembled in the Golgi and then transported to the plasma membrane. Each rosette is composed of six subunits/lobes, which in turn consist of either six monomeric or three dimeric synthetic units, each capable of polymerizing and translocating a single cellulose chain (**Fig. 3**) (Zhu *et al.*, 2016; Haigler and Roberts, 2019; Allen *et al.*, 2021).

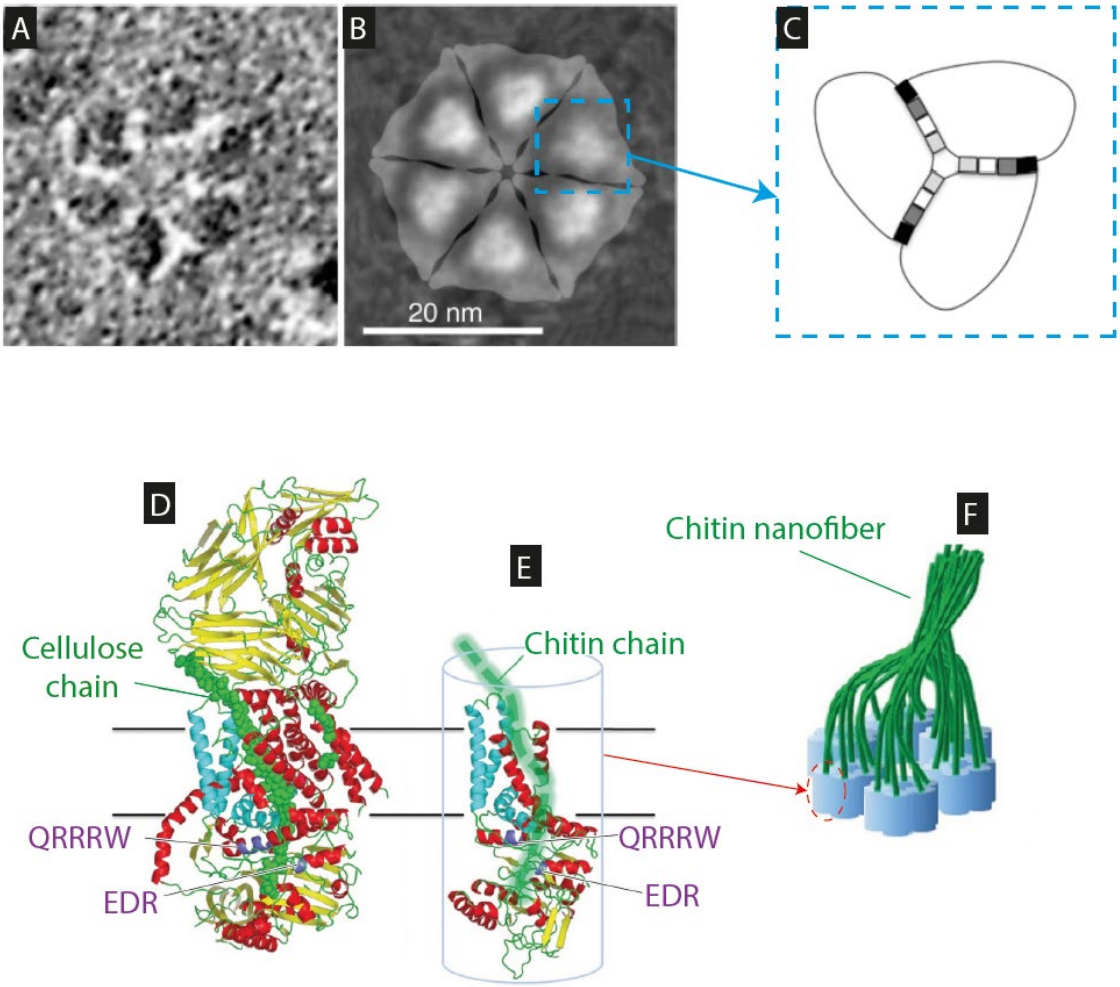

Fig. 3. Cellulose Synthases rosettes. (**A**) TEM image of a rosette transmembrane-helix region of a Cellulose Synthase Complex with six-lobes. The cytosolic regions were below the membrane (adapted from Haigler and Roberts, 2019). (**B**) A schematic representation of a rosette Cellulose Synthase Complex. The cytosolic regions of each lobe are represented by the semi-transparent triangles (adapted from Haigler and Roberts, 2019). (**C**) A schematic representation of a lobe of the rosette composed by three dimeric subunits (adapted from Haigler and Roberts, 2019). (**D**) Crystal structure of cellulose synthase from *Rhodobacter sphaeroides* (adapted from Zhu *et al*., 2016). (**E**) Partial reconstruction of the structure of a single monomer of ChS-A from *Tribolium castaneum*. Green, cellulose/chitin; yellow, β-strands; red, α-helices; cyan, highly conserved α-helices; purple, catalytic site motifs (adapted from Zhu *et al*., 2016). (**F**) Oligomerization model of single catalytic ChS units that oligomerize to form multimeric complexes; sugar chains pre-align for nanofibril formation (adapted from Zhu *et al*., 2016).

In Cellulose Synthase rosette model, it has been proposed that differences in the morphology of either rosettes or their lobes may be responsible for the diversity in cellulose architecture: dispersed rosettes produce widely spaced cellulose microfibrils, whereas dense regions of complexes synthesize highly aggregated crystalline microfibrils (Allen *et al.*, 2021). It has been speculated the existence of other proteins that, perhaps reversibly, associate with the subunits to cause changes in diameter lobe area and shape (Haigler and Roberts, 2019).

It has been predicted that Cellulose Synthase Complexes (CSCs) assemble in the Golgi, with the help of Golgi-localised proteins. CSCs are then transported from the Trans Golgi Network and the Golgi via secretory vesicles (SV) and are delivered to specific sites on the plasma membrane that are marked by proteins linked to microtubules. Myosin IX may also help deliver secretory vesicles containing CSCs to the plasma membrane along actin filaments. Physical interactions between membrane proteins and the exocyst complex with secretory vesicles are required for the insertion of CSCs into the plasma membrane. Various proteins are required for optimal cellulose biosynthesis, associating with CSCs either at the plasma membrane or during trafficking. Intact or degraded CSCs can be internalized into clathrin-coated vesicles (CCV) and undergo clathrin-mediated endocytosis (CME). Internalized CSCs can be recycled back to the plasma membrane (Allen *et al.*, 2021) (**Fig. 4**).

Chitin Synthases may function in a similar way, only after rosette-like complexes have formed. Maybe multitude of different chitin deposition patterns and textures found in nature could have some structural equivalents in the arrangement of single synthetic units within putative chitin synthase super-complexes (Merzendorfer, 2006).

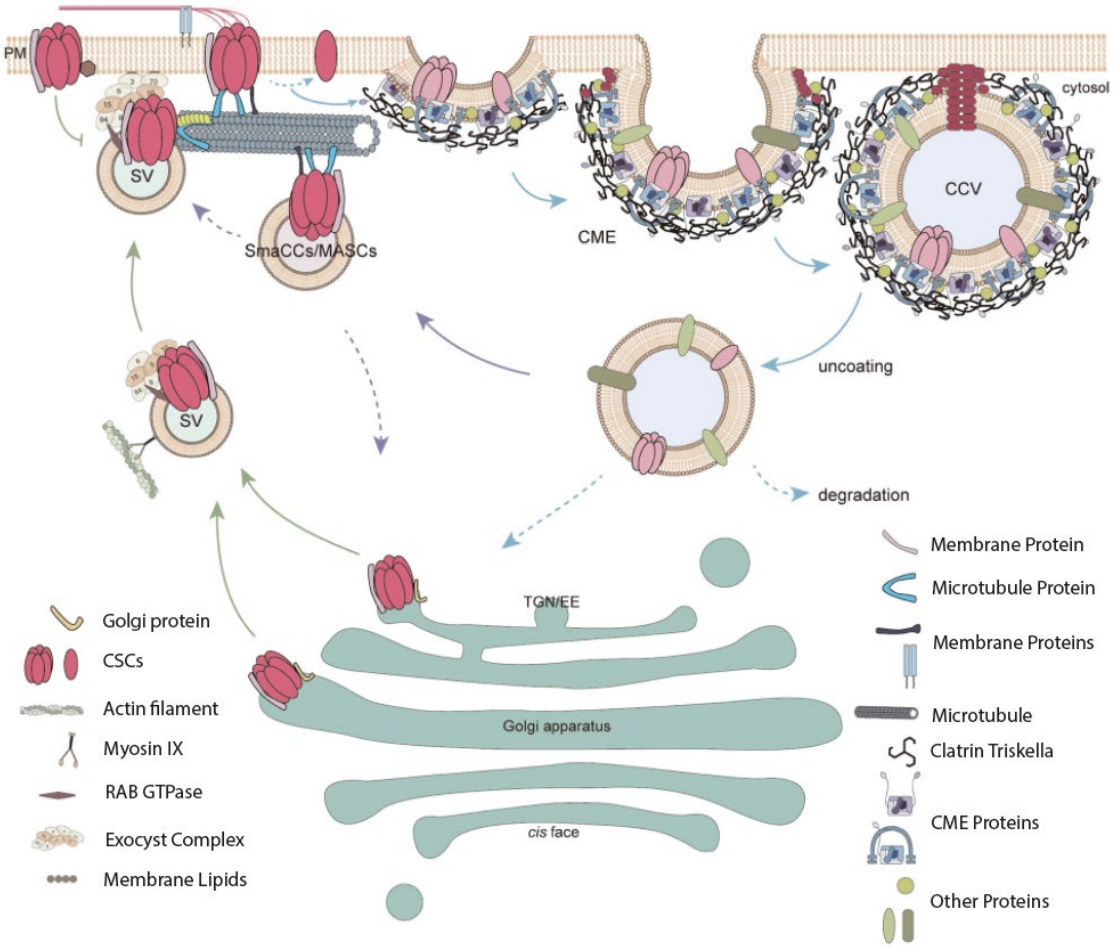

Fig. 4. Trafficking of Cellulose Synthase Complexes. Scheme of Cellulose Synthase complexes trafficking from their assembly in Golgi to the transport to the plasma membrane (adapted from Allen *et al*., 2021). Abbreviations: Plasma Membrane (PM); Secretory Vesicles (SV); Small Cellulose Synthase Compartments (SmaCC); Microtubule Associated SmaCC (MASC); Clathrin-Mediated Endocytosis (CME); Clathrin Coated Vesicle (CCV); Trans Golgi Network (TGN); Early Endosome (EE); Cellulose Synthase Complex (CSC).

1.2.3 Chitin in Peritrophic Matrix

Chitin is also a constituent part of the peritrophic matrices that line the inner surface of the gut in many insects and other invertebrates (Peters, 1992; Lehane, 1997; Barbehenn and Stannard, 2004; Merzendorfer, 2006). The insect gut is comprised of the foregut, midgut (where digestion and nutrient absorption occur) and hindgut (**Fig. 5 A**). The midgut of most, but not all, insects secrete a non-cellular semipermeable biocomposite called the peritrophic matrix (PM) which protects the gut and aids in digestion. The PM

is an invertebrate-unique, semi-permeable apical extracellular matrix with surprisingly complex characteristics (Ramos *et al.*, 1994; Silva and Terra, 1995). The PM creates two compartments within the midgut cavity: the endoperitrophic space (the gut lumen including the food bolus) and the ectoperitrophic space (the space between the PM and epithelium) (**Fig. 5 B**). The presence of the PM increases efficiency of digestion, nutrient acquisition and reuse of hydrolytic enzymes by providing spatial separation of digestive processes (Hegedus *et al.*, 2009). Besides, the PM is a physical barrier protecting the midgut epithelium from materials ingested by an arthropod, including abrasive food particles (mechanichal disruption) and pathogens. It is also a biochemical barrier, sequestering and, in some cases, inactivating ingested toxins (Bolognesi *et al.*, 2001).

The PM is continuously biosynthesized, assembled and degraded in response to feeding and development of the insects. PM are mainly composed of chitin microfibers embedded in the matrix of proteins, glycoproteins and proteoglycans (Terra, 2001). Chitin polymers assemble in nanofibrils in β-conformation (parallel chitin chains) (Zhu *et al.*, 2016). Chitin nanofibrils associated with proteins are then linked together by PM-associated proteins to form microfibrils that are organized into an interconnected mesh-like structure lining the midgut (Hegedus *et al.*, 2009; Liu *et al.*, 2019) (**Fig. 5 C**). Chitin microfibrils in PM are mostly arranged as orthogonal or hexagonal lattices or as random felts (lamellae); multiple laminations of chitin networks are often found especially in the middle and posterior parts of the midgut. There are large pores in the PM that allow for the passage of digestive enzymes secreted by the epithelial cells lining the midgut and for digestion products to pass through the PM in opposite directions (Bolognesi *et al.*, 2008). In PM, chitin polymers are synthesized by class B ChS. ChS-B resides in the apical tips of brush border microvilli of the midgut (Zimoch and Merzendorfer, 2002) (**Fig. 5 B**). When the gene encoding ChS-B in *T. castaneum* is silenced by RNAi, the structural integrity and barrier function of the peritrophic matrix is lost; the loss of the PM's capability to partition digestive enzymes and substrates causes nutritional deficiencies in the larvae, resulting in a starvation phenotype with significantly reduced body weight and a depletion of neutral lipids in fat bodies (Kelkenberg *et al.*, 2015). ChS-B genes are not expressed in the embryonic or pupal stages but ChS-B enzymes are produced by the midgut epithelial cells in the course of PM formation in the larval and adult stages and is probably limited to these feeding stages (Zimoch and Merzendorfer, 2002; Arakane *et al.*, 2005; Muthukrishnan *et al.*, 2012).

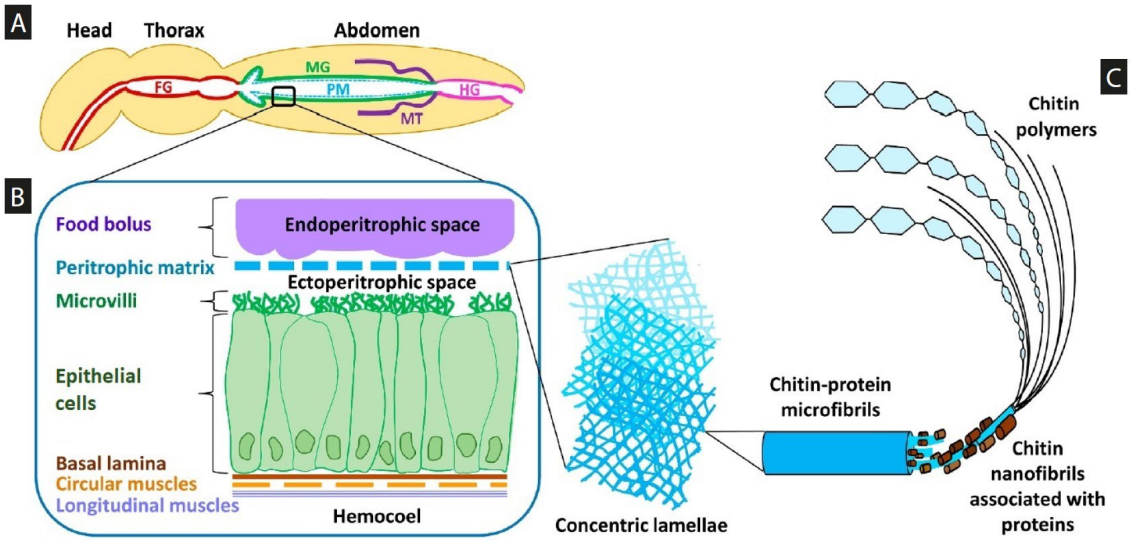

Fig. 5. Insect alimentary canal, detailed midgut structures and hierarchical peritrophic matrix components (adapted from Liu *et al.*, 2019). (**A**) The alimentary canal is comprised of the foregut (FG), midgut (MG), and hindgut (HG). Malpighian tubules (MT) mark the junction between the MG and HG. The MG is lined with the peritrophic matrix (PM), which protects epithelial cells and facilitates digestion. (**B**) The region of the gut lumen within the PM is called the endoperitrophic space, whereas the region outside the PM is the ectoperitrophic space. Microvilli extend from epithelial cells into the ectoperitrophic space to increase surface area for absorption of nutrients and excretion of digestive enzymes and PM. A thin, fibrous, basal lamina made of connective tissue separates the gut epithelium from the circular and longitudinal muscles that encase the gut and propel the bolus. The main body cavity of an insect is the hemocoel. (**C**) The PM itself is comprised of multiple concentric lamellae, each made of chitin-protein microfibrils intertwined to form a porous, mesh-like, laminated layer that can appear as an orthogonal lattice or as irregular fibrils. Protein-chitin microfibrils are comprised of chitin nanofibrils wrapped in PM proteins. Chitin nanofibrils are composed of chitin polymers which are formed by long chains of N-acetylglucosamine monomers linked together by β-1,4-glycoside bonds.

1.3 Development of *Drosophila melanogaster* tracheal system

The tracheal system of insects is a network of epithelial branched tubules that functions as a respiratory organ to supply oxygen to various target organs. It is extended throughout the body cavity and it allows air flow through openings in the body wall, called spiracles, and delivers it to highly ramified tracheal termini, called tracheoles (Wigglesworth, 1972). Tracheal cells have features characteristic of typical epithelia such as apicobasal polarity, maintenance of tissue integrity via cell-cell and cell-extracellular matrix adhesions, a basement membrane and the capacity for directed secretion (Loganathan *et al.*, 2016). Target-derived signalling inputs regulate stereotyped modes of cell specification, branching morphogenesis and collective cell migration in the embryonic stage. Tracheal tube morphogenesis is also regulated by physicochemical interaction of the cell and apical extracellular matrix to regulate optimal geometry suitable for air flow. The tracheal system senses both the external oxygen level and the metabolic activity of internal organs and helps organismal adaptation to changes in environmental oxygen level (Hayashi and Kondo, 2018). Tracheal system development has been studied extensively in the fruit fly *Drosophila melanogaster* (Manning and Krasnow, 1993; Affolter and Caussinus, 2008; Schottenfeld *et al.*, 2010; Loganathan *et al.*, 2016; Hayashi and Kondo, 2018).

1.3.1 *Drosophila melanogaster* as a model organism

Drosophila is a small insect easy and inexpensive to culture in laboratory conditions, it has a short life cycle (around ten days) (**Fig. 6**), it produces a large number of externally laid embryos, its whole genome has been sequenced and it can be genetically modified in numerous ways. Once fertilized, the embryo develops in the egg passing through several embryonic stages (from stage 1 to 17) for around one day at 25°C, then it hatches as a larva. Over five days, the larva eats and grows (going through three molts) until it pupates and undergoes metamorphosis into the adult fly over the course of four days. During metamorphosis, most of the embryonic and larval tissue is destroyed. The adult tissues (e.g., wing, leg, eye) develop from groups of cells known as “imaginal discs” that have been set-aside since early embryonic development. Other tissues, like the tracheal system or the nervous system, do not depend on imaginal origin, and instead they undergo several transformations to produce the adult structure (Jennings, 2011).

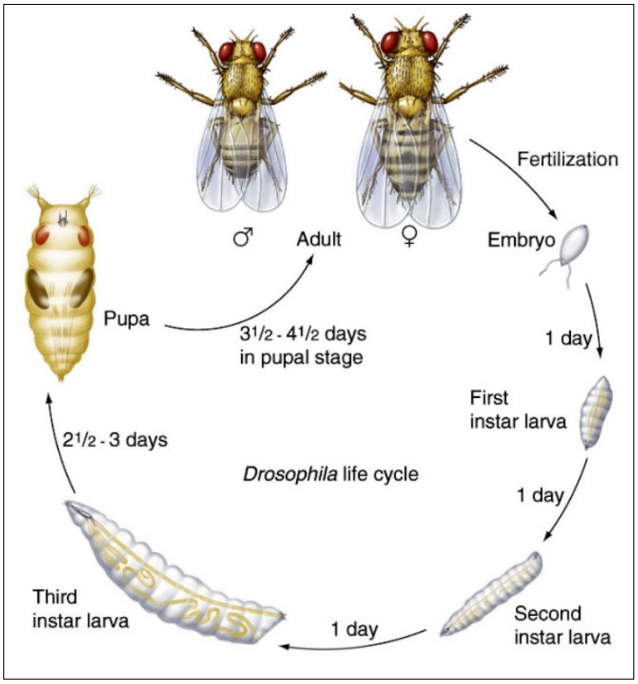

Fig. 6. Life cycle of *Drosophila melanogaster* (adapted from FlyBase)**.** At 25ºC, the *Drosophila* generation time is about ten days and it consists in 1 day of embryogenesis, 1 day of first instar larvae, 1 day of second instar larvae, 2-3 day of third instar larvae and about 4 days of pupal stage.

1.3.2 Morphogenetic events in *Drosophila* trachea

The development of tracheal system can be divided in two big phases, the first one includes morphogenetic events to obtain a branched tubular structure and the second one concerns the maturation of the tubes. The epithelial cells specified to become trachea are recognisable as ten ectodermal placodes (thickened ectodermal plates that form by apico-basal cell elongation) on each side of the stage 9 embryo (Manning and Krasnow, 1993; Uv *et al.*, 2003; Kerman *et al.*, 2006; Affolter and Caussinus, 2008; Schottenfeld *et al.*, 2010; Maruyama and Andrew, 2012). During stage 10, the tracheal placodes invaginate into the underlying mesoderm while maintaining continuity with the epidermis. Coincident with invagination of the tracheal primordia, the approximately forty to forty-five cells in each placode undergo one final round of cell division during early stage 11, from this moment there are around 80 cells per placode and no more cell divisions will

occur. From the second thoracic (T2) through the eighth abdominal (A8) hemisegment, the tracheal metameres (Tr1 through Tr10) form incipient tubes called tracheal pits. The tracheal pits undergo a morphogenetic transformation to become a central stalk-like structure with six distinct buds (**Fig. 7 A, B**). Tracheal primordial cells are not committed to any position or cell type at the time of placode specification (Samakovlis *et al.*, 1996). Therefore, the cell and branch type specification must be determined under the influence of the surrounding environment. Once internalized, the tracheal primordia start expressing the FGF receptor tyrosine kinase Breathless (Btl) (Glazer and Shilo, 1991; Klämbt *et al.*, 1992; Shishido *et al.*, 1993), which is activated by one of the three FGF ligands in *Drosophila*, Branchless (Bnl), (Sutherland *et al.*, 1996), and the process of stereotyped primary branching begins. During stage 12, the buds produce stereotypical primary branch outgrowths in each tracheal metamere. The central stalk, called the transverse connective (TC) supports the outgrowth of dorsal trunk anterior (DTa), dorsal trunk posterior (DTp), dorsal branch (DB), visceral branch (VB), lateral trunk anterior (LTa) and lateral trunk posterior (LTp), the latter producing an offshoot called the ganglionic branch (GB) (**Fig. 7 A, B**). The tubular bridge that remains between the transformed tracheal pits and the epidermis becomes the spiracular branch (SP). During stage 13, the primary branches (DTa, DTp, DB, VB, LTa, LTp/GB) continue to grow towards their targets; for example, the DB toward the dorsal epidermis, the VB toward the intestine and the GB toward the ventral nerve cord. Meanwhile, DTa and DTp from adjacent hemisegments undergo end-on fusions to form the Dorsal Trunk (DT), a multicellular tube along the anterior-posterior axis. Branch outgrowth continues during stages 14 and 15 with the addition of fine unicellular branches (secondary branches) to the tubular repertoire. Later, during stages 15 and 16, additional fine subcellular tubules called terminal branches or tracheoles sprout along various branch termini (LT, DBs, VBs and GBs), thus expanding the coverage of tracheal network with several fine branches (**Fig. 7 A, B**) (Loganathan *et al.*, 2016).

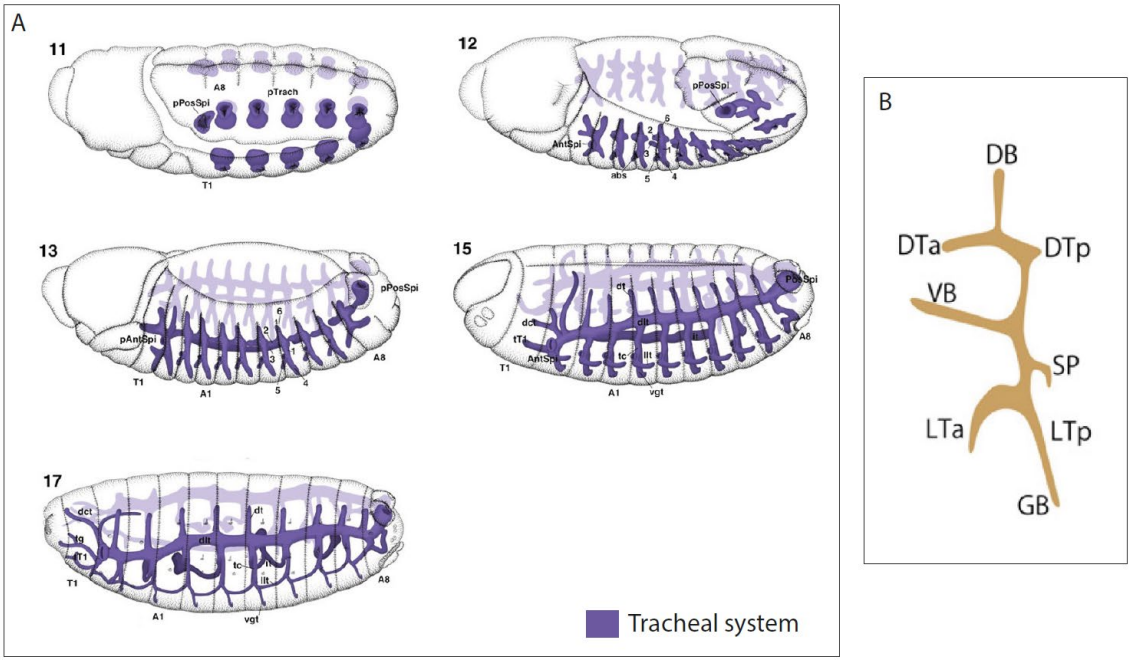

Fig. 7. Development of *Drosophila melanogaster* tracheal system. (**A**) Scheme of the embryonic tracheal development from stage 11 to stage 17 (adapted from Hartestein, 1993). (**B**) Primary branches in stage 12; internalized tracheal primordia form stereotyped primary branches (adapted from Hayashi and Kondo, 2018).

Although a continuous network, the trachea is composed of multicellular, unicellular and subcellular tubules (**Fig. 8 A**). Multicellular primary branches, like the dorsal trunk, are organized by intercellular junctions producing a tubule with a relatively large diameter (**Fig. 8 A**) (Loganathan *et al.*, 2016; Hayashi and Kondo, 2018).

Unicellular branches derive from a morphogenetic event called cell intercalation. While the tube is still multicellular, cell intercalation leads to single cells encircling the lumen aligned along the branch. During the intercalation process, cells originally positioned side-by-side and connected via intercellular junctions, undergo a highly coordinated rearrangement wrapping up the lumen through the formation of autocellular junctions and repositioning in an end-to-end configuration. The proximal and distal continuity of the unicellular lumen is maintained by intercellular adherens junctions that appear as "ring-like" formations at the cell poles (**Fig. 8 A, B**) (Ribeiro *et al.*, 2004).

Subcellular tubes occur as cytoplasmic extensions of unicellular tubes, with absence of adherens junctions; thus, they are also referred as seamless tubes (**Fig. 8 A**) (Loganathan *et al.*, 2020).

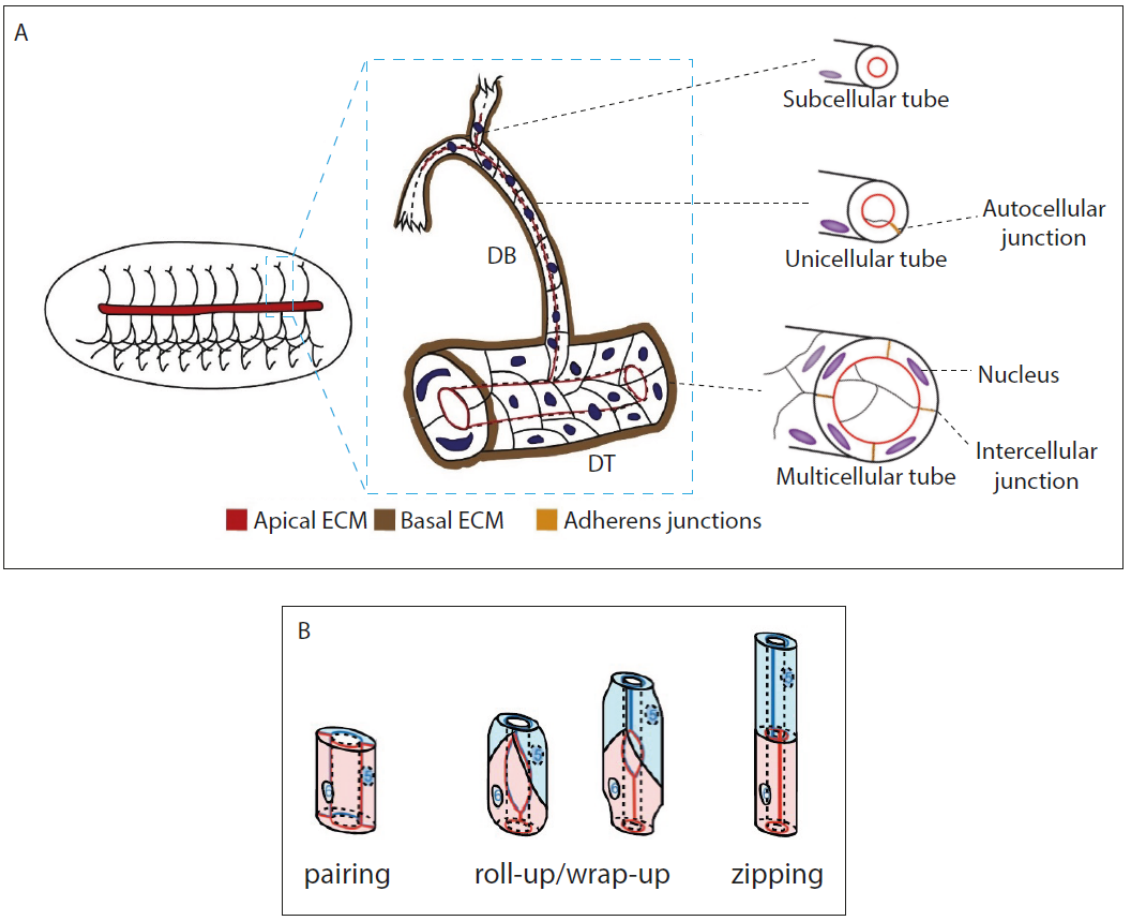

Fig. 8. Multicellular, unicellular and subcellular tubes in *Drosophila melanogaster* tracheal system and cell intercalation event. (**A**) A hemisegment from the ninth metameric unit composed of one unit of the dorsal trunk (DT) and the dorsal branch (DB) highlights the various tubular architectures: a multicellular tubule with intercellular junctions, a unicellular tubule with autocellular junctions, and a subcellular (seamless) tubule devoid of cell junctions (adapted from Loganathan *et al*., 2020). (**B**) Cell intercalation begins with paired cells reaching around their "partners" and making a nascent autocellular junction. As the cells are pulled apart and slide away from each other, the autocellular junctions zipper up, until the end of the cells is reached. At both poles, the ring-like cell adhesions, which are intercellular, maintain the tube continuity (adapted from Loganathan *et al.*, 2016).

1.4 The role of chitin during *Drosophila* tracheal development

Chitin is deposited in two different apical extracellular matrix structures during embryonic tracheal formation: the first one consists of a transient luminal apical extracellular matrix, and the second one consists of a tracheal cuticle decorated by the taenidial folds. This chitin-based ECM is fundamental to regulate tube diameter and length, to maturate the tubes, preventing tube collapse, and to allow gas filling (Manning and Krasnow, 1993; Devine *et al.*, 2005; Tonning *et al.*, 2005; Luschnig *et al.*, 2006; Moussian *et al.*, 2006).

Early in trachea development, starting from embryonic stage 13, the deposition of a chitinous apical extracellular matrix (aECM) begins in the dorsal trunk of the trachea (**Fig. 9 A**). Later, chitin is deposited in the ventral branches (**Fig. 9 B**) and, finally, in the dorsal branches of the trachea (**Fig. 9 C**). At the end of stage 14, the chitinous aECM is present in the lumen of all the tracheal branches (Moussian *et al.*, 2015).

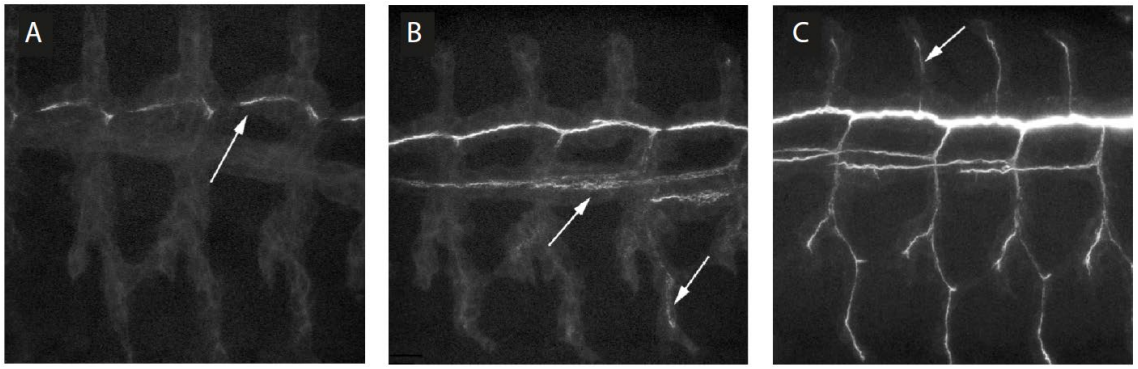

Fig. 9. Luminal chitin deposition in trachea (adapted from Moussian *et al.*, 2015). (**A**) Chitin appears first in the dorsal trunk at stage 13, stronger in the fusion region (arrow). (**B**) During stage 14 it is deposited in visceral branches and in lateral trunks (arrows). (**C**) Finally, chitin appears in dorsal branches and, by the end of stage 14, chitin is deposited in all the branches.

The intraluminal chitin filament is composed of parallel chitin polymers that form a chitin fiber spanning the entire length of the tracheal tubes (**Fig. 10**). Upon deposition of the polysaccharide chitin into intracellular space, luminal components modify chitin structure and contribute to the assembly of the chitin filament (Luschnig *et al.*, 2006; Moussian *et al.*, 2006; Wang *et al.*, 2006). During embryonic development, this chitin filament grows

diametrically as the tracheal tubes expand circumferentially. In the absence of filament, lumen expansion occurs, but in an irregular pattern associated with general dilatation of the tube and constrictions at the level of fusion cells (**Fig. 10**) (Devine *et al.*, 2005; Tonning *et al.*, 2005). Recent studies have identified the chitin filament as an elastic material coupled to the apical cell membrane and have reported that this coupling is required for tube length regulation (Dong and Hayashi, 2015). Overall, it has been proposed that the aECM, composed of the chitin filament and its associated proteins, participates in coordinating apical membrane growth and cell contractility (Öztürk-Çolak, Moussian and Araújo, 2016). However, this filament is a transient structure and towards the end of embryogenesis it is completely cleared from the lumen (Moussian *et al.*, 2006; Tsarouhas *et al.*, 2007).

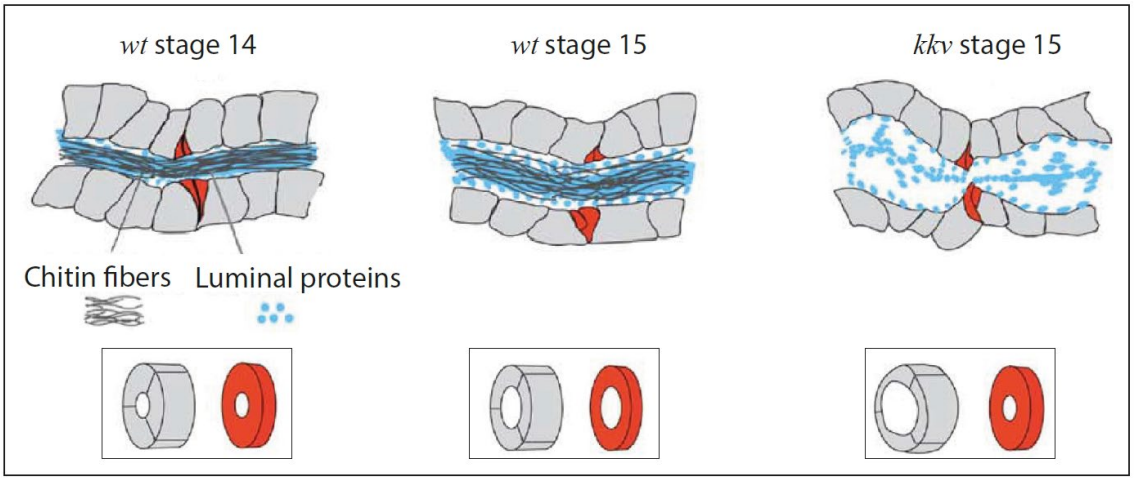

Fig. 10. Chitin role in the trachea. Schematic model for luminal chitinous matrix function during tube expansion. Chitin chains in the expanding lumen assemble into a functional filament by interactions with other luminal components. Loss of chitin abolishes chitinous luminal matrix function and causes lack of fusion cell expansion (red cell) and dilatation in the other part of tube (adapted from Tonning *et al.*, 2005).

Once tracheal tubules reach their final pattern and size, tube maturation starts. The formation of chitinous cuticle layers begin on the apical surface with a circumferential ridge, called taenidial fold, with a pattern corresponding to the cortical F-actin cable arrays formed at an earlier stage (Matusek *et al.*, 2006; Öztürk-Çolak *et al.*, 2016; Öztürk-Çolak, Moussian and Araújo, 2016). At late-stage 16, the chitin luminal filament of the

aECM is further degraded and the taenidia become more conspicuous. Then, the filament is completely removed and the lumen stays filled with liquid. Finally, the taenidia reach their most mature form as the tracheal tubes start to fill with air. The gas is generated independently of the outside atmosphere on part of the cuticle surface, and the gas quickly spreads over the entire tracheal lumen to completely fill the tube with gas (Zhang and Ward, 2009; Öztürk-Çolak, Moussian and Araújo, 2016; Hayashi and Kondo, 2018).

1.4.1 Chitin requirements in *Drosophila* trachea: Expansion and Rebuf

Chitin filaments are the major component of the transient luminal aECM and they are synthesized by *Drosophila* Chitin Synthase A, Kkv (Jürgens *et al.*, 1984; Ostrowski *et al.*, 2002; Moussian *et al.*, 2005; Swanson and Beitel, 2006; Dong and Hayashi, 2015). In the absence of Kkv, tracheal tubes collapse and the inflation with air fails (Moussian *et al.*, 2005). Besides, the tracheal tubes fail to accomplish uniform tube expansion. The apical surface of the dorsal trunk cells of *kkv* mutants show an expanded apical profile, as well as irregular apical accumulation of β-H spectrin. This observation suggests that lack of chitin synthesis causes defects in subapical cytoskeletal organization (Tonning *et al.*, 2005).

Chitin deposition also requires the activity of two MH2-containing proteins, Expansion (Exp) and Rebuf (Reb). The function of Exp and Reb is the same and interchangeable, but they are absolutely required for this process; in fact, Kkv is not able to deposit chitin without Exp/Reb (**Fig. 11**) (Moussian *et al.*, 2015).

Expansion gene (CG13188) was identified in our laboratory during the analysis of gene-expression changes in *Drosophila* embryo after inducing loss and gain of function of the transcription factor Tramtrack, that is involved in several processes during the development of the tracheal system (Araújo *et al.*, 2007). A search for similar proteins to Expansion led to the identification of CG13183, named Rebuf (Reb) (Rotstein *et al.*, 2011; Moussian *et al.*, 2015). These two proteins share 56% amino-acid similarity that is concentrated in the N-terminal part of the sequence. Expansion and Rebuf (Exp/Reb) proteins have been identified in several *Drosophila* species, other insects and arthropods (Iordanou *et al.*, 2014).

Analysis of the protein sequence indicates that Exp and Reb are Smad-like proteins containing a Mad-homology 2 (MH2) domain. Smad proteins are 400–500 amino acids in length, with particularly high similarity in the N-terminal MH1 (Mad-homology 1) domain and the C-terminal MH2 domain (Heldin *et al.*, 1997). The MH2 domain is responsible for interacting with other proteins, whereas the MH1 domain exhibits sequence-specific DNA binding. Generally, Smads are intracellular mediators of the TGF-β signaling pathway (Shi, 2001). Smads that contain only the MH2 domain function as regulators of TGF-β signaling (Tsuneizumi *et al.*, 1997). Exp and Reb contain only an MH2 domain, but no MH1 domain, indicating that they may potentially act as regulators of the TGF-β signaling pathway. However, it has been shown that Exp and Reb do not genetically interact with TGF-β signaling (Iordanou *et al.*, 2014; Beich-Frandsen *et al.*, 2015; Moussian *et al.*, 2015). Moreover, the sequence identity of the Exp/Reb proteins to the Smads is very low and it is restricted to the MH2 domain. Although the structure displays the main features of the MH2 fold, it contains an additional α-helical region that covers the concave site of the MH2 domain and defines the specific structure of the Exp/Reb MH2 domain. Based on this observation, the Exp/Reb MH2 domain has been renamed Nα-MH2 domain, a new member of the FHA/Smad superfamily of MH2 domains. The structural differences between the Smad MH2 and Expansion Nα-MH2 domains could have evolved to host a different range of protein-interaction partners. The differences are not only at the sequence level but also in the localisation of the domain: the Nα-MH2 domain is located in the N-terminal part in Exp/Reb in contrast to a C-terminal position of MH2 in Smad proteins (Beich-Frandsen *et al.*, 2015).

The first role suggested for Exp has been its interaction with receptor tyrosine kinase signaling to control tracheal tube size, suggesting that Exp regulates vesicular trafficking to control tube size (Iordanou *et al.*, 2014). Similarly, in another independent study it was suggested that Reb could be involved in the regulation of the tube size possibly through the endocytosis pathway (Chandran *et al.*, 2018).

However, the most striking phenotypes in embryos deficient for *exp* and *reb* are the absence of the transient luminal chitin filament during the development of the trachea (thus, the trachea remains uninflated) and the lack of chitin in tracheal and epidermal cuticles. Remarkably, these phenotypes are identical to those of *kkv* mutants (Moussian *et al.*, 2015).

The pattern of expression of *exp/reb* genes fully accounts for the timely and spatially regulated chitin deposition. Kkv is present from early stages in all tracheal cells. At stage 13, Reb appears in the DT and Exp in the ventral part of the placode. Chitin accumulation starts in the DT region, where Kkv and Reb are concomitantly expressed. At early stage 14, chitin starts being deposited in regions of concomitant expression of Kkv and Exp. Exp expression progressively expands from the ventral to the dorsal part of the placode, correlating with the deposition of chitin there (**Fig. 11**) (Moussian *et al.*, 2015).

Exp/Reb perform the same function and they are an absolute requirement for chitin deposition. (**Fig. 11**) (Moussian *et al.*, 2015).

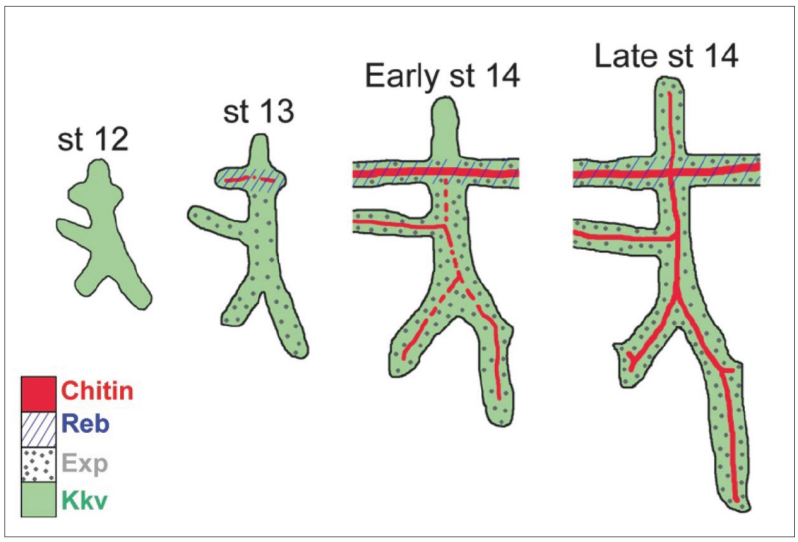

Fig. 11. Timely and spatially regulated chitin deposition (adapted from Moussian *et al.*, 2015). Schematic representation of chitin deposition and Kkv, Exp and Reb expression pattern.

Exp and Reb are not only required but they are also sufficient to bring about early and increased chitin deposition in the presence of Kkv. When *exp/reb* genes are over- or misexpressed, they bring about early and increased chitin deposition in places where Kkv is normally expressed (**Fig. 12 B**). The overexpression of Exp/Reb in trachea leads to strong chitin deposition from early stage 13 in all the branches and not only in the Dorsal Trunk. Later, the branches appear straight and shrank (particularly the DT), and the Lateral Trunk lacks cell intercalation event as cells remain connected by intercellular junctions. In addition, the trachea does not fill with air (**Fig. 12 C**) (Moussian *et al.*, 2015).

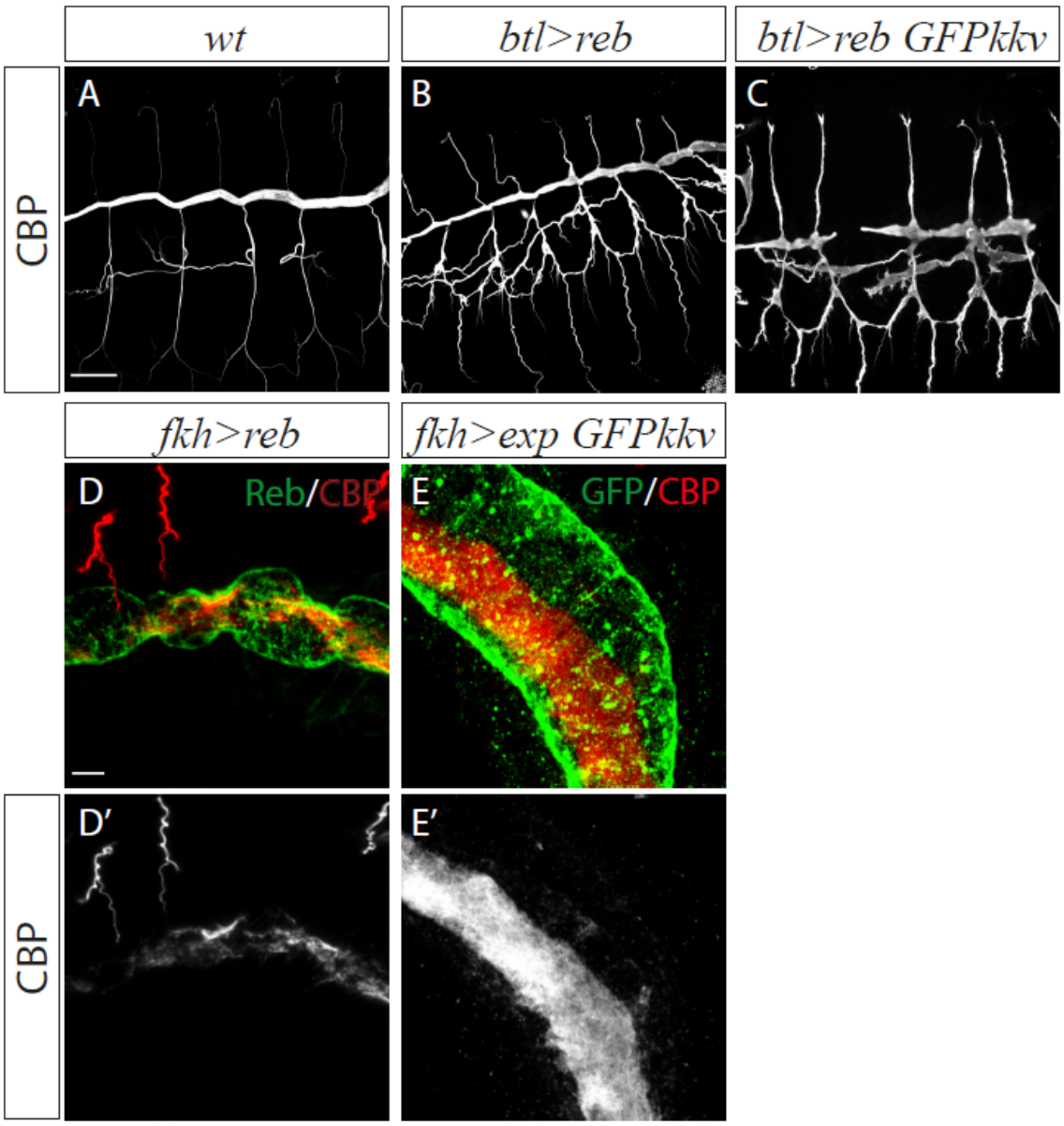

Fig. 12. Exp/Reb overexpression and misexpression. Lateral views of the embryos at stage 15 stained for CBP to detect chitin (grey in A, B, C, D', E' and red in D, E), Reb (green in D) and GFP to visualise Kkv (green in E). (**A**) Wild type embryo (wt), control. (**B**) Overexpression of wildtype form of Reb, note that the branches are straighter than the control. (**C**) The simultaneous overexpression of Reb and GFPKkv in the trachea produces branches that are straighter than the wild type embryo and the dorsal trunk appears discontinuous. (**D-D'**) The expression of Reb in salivary gland leads to ectopic chitin deposition inside the lumen. (**E-E'**) Chitin deposition is more conspicuous when Reb and Kkv are co-expressed. Scale bar 10 µm.

Exp/Reb accumulate strongly at the apical membrane, colocalising with Kkv in an independent manner, in fact Kkv still localises apically in absence of Exp/Reb and Exp/Reb localise apically in absence of Kkv. This subcellular localisation correlates with chitin deposition (Moussian *et al.*, 2015).

Remarkably, the simultaneous misexpression of Kkv and Exp/Reb promotes chitin deposition in ectopic ectodermally-derived tissues. For example, the salivary gland is a chitin-less ectodermal derived tissue, it presents a lumen and Kkv is already expressed at the apical membrane of this organ. The overexpression of Exp/Reb alone trigger chitin deposition in the lumen (**Fig. 12 D, D'**) and the phenotype is even stronger when Exp/Reb is simultaneously co-expressed with Kkv (**Fig. 12 E, E'**) (Moussian *et al.*, 2015).

The activity of Kkv and Exp/Reb has been evaluated in cell culture *in vitro* assays too, using *Drosophila* embryonic S2 cells. The transfection of Kkv alone leads to the formation of small chitin-containing particles intracellularly. The pattern of these particles is not changed when the cells are also co-transfected with Exp, Reb or both, and it is never detected fibrillar chitin deposited extracellularly. Interestingly, Kkv and Exp/Reb do not localise in the cell membrane region, suggesting a strong correlation between the subcellular localisation of these proteins and their activity in chitin deposition (Moussian *et al.*, 2015).

Several lines of evidence suggest that Exp and Reb may participate in chitin polymer translocation across the membrane and/or in the formation of chitin microfibrils. For instance, either in salivary glands (Exp and Reb are absent) or in tracheae deficient for *exp*/*reb*, the overexpression of Kkv alone leads to the formation of intracellular particles of chitin but no luminal chitin is detected. It has been suggested that Exp/Reb could be involved in the translocation of the Kkv-synthesized chitin polymers across the membrane and/or their release into the extracellular domain to form microfibrils (Moussian *et al.*, 2015).

2. Objectives

2. Objectives

Chitin has a recognised importance in physiology but also as a biomaterial. In insects, it is the principal component of the apical extracellular matrix of epidermis, tracheae, foregut and hindgut. In these compartments, chitin is synthesised by the family A of Chitin Synthases, which in *Drosophila* is encoded by the gene *kkv*. Chitin is also the main constituent of the peritrophic matrix that lines the inner surface of the midgut. In this case, the polymer is synthesized by the family B of Chitin Synthases, encoded by *ChS2* in *Drosophila*.

Previous work in our lab showed that Kkv alone is not sufficient to deposit chitin, and that two interchangeable MH2-containing proteins, namely Expansion (Exp) and Rebuf (Reb), are equally required for chitin deposition. It was shown that Kkv and Exp/Reb constitute the minimal genetic program necessary and sufficient for chitin deposition.

Despite the identification of this genetic program and the mentioned importance of chitin, there are still many open questions around the molecular mechanisms of activity of the different chitin-dedicated genes and the molecular mechanisms of chitin deposition. The aim of this work is to gain further insights into these relevant processes. The specific objectives of this Thesis are the following ones:

- **Investigate the molecular mechanism of activity of Exp and Reb**: through a structure-function analysis approach, we aimed to determine the role of Nα-MH2 domain, the only recognisable domain present in these proteins, and we aimed to find out new regions important for Exp/Reb function. Moreover, we aimed to determine whether the observed common functional requirements of *exp/reb* and *kkv* correlated with direct or indirect protein interactions.
- **Investigate the molecular mechanism of activity of Kkv**: we were interested in analysing the function of specific domains in Kkv protein that we speculated could have a role in a direct or indirect interaction with Exp/Reb. In particular, through a structure-function analysis approach, we aimed to determine the role of WGTRE motif and the role of the coiled-coil domain of Kkv.

- **Synthesise chitin *in vitro***: we aimed to produce extracellular chitin in cell culture by providing the cells with Kkv and Exp/Reb activity, with a correct subcellular localisation of the chitin machinery.
- **Compare the molecular mechanisms of activity of Kkv and ChS2**: we aimed to determine how the differences between the two Chitin Synthases Kkv and ChS2 correlate with chitin deposition and with the functional requirement of Exp/Reb.

3. Materials and Methods

3. Materials and Methods

3.1 *Drosophila* strains

All *Drosophila* strains were raised at 25ºC under standard conditions. The strain y^1w^{1188} was used as *wild type* (*wt*). Mutant chromosomes (Chr.) were balanced over *CyO*, *TM3* or *TM6* marked with LacZ, GFP or YFP. For overexpression experiments, we used the Gal4 drivers *btlGal4* (in all tracheal cells) and *fkhGal4* (in salivary glands). The overexpression, rescue and RNAi experiments were performed using the Gal4/UAS system (Brand and Perrimon, 1993). To maximise the expression of the transgenes, crosses were kept at 29°C.

Table 1 shows the list and the description of the strains used in this thesis.

Strain	Chr.	Description	Origin/Reference
btlGal4	II	Gal4 fused to *btl* promoter.	(Shiga *et al.*, 1996)
fkhGal4	III	Gal4 fused to *fkh* promoter.	(Henderson *et al.*, 2000)
Df(2R)BSC329	II	Chromosomal deletion that eliminates *exp* and *reb* among other genes.	(Iordanou *et al.*, 2014)
kkv^{IB22}	III	Nonsense mutation (Q53term) that produces a short protein lacking all the Kkv domains.	(Moussian *et al.*, 2005)
mmy^{H053}	II	Nonsense mutation (W162term) that produces a short protein.	(Araújo *et al.*, 2005)
UAS-GFPKkv	III	UAS construct expressing Kkv marked with GFP under UAS control.	(Moussian *et al.*, 2015)
reb^{LA00773}	II	Insertion of P{Mae-UAS.6.11} element that permits the regulated expression of *reb* under UAS control.	(Bellen *et al.*, 2004; Moussian *et al.*, 2015)
UAS-ChtVis-Tomato	II	UAS construct expressing the chitin binding domain of *B. circulans* chitinase A1 fused to the N- and C-segments of the Dusky-like protein and td-Tomato under the control of UAS. ChtVis-Tomato is secreted and binds to chitin and serves as a reporter of chitin deposition.	BDSC 66512 (Sobala *et al.*, 2016)

UAS-RNAiEps15	III	UAS construct expressing dsRNA for RNAi of Eps-15 under UAS control.	BDSC 33942
UAS-RNAiDap160	III	UAS construct expressing dsRNA for RNAi of Dap160 under UAS control.	BDSC 25879
UAS-Exp$^{\Delta MH2}$	II	UAS construct expressing a mutated form of Expansion protein lacking the MH2 domain under UAS control.	See section 3.3.1
UAS-Reb$^{\Delta MH2}$	II	UAS construct expressing a mutated form of Rebuf protein lacking the MH2 domain under UAS control.	See section 3.3.1
UAS-MH2-Exp	II, III	UAS construct expressing the MH2 domain of Expansion protein under UAS control.	See section 3.3.1
UAS-MH2-Reb	II, III	UAS construct expressing the MH2 domain of Rebuf protein under UAS control.	See section 3.3.1
UAS-Exp$^{\Delta CM}$	II, III	UAS construct expressing a mutated form of Expansion protein lacking the CM domain under UAS control.	See section 3.3.1
UAS-Exp$^{\Delta CM}$(long)	II, III	UAS construct expressing a mutated form of Expansion protein lacking the CM-long domain under UAS control.	See section 3.3.1
UAS- GFP-Kkv$^{\Delta WGTRE}$	II, III	UAS construct expressing a mutated form of Kkv protein, marked with GFP, lacking the WGTRE domain under UAS control.	See section 3.3.1
UAS- GFP-Kkv$^{\Delta CC}$	II, III	UAS construct expressing a mutated form of Kkv protein, marked with GFP, lacking the coiled coil domain under UAS control.	See section 3.3.1
UAS-GFP-ChS2	II, III	UAS construct expressing ChS2 protein marked with GFP under UAS control.	See section 3.3.1
UAS-GFP-ChS2-Kkv	II, III	UAS construct expressing a protein chimera marked by GFP and composed by the N-terminal part of ChS2 until the WGTRE motif and by the C-terminal part of Kkv starting from the coiled-coil domain.	See section 3.3.1
UAS-GFP-Kkv-ChS2	II, III	UAS construct expressing a protein chimera marked by GFP and composed by the N-terminal part of Kkv until the WGTRE motif and the C-terminal part of ChS2 right after the WGTRE motif.	See section 3.3.1

Table 1. List and description of *Drosophila* stocks used in this work.

3.2 Immunohistochemistry

3.2.1 Embryos fixation and immunohistochemistry

Embryos collected from 13 to 24 hours on agar plates were dechorionated with 100% bleach for 2 minutes and rinsed with Triton 0,1%. The embryos were collected and fixed for 20 minutes (10 minutes for E-Cadherin staining) in 4% formaldehyde, PBS (0,1 M Na Cl, 10mM phosphate buffer, pH 7,4) and Heptane 1:1 to generate holes in the vitelline membrane of the embryos. After removing the bottom phase, embryos were washed with methanol three times and used for immunostaining. Fixed embryos were rinsed 3 times, for 20 minutes each wash, with PBT (PBS with 0,1% Tween 20 from Sigma) with 0,5% BSA (Bovine Serum Albumin from Roche). Primary antibody incubation was performed in fresh PBT-BSA over night at 4ºC. The following day, embryos were rinsed 3 times, for 20 minutes each wash, with PBT-0,5% BSA. Secondary antibody incubations were performed in the dark for at least 2 hours at room temperature in PBT-0,5% BSA. Embryos were washed for 1 hour at room temperature in 3 washes of PBT and mounted in Fluoromount-G (Southern biotech), except for super-resolution analysis that preparations were mounted in Vectashield (Vector Laboratories).

Primary and secondary antibodies are listed and described in **Table 2**.

Primary Antibodies				
Name	**Antigen**	**Species**	**Dilution**	**Origin**
Anti-Arl8	Arl8	Rabbit	1:100	DSHB
Anti-Armadillo	Armadillo	Mouse	1:100	DSHB
Anti-ChS2	ChS2	Rabbit	1:100	Produced by our lab (see section 3.3.3)
Anti-Crb	Crumbs	Mouse	1:10	DSHB
Anti-E-Cadh (DCAD2)	De-Cadherin	Rat	1:100	DSHB
Anti-Exp	Expansion	Rat	1:100	Produced by our lab (Moussian *et al.*, 2015)
Anti-FK2	FK2	Mouse	1:50	Enzo Life Sciences
Anti-GFP	GFP	Goat	1:600	Moleculars Probes and Roche
Anti-GFP	GFP	Rabbit	1:600	Moleculars Probes and Roche
Anti-GMAP	GMAP	Goat	1:2000	DSHB
Anti-Golgin245	Golgin245	Goat	1:2000	DSHB
Anti-Golgin84	Golgin84	Mouse	1:100	DSHB

Anti-Hrs27-4	Hrs	Mouse	1:100	DSHB
Anti-KDEL	KDEL	Mouse	1:200	Stress Marq Biosciences
Anti-Kkv	Kkv	Rabbit	1:100	Produced by our lab (see section 3.3.3)
Anti-Rab11	Rab11	Rabbit	1:2000	Provided by T.Nakamura
Anti-Rab7	Rab7	Rabbit	1:100	Provided by T.Nakamura
Anti-Reb	Rebuf	Rat	1:100	Produced by our lab (Moussian *et al.*, 2015)
Anti-RFP	RFP	Rabbit	1:300	AbCam
CBP (probe)	Chitin		1:300	Produced by N. Martín in J. Casanova lab
Secondary antibodies				
Alexa 488		Donkey	1:300	Jackson ImmunoResearch
Alexa 561		Donkey	1:300	Jackson ImmunoResearch
Alexa 647		Donkey	1:300	Jackson ImmunoResearch
Cy2		Donkey	1:300	Jackson ImmunoResearch
Cy3		Donkey	1:300	Jackson ImmunoResearch
Cy5		Donkey	1:300	Jackson ImmunoResearch

Table 2. List of antibodies used in this thesis.

3.2.2 Larval salivary glands fixation and immunohistochemistry

Salivary glands of wandering third instar larvae were dissected while viewed using a stereomicroscope in PBS 1X solution and fixed in PIPES buffer (NaCl 1mM, PIPES 10mM, $MgCl_2 \cdot 6H_20$ 1mM, pH 7,2) and formaldehyde 4% for 30 minutes. Salivary glands were rinsed for 1 hour with PBT-BSA 0,5%. Primary antibody incubation was performed in fresh PBT-BSA over night at 4ºC. The following day, salivary glands were rinsed 3 times, for 20 minutes each wash, with PBT-0,5% BSA. Secondary antibody incubations were performed in the dark for 2 hours at room temperature in PBT-0,5% BSA. Salivary glands were washed for 1 hour at room temperature in 3 washes of PBT and mounted in Vectashield (Vector Laboratories). Salivary glands were stained with the primary antibodies anti-Kkv, anti-Reb and the probe CBP (see **Table 2**).

3.3 Molecular biology techniques

3.3.1 Generation of UAS constructs

From a previous project in our lab (Moussian *et al.*, 2015), several constructs were obtained: the coding sequence of *exp*, *reb*, *GFP-kkv* cloned in the vector pUAST and the coding sequence of *GFP-ChS2* in the vector pJET1.2 (Thermofisher). We digested the DNA from the vector using the following couples of restriction enzymes (New England BioLabs, NEB): EcoRI/XhoI for *expansion*, EcoRI/NotI for *rebuf* and XhoI/XbaI for *GFP-kkv* and we cloned them in the vector pJET1.2. These final constructs were our starting points for the generation of the UAS constructs.

Constructs obtained by directed deletion

To delete specific regions from the DNA, "Q5 Site-Directed Mutagenesis Kit" (NEB) was used. The kit comprehended material to perform PCR, ligation of the fragments and transformation of NEB-α competent cells. Deletions are created by designing primers that flank the region to be deleted, then we performed a PCR obtaining a linear double filament of DNA composed by the original pJET1.2 vector and the flanking regions of the deleted sequence. Upon ligation of the fragment, competent cells were transformed and plated in selective plates. Miniprep to obtain DNA were performed using the kit NZYtech and the DNA was sequenced through the platform Eurofins Genomics. Finally, the new mutated DNA was digest using the restriction enzymes described in the previous paragraph and cloned in pUAST vector for $Exp^{\Delta MH2}$ and $Reb^{\Delta MH2}$ and in pUAST-attB vector (provided by the laboratory of Dr. Gerardo Jimenez) for all the other DNAs. After performing a midiprep (NZYtech), the DNAs were injected in embryos w^{118} by the "*Drosophila* injection Service" of the "Institute for Research in Biomedicine" (IRB, Barcelona) and by the "Transgenesis Service" of the "Centro de Biología Molecular Severo Ochoa" (CBM, Madrid).

The primers used to obtain the constructs are listed in **Table 3**.

Final Construct	Template	Primers
UAS-Exp$^{\Delta MH2}$	*pJET1.2-exp*	Forward: GTGGTGGCCATGGATATG Reverse: GTCGATTTGGGTCCATTTG

UAS-Reb$^{\Delta MH2}$	*pJET1.2-reb*	Forward: AACGTGGTGGCCATGGAC Reverse: GTCGATTTGCTCCCACTTG
UAS-Exp$^{\Delta CM}$	*pJET1.2-exp*	Forward: CGGGCCCGAGTTCCGAAC Reverse: ATATTTCTTATTATCTTTGCCCTTGTCAGATTTACC
UAS-Exp$^{\Delta CM}$(long)	*pJET1.2-exp*	Forward: TCCGGCAAGCCGATACCC Reverse: ATATTTCTTATTATCTTTGCCCTTGTCAGATTTACC
UAS- GFP-Kkv$^{\Delta WGTRE}$	*pJET1.2-GFP-kkv*	Forward: GTGGTGGCTAAGAAGACC Reverse: GGAGACGACGTTTAGGTTG
UAS- GFP-Kkv$^{\Delta CC}$	*pJET1.2-GFP-kkv*	Forward: AGCATGCTGAGCTTCCTTC Reverse: GGTCTTCTTAGCCACCAC

Table 3. List of primers used to perform directed deletions.

Constructs obtained by recombination

To perform recombination of different DNA fragments, the kit "NEBuilder HiFi DNA Assembly" (New England BioLabs) was used. We used the pUAST-attB vector digested by XhoI/KpnI and two different fragments of DNA amplified by PCR. The newly-amplified fragments have two nucleotide tails: the first one is identical to a region of the sequence of the vector, the second tail is identical to a region of the sequence of the other fragment. The recombinations occur between two identical regions. The new plasmid obtained was used to transform competent *E. coli* cells. Then we proceed as described above.

The primers used to obtain the constructs are listed in **Table 4**.

Final construct	Fragment	Template	Primers
UAS-GFP-ChS2-Kkv	*GFP-ChS2-WGTRE*	*pJET1.2-GFP-ChS2*	Forward: TCGTTAACAGATCTGCGGCCGCGGCT CGAGATGGTGAGCAAGGGCGAG Reverse: TCTTAGCCACCACCTCTCGAGTGCCC CACGAAAAC
	WGTRE-Kkv	*pJET1.2-GFP-Kkv*	Forward: GGGCACTCGAGAGGTGGTGGCTAAG AAGACCAAGAAAG

			Reverse: CTTCACAAAGATCCTCTAGAGGTACC TCACAGGCGACCTGTGCC
UAS-GFP-Kkv-ChS2	*GFP-Kkv-WGTRE*	*pJET1.2-GFP-Kkv*	Forward: CTGCGGCCGCGGCTCGAGGGTACCTC TAGATGGTGAGCAAGGGCGAGGAG Reverse: TGAGCACTGGAGCCTCGCGGGTGCCC CAGGA
	WGTRE-ChS2	*pJET1.2-GFP-ChS2*	Forward: GGGCACCCGCGAGGCTCCAGTGCTCA AGGAC Reverse: AGTAAGGTTCCTTCACAAAGATCCTC TAGAACTCGGTGTGCTC

Table 4. List of primers used to amplify fragments to perform recombination.

Other constructs

UAS-GFP-ChS2 was obtained digesting *pJET-GFP-ChS2* with the restriction enzyme SpeI and cloned in pUAST-attB vector.

UAS-MH2-Exp and *UAS-MH2-Reb* were obtained amplifying the MH2 region respectively from *pJET-exp* and *pJET-reb* and cloning the fragment in the pUAST-attB vector using in both cases EcoRI/NotI. The primers used are listed in **Table 5**.

Final construct	Template	Primers
UAS-MH2-Exp	*pJET1.2-exp*	Forward: CGGAATTCATGGACGAGATCTGGGCCAA Reverse: ATAGTTTAGCGGCCGCTCACGGGCGGTTCTTGA
UAS-MH2-Reb	*pJET1.2-reb*	Forward: CGGAATTCATGGACGAGATCTGGGCCAA Reverse: ATAGTTTAGCGGCCGCTCAGCTGCTGTTCGTCAG

Table 5. List of primers used to amplify MH2 fragments.

3.3.2 Generation of RebCherry-Kkv-ExpGFP (RKE) plasmid

From the laboratory of Dr. Rosa Barrio, we received the vector pAc5-STABLE2-Neo (González *et al.*, 2011). This vector permits the multicistronic expression of two proteins fused with mCherry and GFP under the control of the Actin5C constitutive promoter; the

presence of T2A sequences permits the self-cleavage of the polyprotein into individual proteins. The vector contains also a Neomycin-resistance sequence permitting the positive selection of the cell colonies (González *et al.*, 2011).

Our objective was to obtain a plasmid able to express the proteins Reb-Cherry, Kkv and Exp-GFP. First, we amplified a T2A fragment through PCR adding at 5' end the restriction sites for EcoRV and AvrII, and adding at 3' end the restriction sites for PmlI and XbaI; then we cloned it into the pAc5-STABLE2-Neo between mCherry-T2A and GFP-T2A using EcoRV/XbaI; thus, we obtained a vector capable to express a third unmarked protein. Finally, through several steps of DNA digestion and ligation we cloned Rebuf (KpnI/EcoRI), Kkv (EcoRV/AvrII) and Expansion (PmlI/XbaI) in the vector. The primers used for these processes are listed in **Table 6**.

Fragment	Template	Primers
T2A	*pAc5-STABLE2-Neo*	Forward: ATCCCTAGGGGAAGCGGAGAGGGCAGAGGAAGTCTGCTAACTTGC GGTGACGTCGAGGAGAATCCTGGACCTCACGTGT Reverse: CTAGACACGTGAGGTCCAGGATTCTCCTCGACGTCACCGCATGTTA GCAGAGTTCCTCTGCCCTCTCCGCTTCC
Reb	*pJET1.2-reb*	Forward: CGGGGTACCATGATTTCTCGCCGCAAGATC Reverse: CCGGAATTCTTCATGTGCGCTGATCAG
Kkv	*pJET1.2-GFP-Kkv*	Forward: CCGATATCATGTCTGCGATGCGGCATCGC Reverse: GAACCTAGGCAGGCGACCTGTGCCATTA
Exp	*pJET1.2-exp*	Forward: CACGTGATGGTGTCGCGTCGAAAAATT Reverse: GCTCTAGAGTCCCATTCCCCGATGAACATG

Table 6. List of primer used to generate RKE plasmid.

3.3.3 Generation of antibodies

Polyclonal antibodies against Kkv and against ChS2 were generated using fragments not in common to each other. The fragments were amplified by PCR using the primers listed in **Table 7**, we used the restriction sites NdeI/XhoI for Kkv and NcoI/EcoRI for ChS2.

The amplified fragments were cloned into the expression vector pET14b (Novagen) or pROX, which carry an N-terminal His tag. The resulting positive clones were used to transform BL2 (C41) cells (Novagen) for protein expression. Cells were induced with 1

mM IPTG and proteins were expressed at 37ºC during 2 hours. The positive clones were selected and the recombinant proteins (22 KDa for Kkv and 22,8 KDa for ChS2) fused with a His tag were purified through a column of nickel (Quiagen) in denaturalising conditions (8 M urea). The purified proteins were used to inject rabbits by the facility "Production of antibodies" in CID (Centre d'Investigació i Desenvolupament) of Barcelona.

Fragment	Template	Primers
Kkv	*pJET1.2-GFPkkv*	Forward: GGAATTCCATATGGGAATCGATGGCGACTAC Reverse: CCGCTCGAGTCACAGGCGACCTGTGCCATT
ChS2	*pJET1.2-GFPChS2*	Forward: CATGCCATGGACTGGTTTCGAACAGGAGGT Reverse: CCGGAATTCAAAGCCATATTGTTCCG

Table 7. List of primers used to amplify the fragments to generate Kkv and ChS2 antibodies.

3.3.4 Western blot, immunoprecipitation and co-immunoprecipitation

Protein extraction from *Drosophila* embryos

To extract the proteins from *Drosophila* embryos, we used two different solutions. The first solution is composed by TRIS 50mM (pH 8), NaCl 150mM, EDTA 5mM, NP40 0,5%, PMSF 0,1 mM and PIC 1x; the second solution, called RIPA buffer, is composed by TRIS 50mM (pH 8), NaCl 150 mM, NP40 1%, SDS 0,1%, NaDOC 0,5%, PMSF 1 mM and PIC 1x. Embryos collected on agar plates overnight were dechorionated with 100% bleach for 2 minutes and rinsed with Triton 0,1%. We collected 100 µL of dechorionated embryos and we added them in an Eppendorf with 400 µL of one of the two solutions described above; the embryos were homogenised with an Eppendorf homogeniser. Finally, the Eppendorf were incubated for 15 minutes with rotation at room temperature and centrifugated for 15 minutes, at 1600 rpm, at 4ºC; the supernatant was recovered.

Immunoprecipitation and co-immunoprecipitation

Immunoprecipitation (IP) is the small-scale affinity purification of antigens using a specific antibody that is immobilized to a solid support such as magnetic particles. After the immobilization, the complex magnetic beads-antibody is incubated with a cell or embryo lysate containing the target protein. During the incubation period, gentle agitation of the lysate allows the target antigen to bind to the immobilized antibody. The immobilized immune complexes are then collected from the lysate, eluted from the support and analysed.

Co-immunoprecipitation (Co-IP) is an extension of IP that is based on the potential of IP reactions to capture and purify the primary target as well as other macromolecules that are bound to the target by native interactions in the sample solution. Thus, whether or not an experiment is called an IP or Co-IP depends on whether the focus of the experiment is the primary target (antigen) or secondary targets (interacting proteins).

We proceed as following. We transferred 50 µL of magnetic beads (Dynabeads, Thermofisher) in an Eppendorf, we placed the tube on a magnet to separate the beads from the solution and we removed the supernatant. We removed the eppendorf from the magnet to add our antibody (anti-Kkv, anti-Exp or anti-Reb) diluted in 200 µL PBS with Tween 20 and we incubated the tube with rotation for 10 minutes at room temperature. We placed the tube on a magnet and removed the supernatant, we removed the Eppendorf from the magnet and we resuspended the magnetic bead-antibody complex in 200 µL PBS with Tween 20 and we washed by pipetting. We placed the tube on the magnet, we removed the supernatant, we added the embryonic protein extract and we incubated with rotation for 10 min at room temperature to allow the antigen (and eventually its interacting proteins) to bind to the magnetic bead-antibody complex. We washed the magnetic beads-antibody-antigen complex 3 times by gentle pipetting using 200 µL of PBS 1x for each wash placing the tube on the magnet and removing the supernatant between each wash. We resuspended the magnetic beads-antibody-antigen complex in 100 µL of PBS 1x and we transferred the bead suspension to a clean tube. We placed the tube on the magnet and remove the supernatant. We added 20 µL of elution buffer (50 mM glycine pH 2.8), we resuspended the mix and we incubated with rotation for 2 minutes at room temperature to dissociate the complex. We placed the tube on the magnet and transfer the supernatant containing eluted antibody and antigen to a clean tube.

Acrylamide gel electrophoresis (SDS-PAGE)

Acrylamide gel electrophoresis is used to separate proteins according to their molecular weight. The separation occurs in denaturalising conditions with SDS through a polyacrylamide gel matrix (PAGE). The gel is divided in two parts: the stacking gel composed by acrylamide 5%, TRIS 1M pH 6,8, SDS 10%, PSA 10% and TEMED, Roche, and separating gel composed by acrylamide (7% for Exp/Reb gels, 10% for Kkv gels), TRIS 1M pH 6,8, SDS 10%, PSA 10% and TEMED.

We added protein loading buffer (Invitrogen) and β-mercaptoethanol 1,5 M to the samples (full embryonic protein extract or sample derived from IP or Co-IP) and we boiled them for 5 minutes at 95ºC. The samples were loaded in the gel and the separation occurred in Laemmli buffer (1% SDS, glycine 2M, TRIS 250mM, pH 8,3).

Western blot

The proteins were transferred from the gel to a nitrocellulose membrane in transferring buffer (TRIS, glycine, SDS 10%, methanol) for 2 hours, at 4ºC, at 80 Volts. Then, we blocked the membrane (PBT, milk powder 5 g, sodium azide 0.01%) for 2 hours and rinsed 3 times for ten minutes with PBS-tween 0,1%. The membrane was incubated for one hour with the primary antibody and rinsed 3 times for ten minutes with PBS-tween 0,1%. The membrane was incubated with secondary antibody conjugated to peroxidase and rinsed 3 times for ten minutes with PBS-tween 0,1%. The membrane was revealed with Immobilon Western-Chemiluminescent HRP substrate (Millipore), then the membrane was dried and exposed for 5 minutes to an autoradiography film Curix RP2 Plus (Agfa). The film was revealed in a Hyper-processor (Amersham).

3.3.5 Slotblot experiment

The day after cell transfection (see section 3.4.1), we transferred the cells in a new well with fresh culture medium (Schneider's Insect medium, Sigma, with 10% foetal bovine serum, FBS, Gibco) and we incubated them over night, at room temperature with rotation. The following day, we centrifuged the cells for 5 minutes, at 1600 rpm, we recovered the supernatant (the culture medium that we wanted to analyse, we named it supernatant 1), we resuspended the pellet of cells in RIPA buffer and we incubated it for 15 minutes at

room temperature with rotation. Afterwards, we centrifuged the cells for 5 minutes, at 1600 rpm and we recovered the supernatant (the cell lysate to analyse, we named it supernatant 2). Then we put a nitrocellulose membrane in the slotblot apparatus and we load it with the supernatant 1 and 2; after creating the vacuum, the sample were spotted onto the membrane. We let dry the membrane for 1 hour and then we blocked it for 1 hour in blocking solution. We incubated the membrane for 1 hour at room temperature with CBP conjugated to Cy5 in dilution 1:500 and we rinsed it 3 times for ten minutes with PBS-tween 0,1% and once for 10 minutes with PBS 1X. The membrane was dried and signal was detected with Odyssey Fc (Li-Cor) at a length wave of 700 nm.

3.4 *Drosophila* S2 cells culture

Drosophila S2 cells (Invitrogen) were cultured in complete Schneider's Insect medium (Sigma) complemented with 10% foetal bovine serum (FBS, from Gibco) at 28ºC. For general maintenance, cells were passaged at a density of 10^7 cells/mL. The high-density cells were suspended by gentle pipetting and diluted 1:10 in a new flask.

3.4.1 Transient and stable transfection of S2 cells

Drosophila S2 cells were transfected using Effectene Transfection Reagent (Qiagen).

For transient transfection, cells were cultured in Schneider's medium enriched with 10% of FBS and they were used for immunostaining assays or slotblot experiment after 24 hours of expression. The DNA used were generated and described in our lab: actinG4VP16-Crb (Letizia *et al.*, 2013), pAC5.1-Exp, pAC5.1-Reb and pAC5.1-GFP-Kkv (Moussian *et al.*, 2015).

For stable transfection, the cells were passaged 1:10 in selective Schneider's medium enriched with 10% FBS and antibiotic Neomycin (Sigma-Aldrich) 300µg/mL; cells were maintained in selective medium until colonies appeared. In this case, we used the DNA pAC5.1-Stable-RKE described in section 3.3.2.

3.4.2 Fixation and immunohistochemistry of S2 cells

S2 cells were rinsed 2 times with PBS for 10 minutes and suspended in Schneider's medium. Coverslips previously treated with concanavalin A (Sigma) 0,5 mg/mL were put in 12-wells plate; in each well, $4 \cdot 10^6$ cells in a final volume of 2 mL were transferred and incubated overnight at 28ºC. On the next day, each well was rinsed with PBS 1X for 10 minutes with rotation. The cells were fixed for 15 minutes with 100 µL of 4% formaldehyde diluted in PBS 1X. The cells were rinsed first with PBS 1X for 15 minutes and then twice for 10 minutes with PBS-Triton-BSA (PBS 1X, 0,1% Triton X-100, 0,01gr/mL BSA). Primary antibody incubation was performed in fresh PBT-BSA over night at 4ºC. The following day, the cells were rinsed 3 times, for 10 minutes each wash, with PBT-BSA. Secondary antibody incubations were performed in the dark for 1 hour at room temperature in PBT-BSA. Cells were washed twice for 10 minutes in PBT and twice for 10 minutes in PBS 1X. Finally, cells were mounted in Vectashield-DAPI (Vector Laboratories). The primary antibodies used for staining of the cells were anti-GFP, anti-Cherry, anti-Kkv, anti-Crumbs and the probe CBP (**Table 2**).

3.5 Microscopy

Fluorescence confocal images of fixed embryos were obtained with Leica TCS-SPE system using 20x and 63x (1,40-0,60 oil) objectives (Leica). For super-resolution images two different system were used: Elyra PS1- Airyscan (Zeiss) from the "Advanced Digital Microscopy Core Facilty" of the "Institute for Research in Biomedicine" (IRB, Barcelona) and Drangofly 505 (Andor) from "The Molecular Imaging Platform" of the "Institut de Biología Molecular de Barcelona" (IBMB, CSIC); in both cases an 100x (1,40-0,60 oil) objective was used.

The latter system was used also to perform life imaging. In this case, dechorionated embryos were mounted and lined up on a Menzel-Glaser coverslip with oil 10-S Voltalef (VWR) and covered with a membrane (YSI membrane kit). In all movies we used 63x (1,40-0,60 oil) objective. To visualise time-lapse movies, single sections were used.

Fiji (ImageJ) (Schindelin *et al.*, 2012) was used for measurement and adjustment. Otherwise indicated in the text, confocal images are maximum-intensity projections of Z-stack sections. Figures were assembled with Adobe Illustrator CC 2021.

3.6 Quantification and statistics

Total number of cells is provided in the text and figure. Measurement was imported and treated into Prism software 4.7, where graphic was generated. Error bars graphic denote standard deviation. Statistical analysis was performed applying t-test. Difference was considered significant when $p<0,05$. In graphic *** means $p<0.001$.

4. Results

4. Results

4.1 Structure-function analysis of Expansion and Rebuf

To investigate the molecular and cellular mechanism of activity of Expansion (Exp) and Rebuf (Reb) we decided to use a structure-function approach. We examined a domain already described in literature, the Nα-MH2 domain (Beich-Frandsen *et al.*, 2015), and we looked for other possible conserved domains not yet characterized.

4.1.1 Nα-terminal MH2 domain is required for chitin deposition

It has already been described that the only recognisable domain in Exp and Reb proteins is a Nα-MH2, a new member of the Smad/FHA superfamily (Beich-Frandsen et al., 2015; Moussian et al., 2015). Typically the MH2 domains are involved in protein-protein interactions (Qin *et al.*, 1999; Wu *et al.*, 2002), but the role of Nα-MH2 and its possible interactions have not been determined.

To study the role of Nα-MH2 domain we chose to generate new UAS constructs for Exp and Reb lacking this domain: UASExp$^{\Delta MH2}$ and UASReb$^{\Delta MH2}$. The results obtained with each construct were comparable. When we overexpressed the wildtype form of Exp or Reb, we observed an increased and advanced accumulation of chitin, therefore the branches of the trachea were straighter than the control (**Fig. 13 A, B**). In contrast, when we overexpressed Exp$^{\Delta MH2}$ in the trachea of a wildtype embryo, no detectable effect was found and chitin was normally deposited in the lumen according to the spatio-temporal pattern (**Fig. C**). This suggested that Exp$^{\Delta MH2}$ and Reb$^{\Delta MH2}$ proteins are unable to exert the same function as the wildtype proteins. To assess this hypothesis, we tested the ability of Exp$^{\Delta MH2}$ and Reb$^{\Delta MH2}$ to rescue the lack of chitin deposition produced by the absence of Exp and Reb. To test this condition, we used a deficiency (BSC879) that uncover *exp*, *reb* and other genes (Moussian *et al.*, 2015). Embryos homozygous for the deficiency lacks chitin but the overexpression of the wildtype form of Exp/Reb proteins was able to revert the absence of chitin (**Fig. 13 E**). Instead, the overexpression of the ΔMH2 forms

in an *exp*/*reb* deficient background was unable to rescue the lack of chitin (**Fig. 13 F**). These results indicate that Exp or Reb proteins lacking the Nα-MH2 domain are not functional and that the Nα-MH2 domain is absolutely required for chitin deposition.

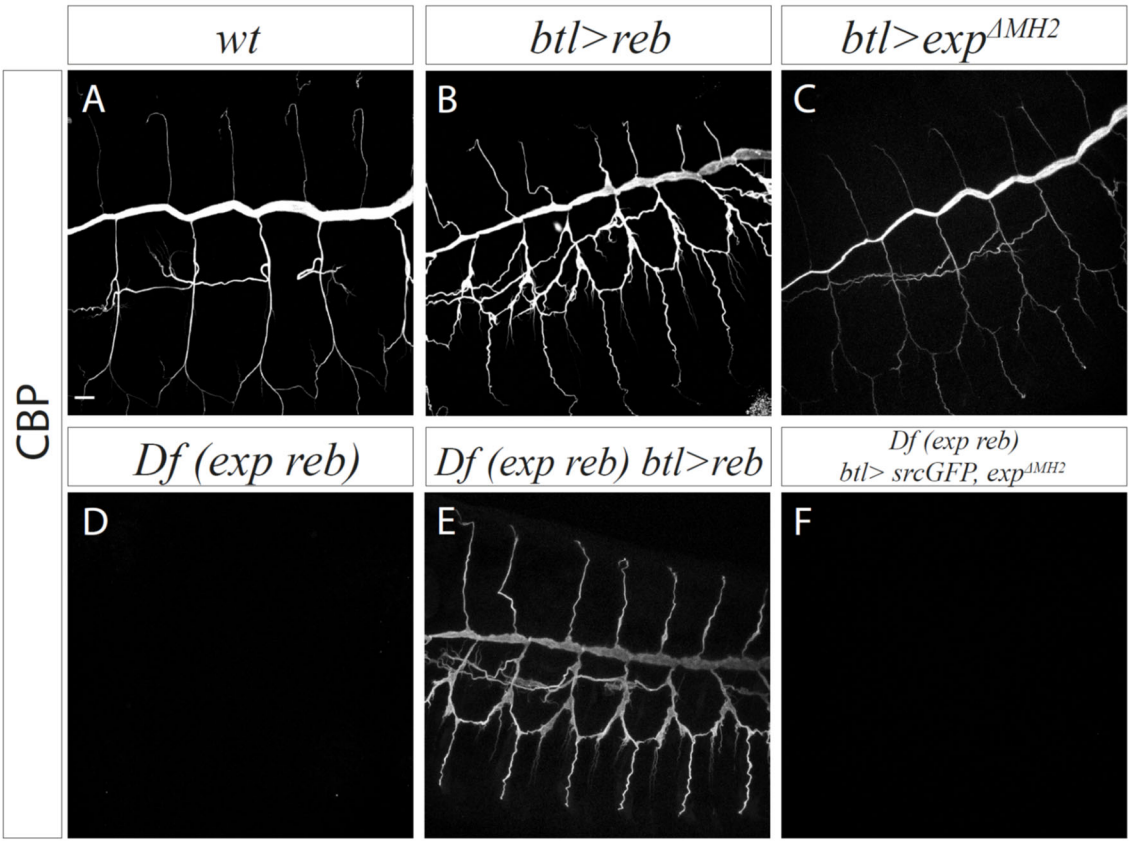

Fig. 13. Analysis of the overexpression of Exp$^{\Delta MH2}$ in trachea. Lateral views of the embryos at stage 15 stained for CBP to detect chitin (grey). (**A**) Control embryo. (**B**) Overexpression of wildtype form of Reb, note that the branches are straighter than the control. (**C**) The overexpression of Exp$^{\Delta MH2}$ is comparable to the control. (**D**) In a deficiency background for *exp* and *reb*, chitin is missing in the embryo. (**E**) The overexpression of a wildtype form of Reb in a deficient background for *exp* and *reb* rescues the absence of chitin. (**F**) The overexpression of Exp$^{\Delta MH2}$ in a deficient background for *exp* and *reb* does not rescue the lack of chitin. Scale bar 10µm.

The co-expression of Kkv and Exp or Reb can deposit excessive and advanced chitin in tissues that normally deposit chitin, such as in trachea (**Fig. 14 A-A''**), or can deposit ectopic chitin in ectodermal derived tissues that normally lack chitin, like in salivary glands (**Fig. 15 A**). We reasoned that Exp$^{\Delta MH2}$ and Reb$^{\Delta MH2}$ would be unable to produce these effects. As expected, the concomitant overexpression in trachea of Kkv and

Exp$^{\Delta MH2}$ or Reb$^{\Delta MH2}$ did not generate excessive or advanced chitin; the polymer was still present in the lumen, likely due to the presence of the endogenous Exp and Reb proteins (**Fig. 14 B-B'**). In agreement with this, we found that in embryos deficient for *exp* and *reb*, the simultaneous overexpression of Kkv and Exp$^{\Delta MH2}$ or Reb$^{\Delta MH2}$ did not lead to chitin deposition in the lumen of the trachea (**Fig. 14 E-E'**). However, the co-expression of Kkv and Exp$^{\Delta MH2}$ or Reb$^{\Delta MH2}$ in the trachea produced a very clear phenotype: we identified the presence of many intracellular particles of chitin (**Fig. 14 B-B'**) and presence of vesicles containing Kkv (**Fig. 14 B, B''**). Largely, Kkv and chitin vesicles do not colocalise (see section 4.1.4). The presence of Kkv and chitin vesicles was also observed in conditions of absence of endogenous *exp* and *reb*. These results indicate that, in absence of the Nα-MH2 domain of Exp and Reb, chitin can still be synthesised, but it cannot be deposited extracellularly. Thus, the Nα-MH2 domain is required for chitin deposition but it is dispensable for chitin synthesis.

It was already shown that Exp and Reb are not yet functional at early stages (stage 11-12) in the trachea, because they are not present (Moussian *et al.*, 2015). Interestingly, we observed that at early stages (**Fig. 14 C-C'**) as well as in mutants deficient for *exp* and *reb* (**Fig. 14 F-F'**), the overexpression of Kkv alone produced intracellular chitin particles. In contrast, at later stages, the overexpression of only Kkv in an otherwise wild type background, did not produce intracellular chitin particles (**Fig. 14 D-D'**). We attribute the presence of chitin particles to an excess of Kkv activity: due to the absence of Exp and Reb, the extra chitin synthesised cannot be processed and deposited to the lumen. When we added Exp$^{\Delta MH2}$ or Reb$^{\Delta MH2}$ to the overexpression of Kkv (**Fig. 14 B, B', E, E'**), we found many more intracellular chitin particles suggesting that the presence of extra Exp and Reb proteins promotes Kkv-dependent chitin synthesis.

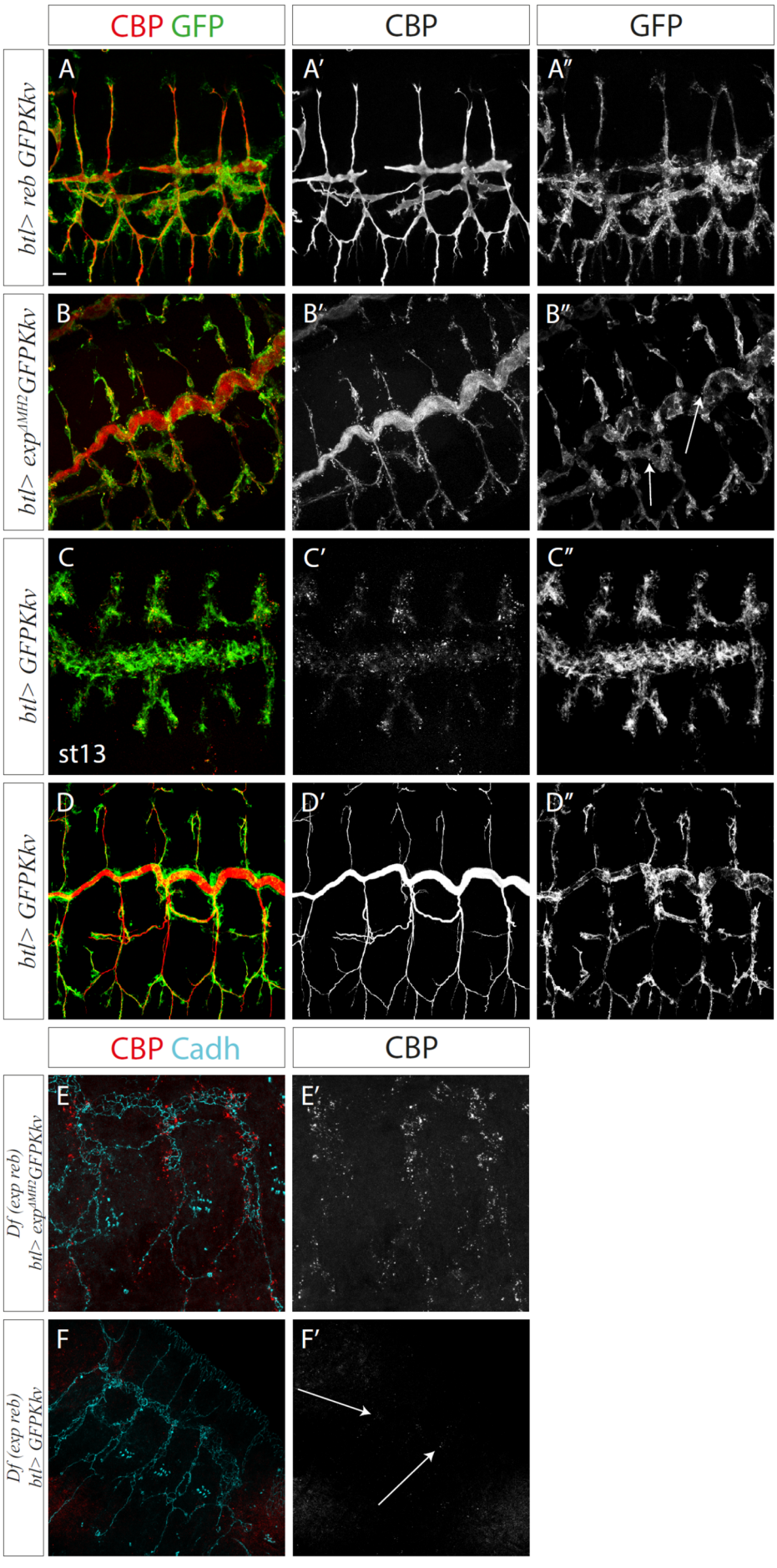
CBP GFP
CBP
GFP
btl> reb GFPKkv
A
A′
A″
btl> exp^ΔMH2 GFPKkv
B
B′
B″
btl> GFPKkv
C
C′
C″
st13
btl> GFPKkv
D
D′
D″
CBP Cadh
CBP
Df (exp reb)
btl> exp^ΔMH2 GFPKkv
E
E′
Df (exp reb)
btl> GFPKkv
F
F′

Fig. 14. Analysis of the co-expression of Exp$^{\Delta MH2}$ and Kkv in trachea; comparison with the overexpression of Kkv alone. Lateral views of the embryos at stage 15, otherwise indicated differently, stained for GFP to reveal Kkv accumulation (green, grey) in A-D, CBP to detect chitin (red, grey) and E-Cadherin to visualise the apical domain of cells (cyan, grey) in E-F**.** (**A**) The simultaneous overexpression of Reb and GFPKkv in the trachea produces branches that are straighter than the control (**Fig. 3 A**) and the dorsal trunk appears discontinuous. (**B**) The simultaneous overexpression of Exp$^{\Delta MH2}$ and GFPKkv in wildtype embryo does not affect chitin deposition in the lumen, probably due to the presence of endogenous Exp and Reb, and it leads to the presence of intracellular chitin particles and GFPKkv vesicles; arrows indicate GFPKkv vesicles. (**C**) The overexpression of GFPKkv in the trachea of an embryo at early stage leads to presence of intracellular chitin and GFPKkv vesicles. (**D**) The overexpression of GFPKkv in the trachea of an embryo at late stage produces no detectable effects. (**E**) The simultaneous overexpression of Exp$^{\Delta MH2}$ and GFPKkv in an embryo deficient for *exp* and *reb* results in no chitin deposition in the lumen, and instead intracellular particles of chitin are present. (**F**) The overexpression of GFPKkv in the trachea of an embryo deficient for *exp* and *reb* leads to chitin absence in the lumen of the trachea, but intracellular particles of chitin are present; arrows indicate chitin particles. Scale bar 10µm.

We intended to confirm these observations in the salivary glands. As already described above, the simultaneous mis-expression of Kkv and Exp or Reb in this tissue led to ectopic chitin deposition in the lumen (**Fig. 15 A, A'**). Instead, the co-expression of Kkv and Exp$^{\Delta MH2}$ or Reb$^{\Delta MH2}$ in salivary gland resulted in the accumulation of many intracellular chitin particles, but no extracellular chitin deposition (**Fig. 15 B, B'**); we detected Kkv vesicles too (**Fig. 15 B, B''**). Again, the presence of intracellular chitin particles was increased compared to the overexpression of Kkv alone (**Fig. 15 C, C'**). The results confirmed that the Nα-MH2 domain is not required for chitin synthesis, but it is necessary for chitin deposition to the extracellular compartment. Furthermore, the results further indicated that the presence of Exp or Reb promotes Kkv-dependent chitin synthesis.

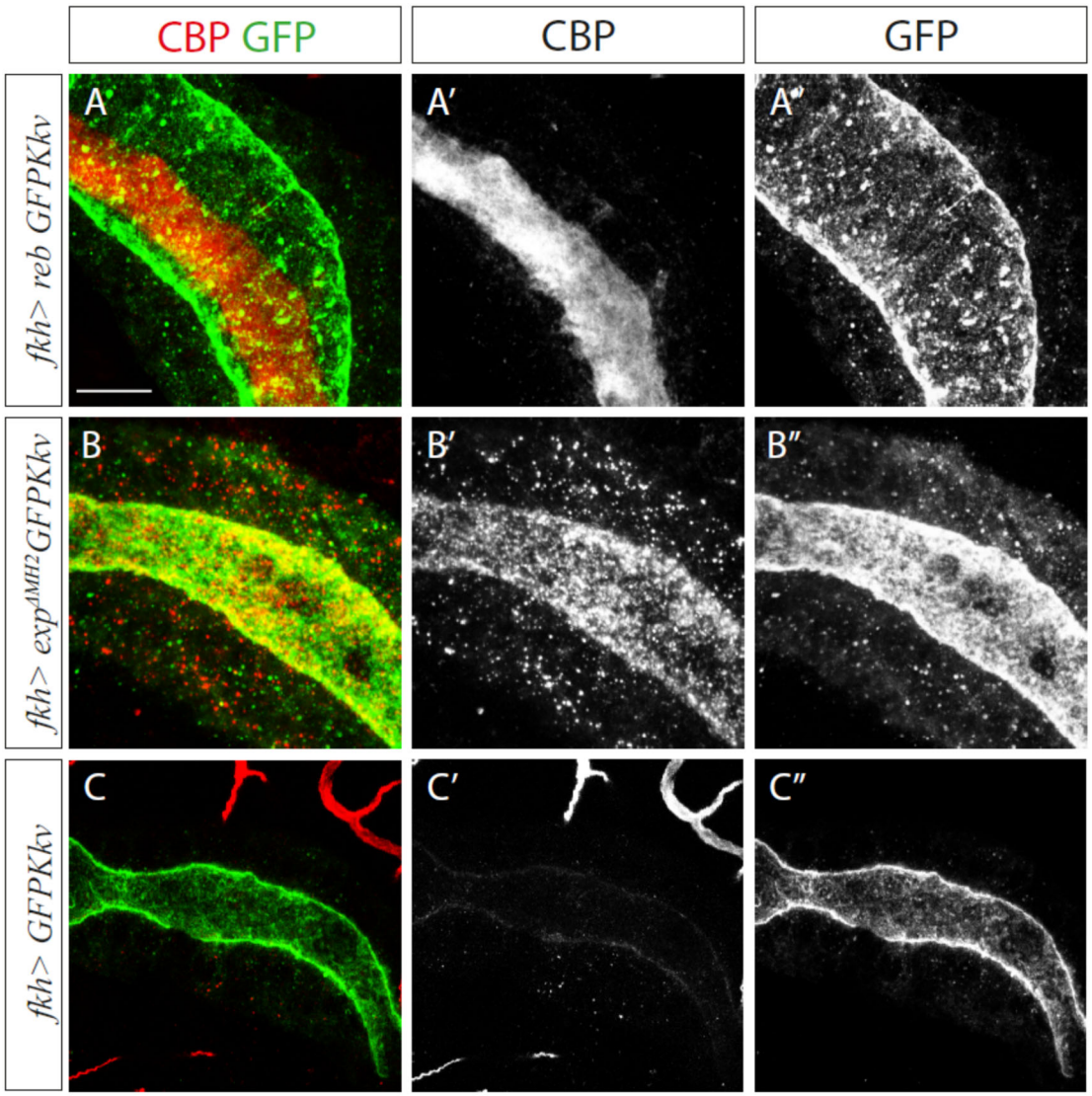

Fig. 15. Analysis of the concomitant misexpression of Exp$^{\Delta MH2}$ and Kkv in embryonic salivary gland. Lateral views of the embryos at stage 15, stained for GFP to reveal Kkv accumulation (green, grey) and CBP to detect chitin (red, grey). (**A-A''**) The simultaneous overexpression of Reb and GFPKkv in salivary gland leads ectopic chitin deposition inside the lumen. (**B-B''**) The simultaneous overexpression of Exp$^{\Delta MH2}$ and GFPKkv in salivary gland produces intracellular chitin punctae and GFPKkv vesicles. (**C-C''**) The overexpression of GFPKkv alone in salivary gland produces few intracellular chitin particles and GFPKkv vesicles. Scale bar 10µm.

To further investigate the role of the Nα-MH2 domain in chitin deposition, we asked if it is important for the localisation of Exp and Reb or if it affects the localisation of Kkv. To analyse the localisation of Exp and Reb, we used two antibodies raised in our laboratory few years ago (Moussian *et al.*, 2015). The full endogenous Exp and Reb proteins localise

mainly apically at the membrane (**Fig. 16 A**), although a bit of the protein can be detected intracellularly. Our antibodies could recognise $Exp^{\Delta MH2}$ and $Reb^{\Delta MH2}$ and it was clear that the absence of the Nα-MH2 domain did not compromise the normal pattern and also in this case the proteins localised mainly apically (**Fig. 16 B**). To investigate the localisation of Kkv, we generated an antibody against Kkv. We found that this antibody recognised endogenous Kkv protein, as in Kkv mutants no signal was detected, validating our antibody. As expected, Kkv protein localised at the apical membrane of tracheal cells in a wild type embryo (**Fig. 16 C**). In addition, we detected protein accumulation in the apical domain of salivary gland cells (**Fig. 16 E-E'**). The overexpression of $UASExp^{\Delta MH2}$ in the trachea did not detectably affect Kkv localisation, as we could still observe Kkv at the apical membrane of tracheal cells (**Fig. 16 D**). These results suggest that Nα-MH2 domain is dispensable for Exp/Reb localisation and for Kkv localisation.

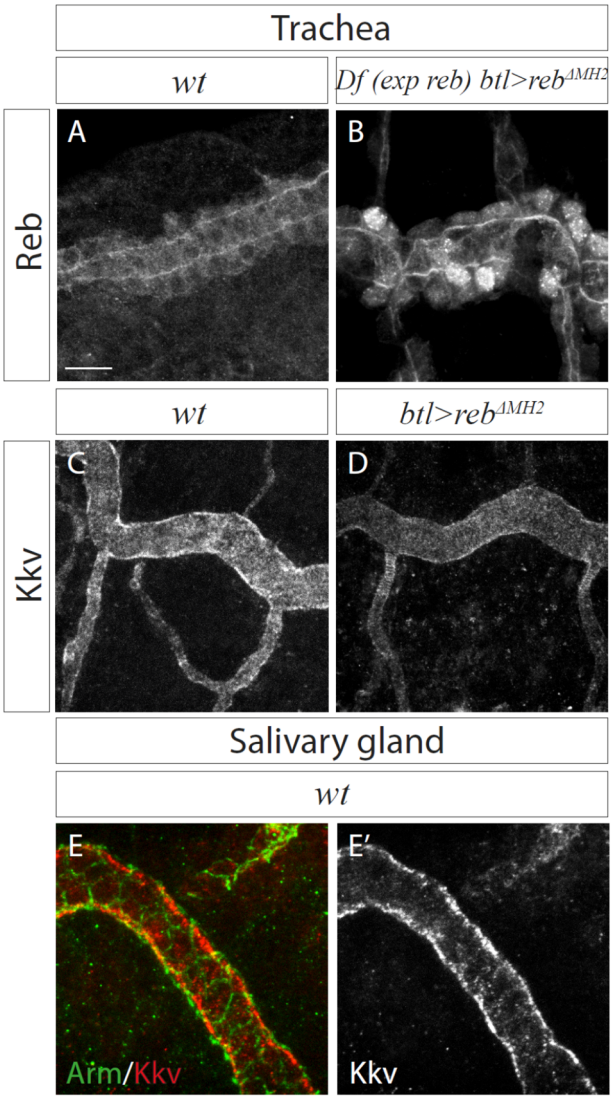

Fig. 16. Analysis of Exp and Reb localisation. Lateral views of the embryos at stage 15, stained for Exp (grey in A, B), Kkv (grey in C, D, E'; red in E) and Armadillo to visualise the apical membrane of the cells (green in E). (**A**) In a wildtype embryo, Reb accumulates mainly at the apical membranes. (**B**) The overexpression of $Reb^{\Delta MH2}$ in an embryo deficient for exp/reb appears mainly apical. (**C**) In a wildtype embryo, Kkv accumulates at the apical membranes. (**D**) When $UASReb^{\Delta MH2}$ is overexpressed, Kkv still localises at the apical membranes. (**E-E'**) Kkv localises apically in salivary glands. Scale bar 10µm.

4.1.2 Analysis of Nα-MH2 domain alone

The inability of $Exp^{\Delta MH2}$ and $Reb^{\Delta MH2}$ proteins to allow chitin deposition indicated an essential role of this domain. We asked whether in addition to being required, the Nα-MH2 domain was sufficient to provide the function of Exp/Reb. Hence, we generated new UAS constructs with only the Nα-MH2 domain of Exp and of Reb (MH2-Exp and MH2-Reb). Also in this case, the results obtained with each construct were comparable. As already described in the previous paragraph, the overexpression of a wildtype form of Exp or Reb proteins in the trachea led to an excessive and advanced chitin deposition (**Fig. 17 B**). Instead, the overexpression of UASMH2-Exp in a wildtype background did not produce any clear effect (**Fig. 17 C**) and the phenotype was comparable to the one of a wildtype embryo (**Fig. 17 A**). In addition, we tested if these constructs were able to rescue the absence of chitin produced by a deficiency uncovering both *exp* and *reb*, as a UAS-Exp or -Reb wildtype does (**Fig. 17 D**) (Moussian *et al.*, 2015), but chitin was not deposited (**Fig. 17 E**). Therefore, the results indicated that the MH2 domain alone is not able to deposit chitin. We asked whether MH2-Exp and $Exp^{\Delta MH2}$ would complement each other, and we co-expressed these Exp mutant proteins in an *exp*/*reb* deficient background. We found no rescue of chitin deposition (**Fig. 17 F**).

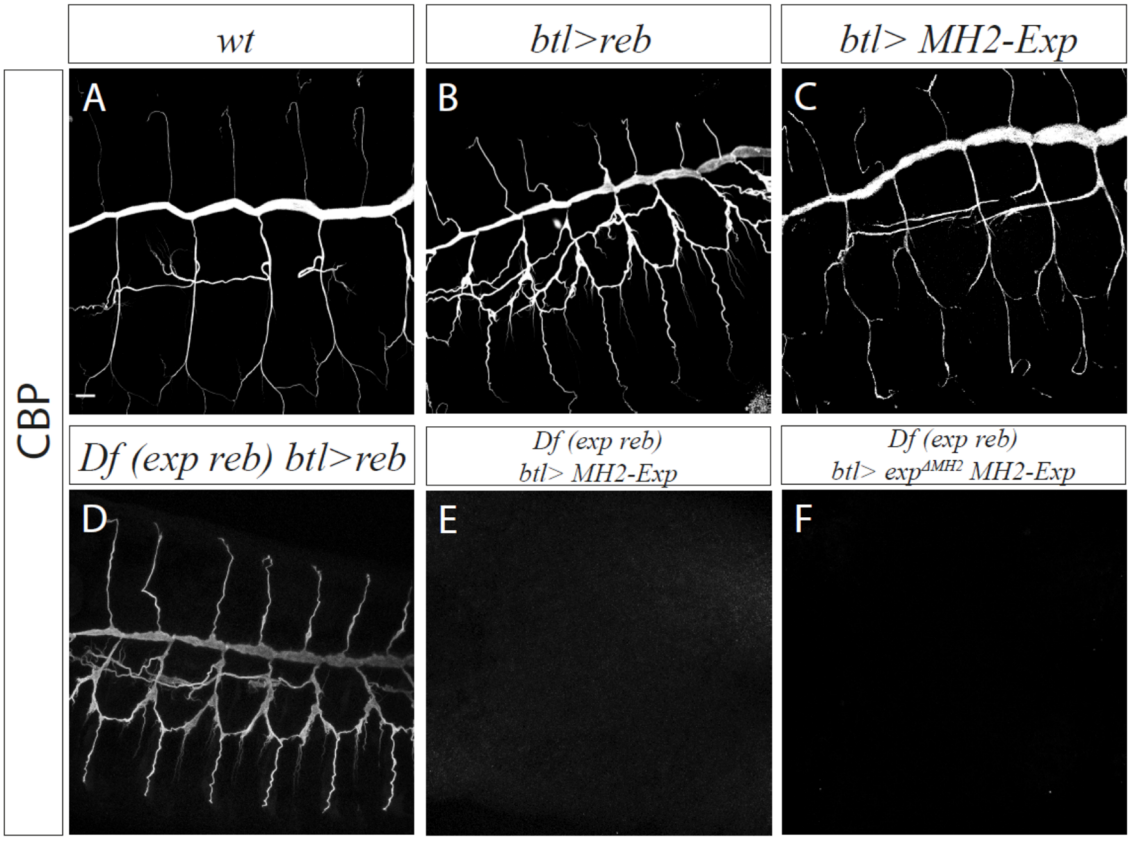

Fig. 17. Analysis of the overexpression of MH2-Exp in trachea. Lateral views of the embryos at stage 15 stained for CBP to detect chitin (grey). (**A**) Control embryo. (**B**) Overexpression of wildtype form of Reb; note that the branches are straighter than the control. (**C**) The overexpression of MH2-Exp is comparable to the control. (**D**) The overexpression of a wildtype form of Reb in a deficient background for *exp* and *reb* rescues the absence of chitin. (**E**) The overexpression of MH2-Exp in a deficient background for *exp* and *reb* does not rescue the lack of chitin. (**F**) The co-expression of $Exp^{\Delta MH2}$ and MH2-Exp in a deficient *exp*/*reb* background does not permit chitin deposition in the lumen. Scale bar 10µm.

Furthermore, we decided to co-express simultaneously Kkv and MH2-Exp or MH2-Reb. Surprisingly, also in this case we obtained intracellular Kkv and chitin vesicles in the trachea of early embryo when Exp/Reb are not yet functional (**Fig. 18 A**), at later stages when Exp/Reb are functional (**Fig. 18 B**), in salivary glands (**Fig. 18 C**) and in embryos deficient for *exp*/*reb* (**Fig. 18 D**). These results indicated that Nα-MH2 domain is able to promote chitin synthesis, but it is unable to deposit chitin.

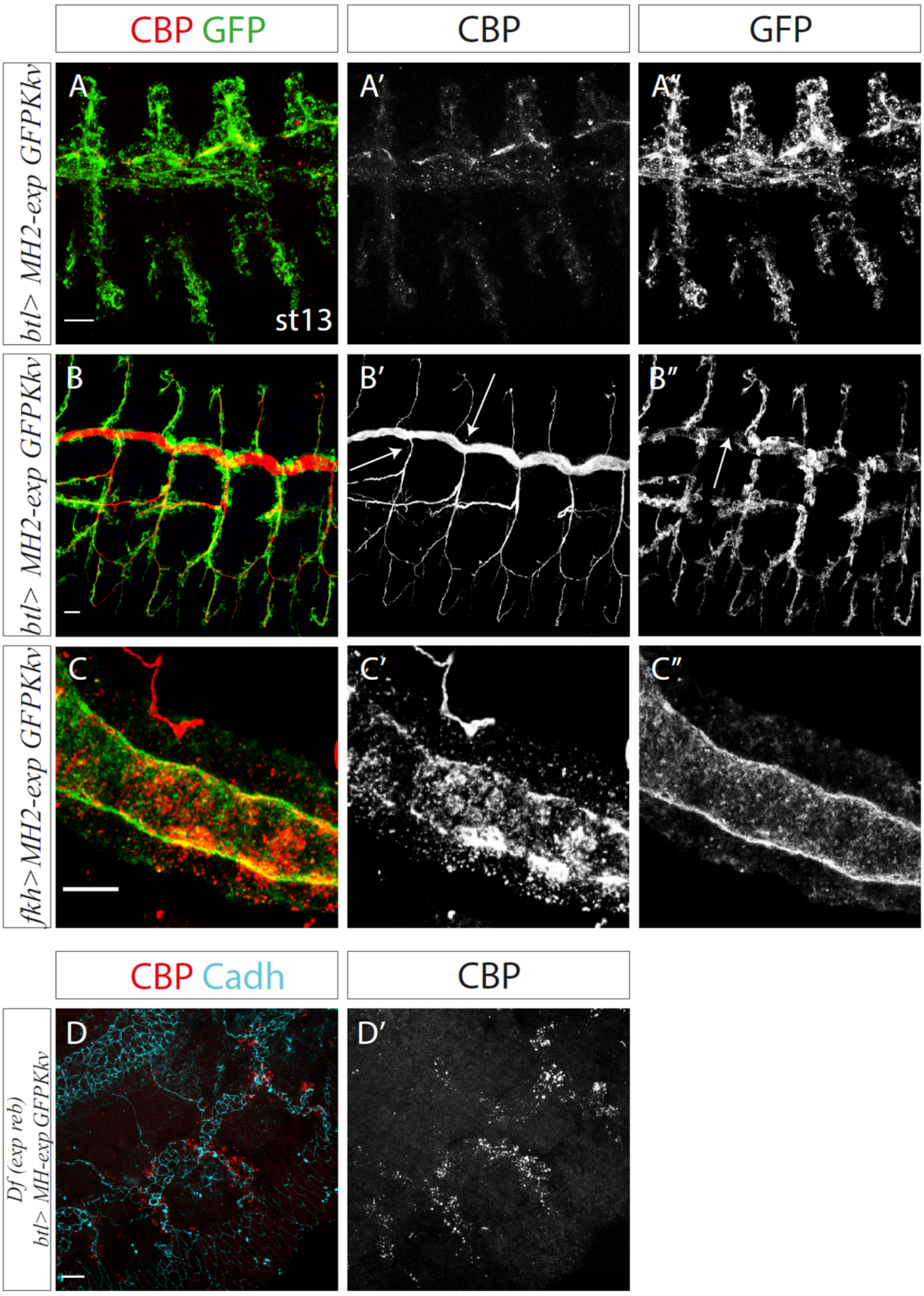
CBP GFP
CBP
GFP
btl> MH2-exp GFPKkv
A
A′
A″
st13
B
B′
B″
fkh>MH2-exp GFPKkv
C
C′
C″
CBP Cadh
CBP
Df (exp reb)
btl> MH-exp GFPKkv
D
D′

Fig. 18. Analysis of the simultaneous expression of Kkv and MH2-Exp. Lateral views of the embryos stained for GFP to reveal Kkv accumulation (green, grey) in A-C, CBP to detect chitin (red, grey) in A-D and Cadherin to visualise the apical domain of cells (cyan) in D**.** (**A**) During the co-expression of GFPKkv and MH2-Exp in an embryo at stage 13, chitin deposition starts in the Dorsal Trunk because Reb here begins to be functional, although many intracellular chitin and GFPKkv vesicles are present. (**B**) During the co-expression at stage 15, chitin is deposited in the lumen due to the presence of endogenous Exp/Reb proteins, and few chitin and GFPKkv vesicles are still detectable (arrows). (**C**) No luminal chitin is deposit in the co-expression of GFPKkv and MH2-Exp in salivary gland but there is a strong presence of intracellular chitin and GFPKkv vesicles. (**D**) During the co-expression in stage 15 embryos deficient for *exp*/*reb*, chitin deposition does not occur, while several intracellular chitin particles are visible. Scale bar 10µm.

Finally, we asked if the Nα-MH2 domain was able to localise apically like Exp/Reb proteins do and if it is important for the localisation of Kkv. The full endogenous Exp and Reb proteins localise mainly apically at the membrane (**Fig. 19A**), although a bit of the protein can be detected intracellularly. Our antibodies could recognise the Nα-MH2 domain but the mutant protein was not able to localise apically (**Fig. 19 B**). The overexpression of UAS-Nα-MH2 in the trachea did not detectably affect Kkv localisation, as we could still observe Kkv at the apical membrane of tracheal cells (**Fig. 19 D**). These results suggest that Nα-MH2 domain is not able to localise apically and it does not affect Kkv localisation.

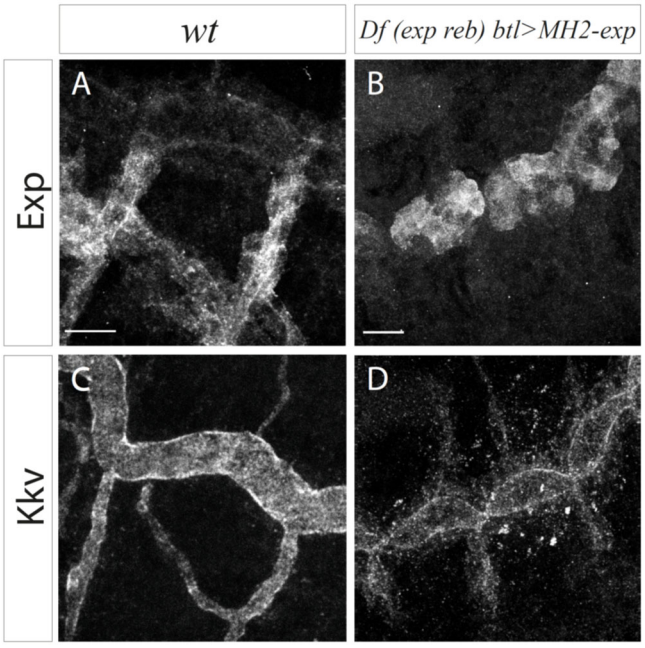

Fig. 19. Analysis of Nα-MH2 localisation. Lateral views of the embryos at stage 15, stained for (A, B) Exp in grey and (C, D) Kkv in grey. (**A**) In a wildtype embryo, Exp accumulates mainly at the apical membranes. (**B**) In an embryo deficient for *exp/reb*, Nα-MH2 is not able to localise apically. (**C**) In a wildtype embryo, Kkv accumulates at the apical membranes. (**D**) When Nα-MH2 is overexpressed, Kkv still localises at the apical membranes. Scale bar 10µm.

4.1.3 The Conserved Motif is dispensable for chitin synthesis and deposition

We previously described in the lab that the only recognisable domain in Exp and Reb proteins is a Nα-MH2 domain (Beich-Frandsen *et al.*, 2015). To find out regions that could be important for Exp/Reb functions, we decided to look for highly conserved regions comparing the amino acids sequences of proteins homolog to Exp and Reb in other organisms (**Fig. 20**). We found a highly conserved region not yet described in literature, neither in Exp/Reb protein nor in any other protein, and we called it Conserved Motif (CM) (blue square in **Fig. 20**).

Fig. 20. Alignment of amino acids sequences of Exp/Reb and its homologs. Partial amino acids sequence of isoform B of Exp (amino acids 356-433) and its homologs; the highly conserved region is highlighted by a blue square and a red square.

Thus, to investigate the importance of this motif, we generated new transgenic flies lacking the CM, UASExp$^{\Delta CM}$. The overexpression of the new constructs produced a phenotype similar to the overexpression of the wildtype form of Exp or Reb (**Fig. 21 A**), an excessive and advanced chitin deposition (**Fig. 21 B**). This result indicated that this

mutated protein can still elicit the function of the wildtype protein. In addition, we found that $Exp^{\Delta CM}$ protein was able to rescue the lack of chitin deposition in *exp*/*reb* mutants, giving rise to a phenotype of Exp/Reb overexpression (**Fig. 21 C**). When we co-expressed $Exp^{\Delta CM}$ with Kkv in trachea, we found a strong phenotype with an excessive and advanced chitin deposition (**Fig. 21 E**) comparable to the overexpression of Kkv and Exp/Reb wildtype (**Fig. 21 D**). Similarly, expression of $Exp^{\Delta CM}$ in salivary glands produced ectopic chitin deposition in the luminal space (**Fig. 21 F-F'**). The results indicated that the $Exp^{\Delta CM}$ protein behaves as the full-length Exp/Reb protein, and it is able to deposit chitin extracellularly. Hence, the Conserved Motif is not required for Exp activity, although it is highly conserved throughout evolution. Finally, we asked if the CM was able to localise apically like Exp/Reb proteins do. The full endogenous Exp and Reb proteins localise mainly apically at the membrane (**Fig. 21 G**), although a bit of the protein can be detected intracellularly. Instead, most of $Exp^{\Delta CM}$ protein is detected intracellularly, although a bit of the protein localises at the apical membrane (**Fig. 21 H**). These results suggest that the CM is involved in Exp/Reb localisation.

Fig. 21. Analysis of the overexpression of $Exp^{\Delta CM}$. Lateral views of the embryos at stage 15 stained for CBP to visualise chitin deposition (grey in A-E and F', red in F), Armadillo to visualise the apical membrane of the cells (green in F) and Exp (grey in G-H). (**A**) During the overexpression of wildtype form of Reb in trachea, advanced and excessive luminal chitin deposition is detected. (**B**) The expression of $Exp^{\Delta CM}$ does not produce any clear defect, so the phenotype is similar to the overexpression of Exp/Reb wildtype. (**C**) The overexpression of $Exp^{\Delta CM}$ in the trachea of a deficient embryo for *exp*/*reb* rescues the lack of chitin deposition, additionally it produces an Exp/Reb overexpression effect. (**D**) The simultaneous overexpression of Reb and GFPKkv in the trachea produces branches that are straighter than the control and the dorsal trunk appears discontinuous. (**E**) The co-expression of $Exp^{\Delta CM}$ and GFPKkv in the trachea of a wildtype embryo is analogous to the overexpression of Exp/Reb wildtype and Kkv; arrows indicate chitin discontinuity. (**F-F'**) During the overexpression of $Exp^{\Delta CM}$ in salivary gland, luminal chitin deposition is detected. (**G**) In a wildtype embryo, Exp accumulates mainly at the apical membranes. (**H**) $Exp^{\Delta CM}$ localises mainly intracellularly but a bit of the protein can be detected at the apical membrane; arrow indicates apical accumulation. Scale bar 10µm.

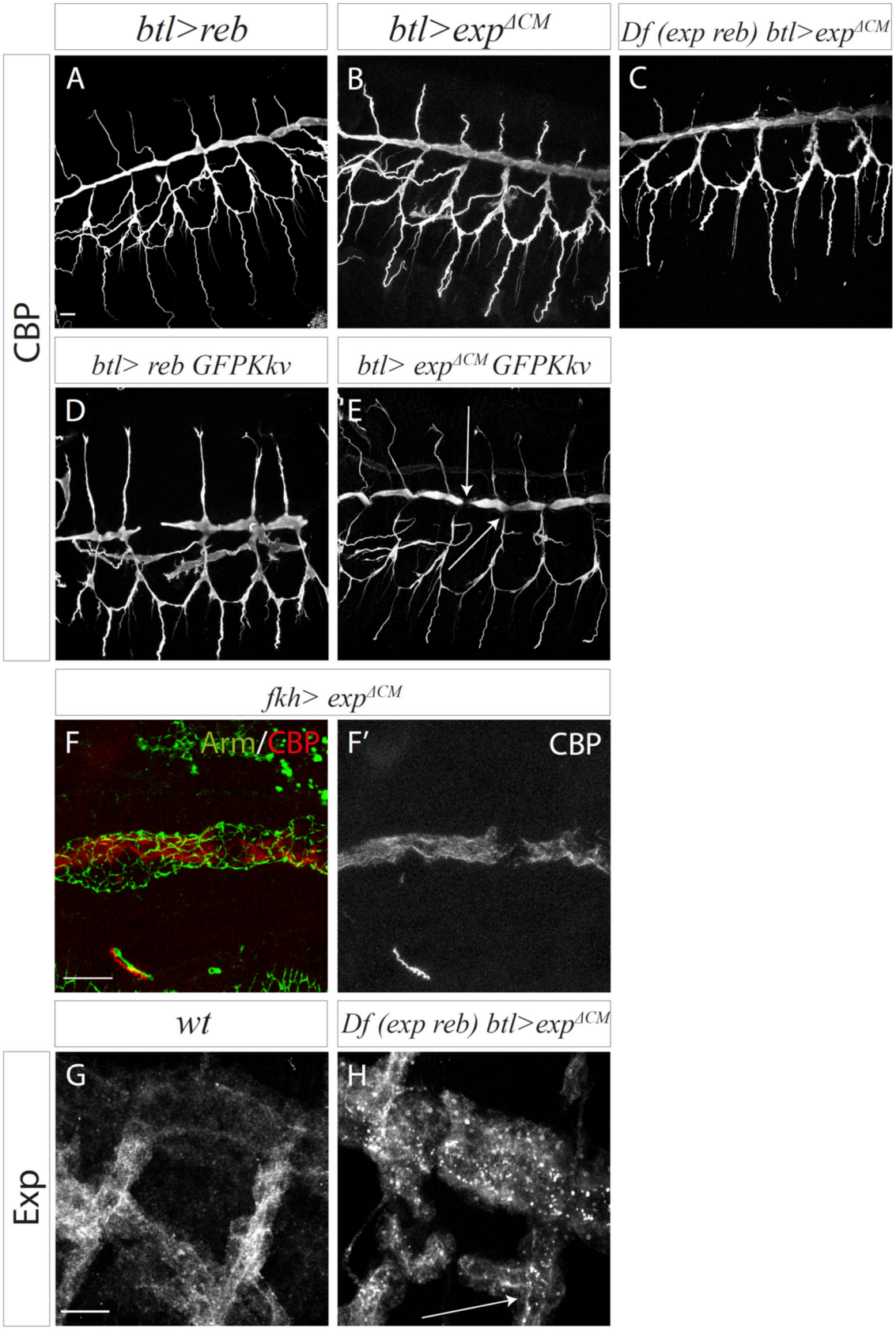
btl>reb
btl>exp^ΔCM
Df (exp reb) btl>exp^ΔCM
CBP
A
B
C
btl> reb GFPKkv
btl> exp^ΔCM GFPKkv
D
E
fkh> exp^ΔCM
F
Arm/CBP
F'
CBP
wt
Df (exp reb) btl>exp^ΔCM
Exp
G
H

After these results, and because we were surprised that the CM did not show any effect, we decided to consider as Conserved Motif a bigger region (red square in **Fig. 20**). Actually, we observed that the nine amino acids following the initial CM are still highly conserved through evolution (**Fig. 20**). Thus, we generated transgenic flies without the longer sequence of Conserved Motif and we repeated the same experiments. Unfortunately, the results were similar to the previous ones and we could confirm that the Conserved Motif is not required for the function of Exp/Reb in chitin synthesis and deposition.

4.1.4 Biological nature of Kkv vesicles and chitin punctae

As already shown, when we overexpress Kkv alone (**Fig. 14 C, D, F** and **Fig. 15 C**) and when we simultaneously overexpress it with $Exp^{\Delta MH2}$/$Reb^{\Delta MH2}$ (**Fig. 14 B, E** and **Fig. 15 B**) or Nα-MH2-Exp/-Reb (**Fig. 18 A-D**), we found a particular phenotype: the presence of intracellular vesicles of Kkv and intracellular punctae of chitin. We speculated that this phenotype could be reflecting the endogenous pathway of Kkv and chitin synthesis; as we were saturating the chitin synthesis machinery and preventing its extracellular deposition, we were detecting the presence of intracellular chitin punctae. We thought about two different conditions in which chitin punctae could be generated: in the first one, chitin is synthesised in Kkv vesicles while it is secreted; in the second one, chitin is synthesised at the membrane level but it is internalised instead of being deposited in the lumen.

Hence, we analysed the biological nature of the vesicles to validate any of these two possibilities. We overexpressed Kkv and $Exp^{\Delta MH2}$ in the salivary gland and we stained the embryos for markers for different intracellular compartments. We chose the salivary glands because the presence of vesicles was more conspicuous as compared to the trachea. We observed that, in most of the cases, KkvGFP and chitin did not colocalise; only few vesicles presented both.

We first analysed the exocytic pathway. We found colocalisation between Kkv vesicles and markers for Golgi rims (Golgin84, **Fig. 22 A-A''**) and for Trans-Golgi Network (Golgin245, **Fig. 22 B-B''**).

We then analysed the endocytic pathway. We found a clear colocalisation of KkvGFP with Hrs, a marker for maturing endosomes (**Fig. 22 C-C''**). We also detected a high colocalisation with Rab7 (**Fig. 22 D-D''**). These results suggested that most Kkv vesicles are the product of endocytosis. To understand whether Kkv was then following the degradation pathway or was recycled back to the membrane we used lysosomal markers and markers for vesicle recycling. We found no colocalisation with the lysosomal marker Arl8. In contrast, we found some colocalisation with Rab11, a marker for recycling (**Fig. 22 E-E''**). In contrast to these results for KkvGFP, we could not find clear colocalisation of chitin and any of these markers. Occasionally, we found colocalisation of chitin with Hrs and KkvGFP (**Fig. 22 C-C'''**). These results suggested that Kkv, or Kkv complex, is formed at the level of Golgi rims and Trans-Golgi Network and then is translocated to the membrane. Then, Kkv is endocytosed but it is recycled rather than degraded.

Chitin is more uncertain. Unfortunately, we have not been able so far to determine whether the intracellular punctae of chitin correspond to vesicles or correspond to short chitin microfibers floating in the cytoplasm.

Fig. 22. Biological nature of Kkv vesicles and chitin particles. Lateral views of the embryos at stage 15 overexpressing GFPKkv and $Exp^{\Delta MH2}$ in salivary gland, all the embryos are stained with GFP to visualise KKv (green and grey) and a marker for intracellular trafficking (red and grey); in C, embryo is also stained with CBP to detect chitin (in blue and in grey); arrows indicate colocalisation. (**A-A''**) Embryo stained for Golgin84 (Golgi rims). (**B-B''**) Embryo stained for Golgin245 (Trans Golgi Network). (**C-C'''**) Embryo stained for Hrs (maturing endosome). (**D-D''**) Embryo stained for Rab7 (maturing endosome). (**E-E''**) Embryo stained for Rab11 (recycling). Scale bar 10µm.

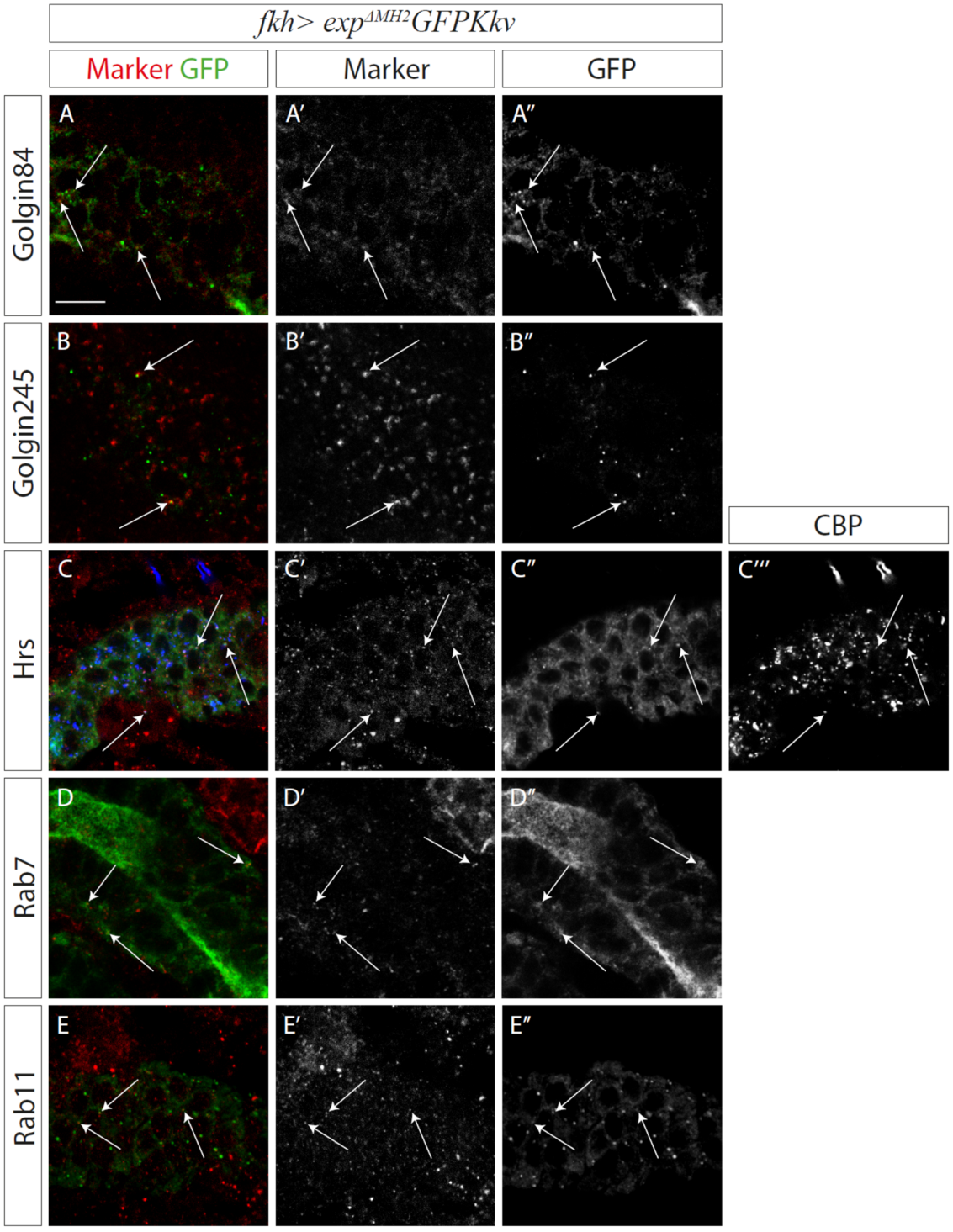

To further understand the process of chitin deposition, we performed live imaging using a live-probe for chitin and KkvGFP. The results indicated that KkvGFP and chitin vesicles did not colocalise perfectly and in most of the cases the two types of punctae where next to each other (**Fig. 23 A-A'', B-B''**). In few cases we found that the KkvGFP and chitin were separating from each other (**Fig. 23 A'', B''**). and we found some cases

of vesicles with only KkvGFP (**Fig. 23 A'**) or chitin signal (**Fig. 23 A**). More improvement in time and space of the live imaging are necessary to better understand the dynamics between KkvGFP vesicles and chitin.

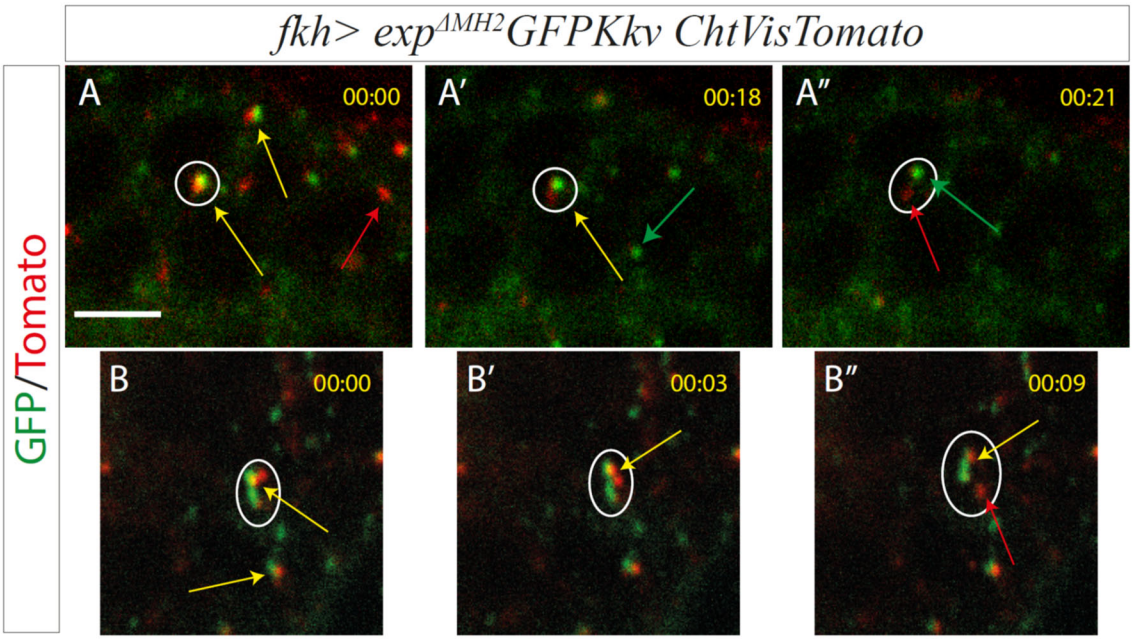

Fig. 23. Live imaging of Kkv vesicles and chitin particles. Lateral views of the embryos at stage 15 overexpressing GFPKkv, ChtVisTomato and Exp$^{\Delta MH2}$ in salivary gland, GFP marks Kkv (green) and Tomato marks chitin (red). Each panel shows a time-laps image of **movie 1** (**A-A''**) and **movie 2** (**B-B''**), time format mm:ss. The ellipses highlight couples of KkvGFP vesicles and chitin that separate from each other. Yellow arrows indicate partial colocalisation between KkvGFP and chitin, green arrows indicate KkvGFP vesicles and red arrows indicate chitin punctae. Scale bar 5µm.

4.2 Analysis of Expansion, Rebuf and Kkv: a biochemical approach

With the results obtained, we found no evidence of a direct or indirect physical interaction between Exp/Reb and Kkv. Thus, we decided to use a biochemical approach to better investigate a possible interaction between these proteins. First, we tested if the new antibody raised against Kkv was able to recognise the protein in a western blot analysis. We detected a band with the expected weight (182kDa) in a total protein extract of control

embryos (**Fig. 24 A**) and in an extract using a more stringent lysis buffer (**Fig. 24 C**); the band was absent in a protein extract of embryos mutant for *kkv* (**Fig. 24 B**). In an immunoprecipitation experiment, Kkv antibody was able to immunoprecipitate Kkv protein (**Fig. 24 E**), it did not happen with a control immunoprecipitation (**Fig. 24 D**); hence, the antibody is suitable for biochemical experiments. Unfortunately, we did not obtained clear results when we performed these same experiments with the Exp antibody; we did not visualise a band of the expected molecular weight and it is necessary to characterise better Exp antibody (for example using embryos deficient for *exp* or using different lysis buffer).

In a protein extract from control embryos, Reb antibody was able to recognise a band with the molecular weight of Reb (48 kDa) (**Fig. 24 F**), but Reb protein did not co-immunoprecipitate with Kkv (**Fig. 24 H**). Hence, with this experiment we cannot say if there is a physical interaction between Kkv and Reb. Several aspects can interfere during a co-immunoprecipitation experiment, for instance the lysis buffer we used could disrupt a possible interaction between Reb and Kkv or another possibility is that the interaction between Reb and its respective antibody could affect the interaction between Reb and other proteins.

In any case, our biochemical approach did not support a physical interaction between Kkv and Exp or Reb, although we cannot discard this possibility.

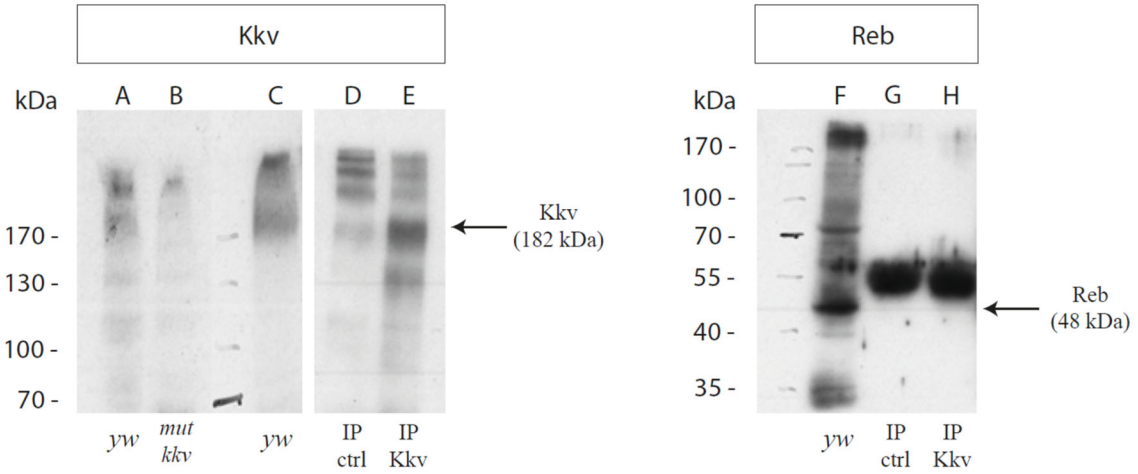

Fig. 24. Western blot, immunoprecipitation (IP) and co-immunoprecipitation (CO-IP) experiments of Kkv and Reb. (**A-E**) Membrane revealed with Kkv antibody. (**A**) Protein extract from *yw* (control) embryos. (**B**) Protein extract from *kkv* mutant embryos. (**C**) Protein extract from *yw* embryos with a more stringent buffer (RIPA buffer). (**D**) Control IP. (**E**) IP of Kkv. (**F-H**) Membrane revealed with Reb antibody. (**F**) Protein extract from *yw* embryos. (**G**) Control IP. (**H**) IP of Kkv, CO-IP of Reb.

4.3 Structure-function analysis of Kkv

To analyse the molecular and cellular mechanism of activity of Kkv protein, we decided to use a structure function approach. In particular, we were interested in domains that we speculated could have a role in a direct or indirect interaction with Exp/Reb. The candidates were the conserved motif WGTRE, with an unclear function, and a coiled-coil domain, with a putative role in protein-protein interactions.

4.3.1 The Conserved Motif WGTRE is required for Kkv localisation

The conserved motif WGTRE is an essential domain for Kkv activity: it has been described that a point mutation changing the glycine into an aspartic acid gives rise to an inactive Kkv protein (Ostrowski *et al.*, 2002). The WGTRE motif has been suggested to be involved in oligomerisation or interactions with other factors (Zhu *et al.*, 2002; Moussian *et al.*, 2005; Van Leeuwen *et al.*, 2012); thus, we wanted to test if it could be involved in interactions with Exp/Reb. We generated a protein lacking this domain, GFP-Kkv$^{\Delta WGTRE}$.

The overexpression of the mutant protein in the trachea, in an otherwise wild type background, did not produce any detectable defect in chitin deposition (**Fig. 25 A, B**). To determine the activity of this protein we assayed its rescuing capacity in a *kkv* mutant background. To test this condition, we used embryos with *kkv*^{IB22} mutation, a nonsense mutation producing a short protein lacking all Kkv domains and generating phenotypes similar to the absence of Kkv (Moussian *et al.*, 2005). A wild type form of Kkv can rescue the lack of chitin produced by this Kkv mutant form (Moussian *et al.*, 2015); instead,

GFP-Kkv$^{\Delta WGTRE}$ was not able to rescue this phenotype and trachea was defective (**Fig. 25 C**). This indicated that the protein is not functional.

The overexpression of Reb alone in trachea (**Fig. 25 D**) or in salivary gland (**Fig. 25 G, G'**) is able to produce excessive chitin due to the presence of endogenous Kkv. The phenotype is even stronger when Reb is overexpressed simultaneously with Kkv either in trachea (**Fig. 25 E**) or in salivary gland (**Fig. 25 H, H'**) (Moussian *et al.*, 2015). However, the co-expression of Reb and GFP-Kkv$^{\Delta WGTRE}$ did not increase the Reb phenotype neither in trachea (**Fig. 25 F**) nor in salivary gland (**Fig. 25 I, I'**). This result confirmed that GFP-Kkv$^{\Delta WGTRE}$ is not functional and that the WGTRE domain is essential for chitin deposition. In addition, it also shows that the domain is essential for chitin synthesis, as we found no intracellular chitin particles when we overexpressed GFP-Kkv$^{\Delta WGTRE}$.

Fig. 25. Analysis of the overexpression of GFP-Kkv$^{\Delta WGTRE}$. Lateral views of the embryos at stage 15 stained for CBP to detect chitin (grey in A-F and in G', H', I'; red in G, H, I), Reb (green in G) and GFP to detect GFP-Kkv in H and GFP-Kkv$^{\Delta WGTRE}$ in I (green). (**A**) Wild type embryo. (**B-F**) Overexpression in the trachea. (**B**) The overexpression of GFP-Kkv$^{\Delta WGTRE}$ in a wild type embryo do not affect chitin deposition. (**C**) The overexpression of GFP-Kkv$^{\Delta WGTRE}$ in an embryo mutant for *kkv* does not rescue the absence of chitin. (**D**) The overexpression of Reb in a wild type embryo leads to an excessive and advanced chitin deposition. (**E**) The co-expression of Reb and GFP-Kkv in a wild type embryo in the trachea produces a stronger phenotype than the overexpression of Reb alone and the dorsal trunk appears discontinuous. (**F**) The co-expression of Reb and GFP-Kkv$^{\Delta WGTRE}$ in a wild type embryo produces a similar phenotype to the Reb overexpression. (**G-I**) Overexpression in salivary gland. (**G-G'**) The overexpression of Reb produces mild chitin deposition. (**H-H'**) The concomitant overexpression of Reb and GFPKkv produces strong chitin deposition. (**I-I'**) The concomitant overexpression of Reb and GFP-Kkv$^{\Delta WGTRE}$ produces mild chitin deposition, it is comparable to the overexpression of Reb alone. Scale bar 10µm.

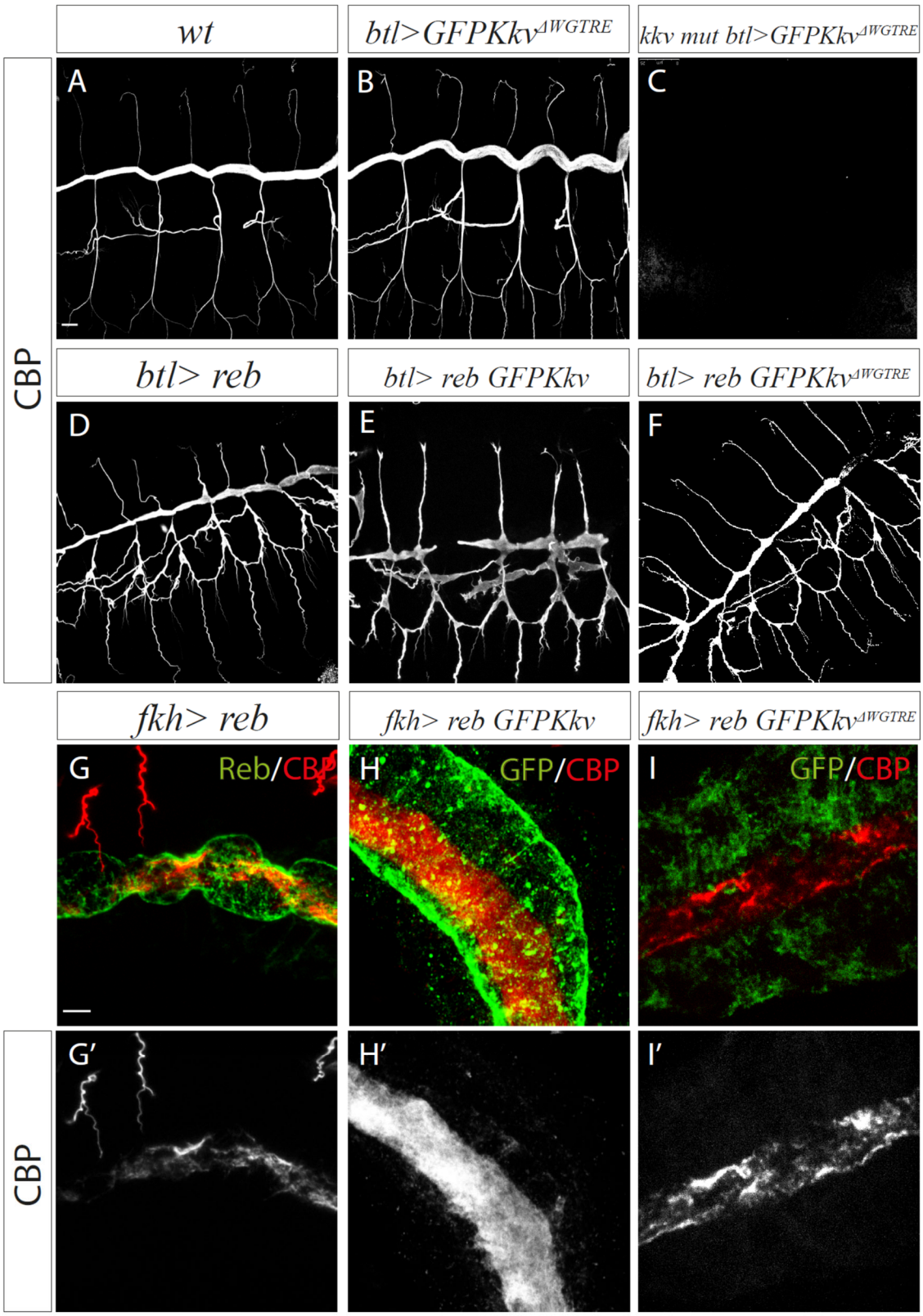

To understand the role of this domain we analysed the localisation of the GFP-Kkv$^{\Delta WGTRE}$ protein. In a wild type situation, endogenous Kkv localises apically at the membrane (**Fig. 26 A**). Instead, we found no apical accumulation of GFP-Kkv$^{\Delta WGTRE}$ protein, neither in a wild type background (**Fig. 26 B**) nor in a *kkv* mutant background (**Fig. 26 C**). We found

a generalised pattern in the cytoplasm excluding the nucleus. Hence, we co-stained with different markers to determine the localisation. Interestingly, we found that GFP-Kkv$^{\Delta WGTRE}$ largely co-localised with KDEL, a marker of the Endoplasmic Reticulum (ER) (**Fig. 26 D-D''**). The results indicated that GFP-Kkv$^{\Delta WGTRE}$ is retained in the ER.

ER retention maybe due either to a defective folding of the protein or to a specific effect of this domain in Kkv trafficking to the membrane. Proteins with a defective folding can be degraded from ER upon ubiquitination (Tsai and Weissman, 2010). To distinguish between these two possibilities, we used the FK2 antibody that recognises mono- and polyubiquitinated conjugates, but not free ubiquitin (Fujimuro, *et al.*, 1994). We found no colocalisation between GFP-Kkv$^{\Delta WGTRE}$ and FK2 (**Fig. 26 E-E''**), indicating that the protein is not ubiquinated. The results strongly suggest a role for the WGTRE domain in Kkv trafficking.

Fig. 26. GFP-Kkv$^{\Delta WGTRE}$ localisation and ER retention. Lateral views of the embryos at stage 15. (**A**) Wild type embryo stained with Kkv (grey) shows apical localisation for Kkv protein. (**B**) The overexpression of GFP-Kkv$^{\Delta WGTRE}$ in a wild type background stained with GFP to visualise GFP-Kkv$^{\Delta WGTRE}$ (grey) shows that the mutant protein does not localise apically. (**C**) The overexpression of GFP-Kkv$^{\Delta WGTRE}$ in a mutant background for *kkv*, stained with GFP to visualise GFP-Kkv$^{\Delta WGTRE}$ (grey), shows that the mutant protein does not localise apically. (**D-D''**) The overexpression of GFP-Kkv$^{\Delta WGTRE}$ in a wild type background stained with KDEL, to visualize ER compartment (red in D, grey in D'), and GFP, to visualise GFP-Kkv$^{\Delta WGTRE}$ (green in D, grey in D''), shows that there is colocalisation. (**E-E''**) The overexpression of GFP-Kkv$^{\Delta WGTRE}$ in a wild type background stained with FK2 that recognises mono- and poliubiquinated conjugates (red in E, grey in E') and GFP to visualise GFP-Kkv$^{\Delta WGTRE}$ (green in E, grey in E''), shows that there is no colocalisation. Scale bar 10µm.

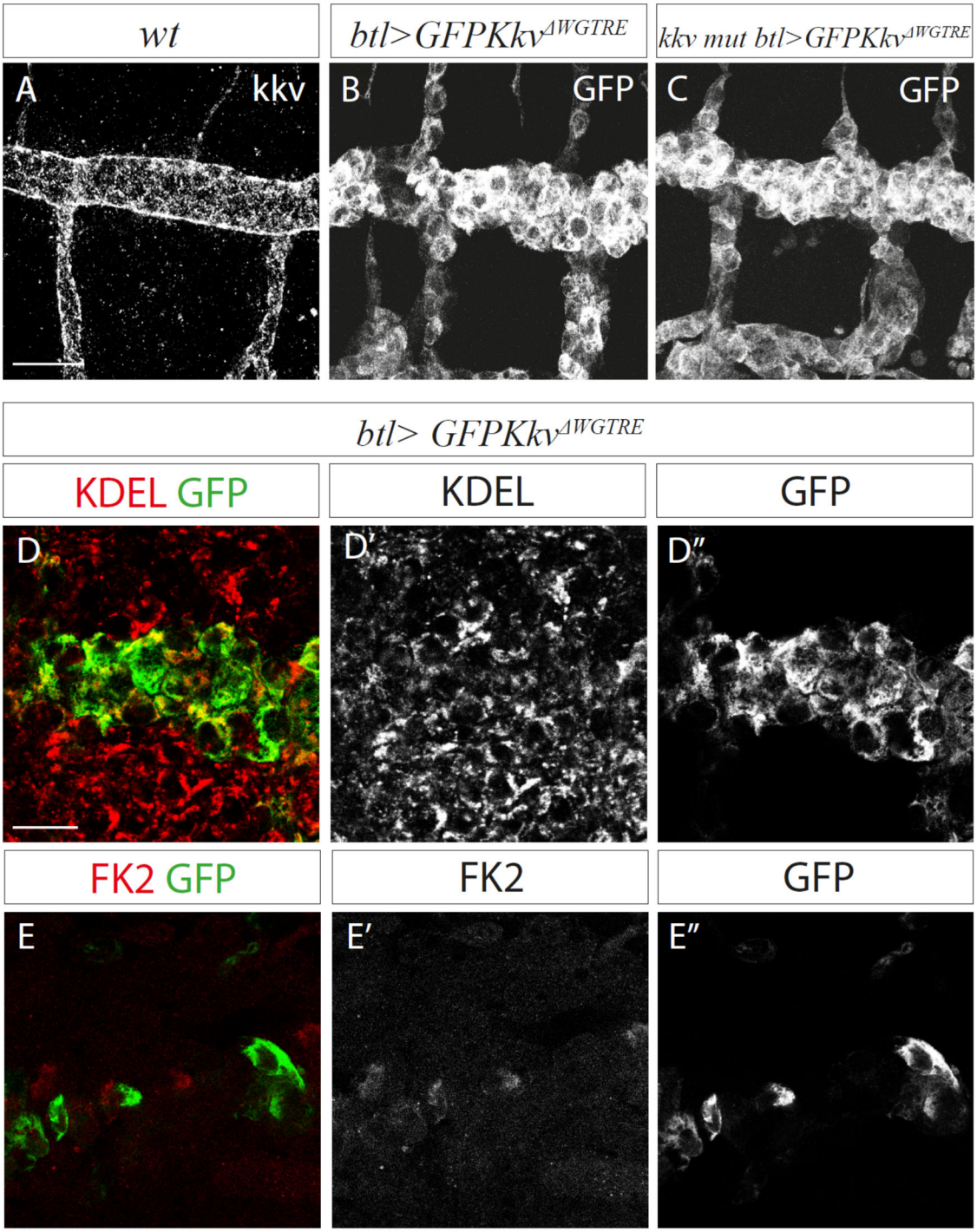

4.3.2 The SWG motif of Kkv is not a target of EH-domain containing proteins

The results suggested a specific role of the WGTRE motif in Kkv trafficking. An amino acids sequence alignment among proteins homolog to Kkv in different species allowed us to identify that an S residue before the WGTRE motif was highly conserved and that, actually, the most conserved region was a SWG motif. This motif can be a target for EH

(Eps15 Homology) domain containing proteins (Paoluzi *et al.*, 1998). The EH domain is a protein-protein interaction module of approximately 100 residues; it was found in several proteins implicated in endocytosis, vesicle transport and signal transduction. EH domains have been shown to bind specifically but with moderate affinity to peptide containing short, unmodified motifs through predominantly hydrophobic interactions. One of the target motifs comprises the class II, including the SWG motif (Santolini *et al.*, 1999; Bhattacharyya and Pucadyil, 2020). In *Drosophila melanogaster*, only four proteins are known to contain an EH domain: Dap160, Reps, Eps15 and Past1. We decided to test whether in conditions for downregulation of each of them, by RNA interference, we could detect any effect in the pattern of chitin or Kkv accumulation. We observed no effect neither in chitin deposition nor in Kkv localisation. Our analysis of downregulation of the known EH-domain containing proteins did not suggest that the SWG motif of Kkv is a target of these proteins (**Fig. 27**). However, null conditions for these proteins (including null maternal contributions) and analysis of redundancy between them should be performed to confirm this suggestion.

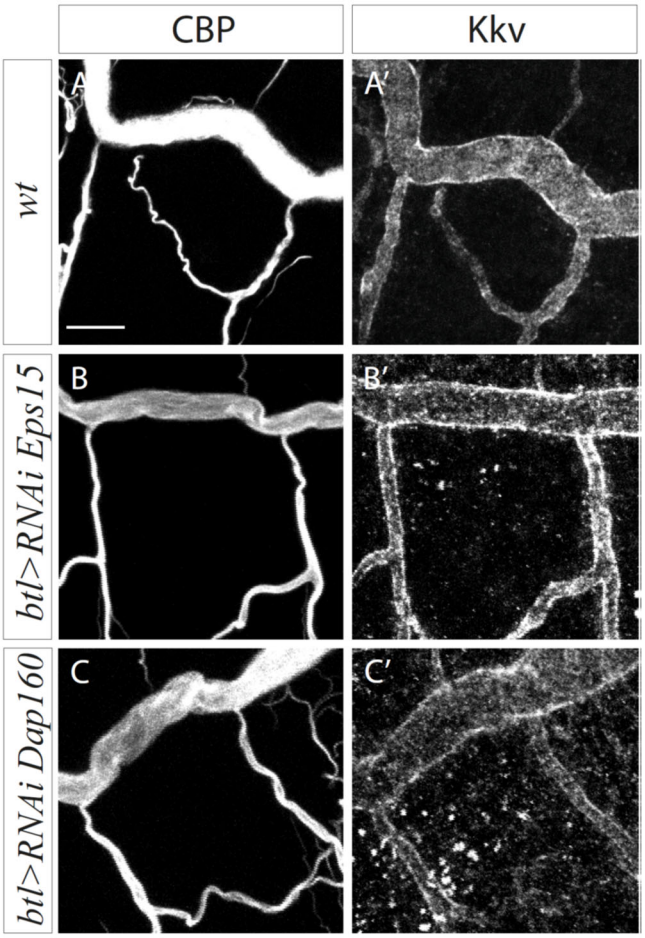

Fig. 27. Downregulation of EH-protein. Lateral views of the embryos at stage 15 stained for CBP to detect chitin (grey in A, B, C) and Kkv (grey in A', B', C'). (**A-A'**) Wild type embryo. (**B-B'**) Embryo with downregulation for the EH-protein Eps15. (**C-C'**) Embryo with downregulation for the EH-protein Dap160. No difference is detected among the three conditions. Scale bar 10µm.

4.3.3 The coiled-coil domain of Kkv is dispensable for its activity

The main difference between class A and class B chitin synthases (respectively, Kkv and ChS2 in *Drosophila melanogaster*) is the presence of a coiled-coil domain, C-terminal to the active centre in class A enzymes. This domain is not present in class B, suggesting that it may contribute to the specificity of epidermal chitin synthases. Potentially, the coiled-coil domain mediates an association to a yet unknown partner assisting chitin synthase localisation or activity (Moussian, 2013). It is predicted to face the extracellular space and may be involved in protein–protein interaction or oligomerization (Merzendorfer, 2006; Adler, 2019).

To investigate the role of this coiled-coil domain, we generated a protein lacking this region, GFP-Kkv$^{\Delta CC}$. When we expressed the mutant protein in a wild type background, we observed that the protein localised mainly apically (**Fig. 28 B**), as wildtype Kkv does (**Fig. 28 A**). This indicated that the coiled-coil domain is dispensable for Kkv localisation. We did not detect any defect of GFP-Kkv$^{\Delta CC}$ overexpression in chitin deposition (**Fig. 28 D**) and the phenotype was comparable to a wild type embryo (**Fig. 28 C**). The overexpression in a mutant background for *kkv* rescued the absence of chitin (**Fig. 28 E**), this indicated that the protein is functional and that the coiled-coil domain is not necessary for Kkv function. In agreement with this, we found that the overexpression of GFP-Kkv$^{\Delta CC}$ in salivary gland produced chitin punctae (**Fig. 28 G-G'**) as the overexpression of wild type Kkv does (**Fig. 28 F-F'**), confirming that this new protein is functional.

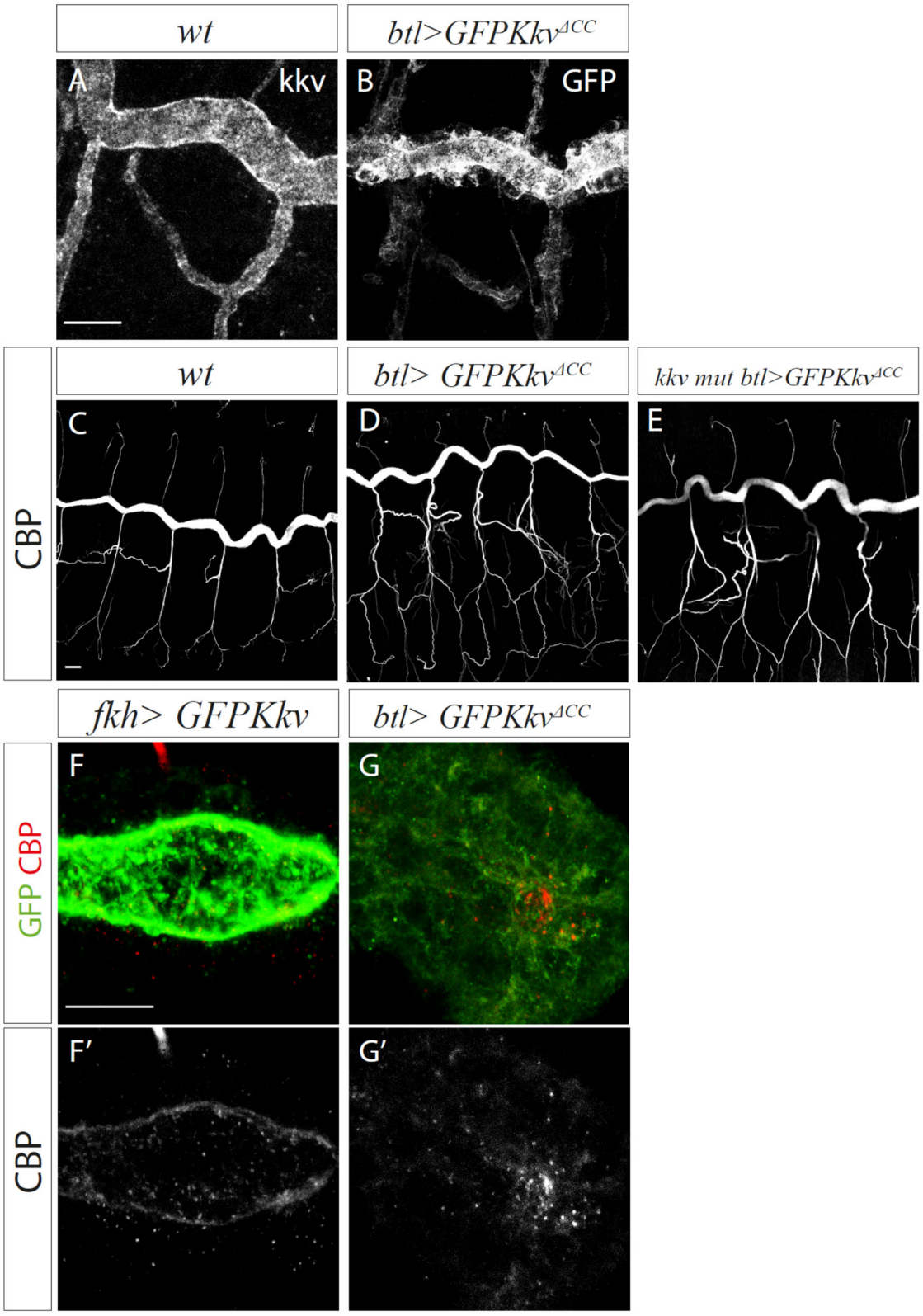
wt
btl>GFPKkv^ΔCC
A
kkv
B
GFP
CBP
wt
btl> GFPKkv^ΔCC
kkv mut btl>GFPKkv^ΔCC
C
D
E
fkh> GFPKkv
btl> GFPKkv^ΔCC
GFP CBP
F
G
CBP
F′
G′

Fig. 28. Analysis of the expression of GFP-Kkv$^{\Delta CC}$. Lateral views of the embryos at stage 15, stained for Kkv (grey in A), GFP to visualise GFP-Kkv$^{\Delta CC}$ (grey in B, green in G) and to visualise GFP-Kkv (green in F) and CBP to detect chitin (grey in C, D, E, F' and G', red in F, G). (**A**) In a wild type embryo, Kkv accumulates apically in the trachea. (**B**) GFP-Kkv$^{\Delta CC}$ localises mainly apically in the trachea. (**C**) Tracheal chitin pattern of a wild embryo. (**D**) The expression of GFP-Kkv$^{\Delta CC}$ in the trachea of a wild type embryo does not produce any defect in chitin deposition. (**E**) The expression of GFP-Kkv$^{\Delta CC}$ in the trachea of an embryo mutant for *kkv* is able to rescue the lack of chitin. (**F-F'**) The expression of Kkv in salivary gland produces few intracellular particles of chitin. (**G-G'**) The expression of GFP-Kkv$^{\Delta CC}$ in trachea produces few intracellular particles of chitin. Scale bar 10µm.

In salivary gland, the concomitant expression of Reb and GFP-Kkv$^{\Delta CC}$ produced intraluminal chitin deposition (**Fig. 29 B-B'**), similar to the simultaneous expression of Reb and wild type Kkv (**Fig. 29 A-A'**). As already described, the overexpression of Reb and Kkv in the trachea produces a strong effect of advanced and excessive chitin deposition (**Fig. 29 C**). Surprisingly, the concomitant overexpression of Reb and GFP-Kkv$^{\Delta CC}$ in the trachea rescued the phenotype of Reb overexpression: tubes and chitin deposition appeared normal (**Fig. 29 D**). Altogether these results indicate that the coiled-coil domain is dispensable for Kkv activity and localisation, but it is acting differently to the full length Kkv protein.

Fig. 29. Analysis of the co-expression of GFP-Kkv$^{\Delta CC}$ and Reb. Lateral views of the embryos at stage 15, stained for CBP to detect chitin (red in A, B; grey in A', B', C, D) and GFP to visualise Kkv (in green in A-B). (**A-A'**) The co-expression of Kkv and Reb in salivary gland produces ectopic chitin deposition inside the lumen. (**B-B'**) The co-expression of GFP-Kkv$^{\Delta CC}$ and Reb in salivary gland produces intraluminal chitin deposition. (**C**) The simultaneous overexpression of Reb and GFPKkv in the trachea produce branches that are straighter than the control and the dorsal trunk appears discontinuous. (**D**) During the simultaneous overexpression of Reb and GFP-Kkv$^{\Delta CC}$ in the trachea of a wild type embryo, the phenotype of excessive chitin deposition is rescued, chitin pattern and tubes appear normal, comparable to a wild type embryo (Fig. 28 C). Scale bar 10µm.

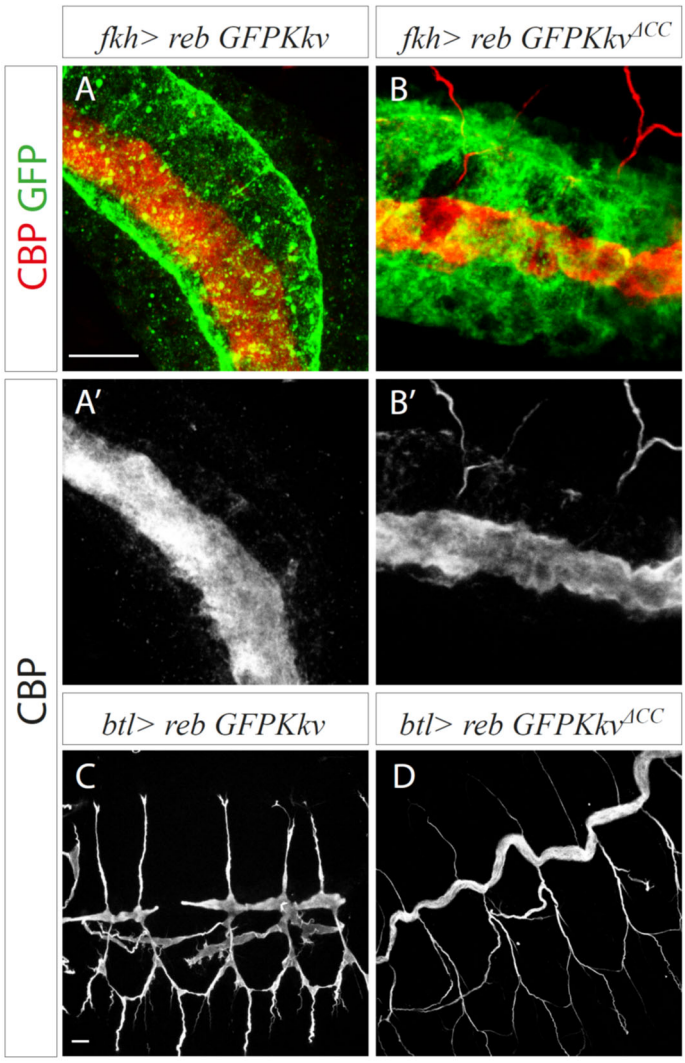

4.4 Kkv distribution at the apical membrane and relation with Exp/Reb

It has been proposed that Chitin Synthases could be organized at the plasma membrane in a quaternary structure forming rosettes. This hypothesis come from the comparison between Chitin Synthases and the closely related Cellulose Synthases: both enzymes belong to family 2 of glycosyltranferases, they produce polymers with similar molecular structure (they differ only for a hydroxyl group) and several motifs in the amino acids structure are conserved, among them the catalytic domain QxxRW and several transmembrane domains (Merzendorfer, 2006; Bi *et al.*, 2015). Cellulose Synthases seem to be organized as hexagonal structures with sixfold symmetries (rosettes), which are assembled in the Golgi and then transported to the plasma membrane. Each rosette is composed of six subunits/lobes, which in turn consist of either six monomeric or three

dimeric synthetic units, each capable of polymerizing and translocating a single cellulose chain. It has been proposed that differences in the morphology of either rosettes or their lobes may be responsible for the diversity in cellulose architecture: dispersed rosettes produce widely spaced cellulose microfibrils, whereas dense regions of complexes synthesise highly aggregated crystalline microfibrils (Allen *et al.*, 2021). It has been speculated the existence of other proteins that, perhaps reversibly, associate with the subunits to cause changes in diameter lobe area and shape (Haigler and Roberts, 2019). Chitin Synthases could function in a similar way, only after rosette-like complexes have formed. Possibly, multitude of different chitin deposition patterns and textures found in nature could have some structural equivalents in the arrangement of single synthetic units within putative chitin synthase super-complexes (Merzendorfer, 2006).

We decided to test whether Exp/Reb could have a role in the quaternary structure of Kkv, maybe producing changes in the distribution of Kkv complexes. We had previously shown that Exp/Reb are not required for apical localisation of Kkv, and we confirmed this in our experiments. We now checked at high resolution, using super-resolution microscopy, the pattern of Kkv at the apical membrane of the trachea of *yw* (control) embryos and of embryos deficient for *exp*/*reb*. At stage 14, in both *yw* and *exp*/*reb* deficient embryos, Kkv was not completely apical, many intracellular Kkv vesicles were present and Kkv pattern was non-uniform in intensities and in distribution (**Fig. 30 A, B**). At stage 16, control embryos showed an apical distribution of Kkv in stripes, probably following the taenidial folds and Kkv vesicles were mainly absent (**Fig. 30 C**). In contrast, in embryos deficient for *exp* and *reb*, Kkv was apical too, but it was not distributed in lines, and we detected several regions in which the protein had different intensities and non-uniform distribution (**Fig. 30 D**). As indicated, the apical accumulation of Kkv at stage 16 follows the taenidia, and in *exp*/*reb* mutants taenidia are not formed, raising the possibility that the defects observed are due to the absence of these supracellular structures. Therefore, we aimed to analyse a condition in which the chitinous cuticle is not yet deposited but chitin is strongly deposited in the intracellular filament. We analysed Kkv accumulation in control at stage 15 embryos and detected a uniform and homogeneous pattern of the enzyme, in terms of distribution and intensity; the amount of Kkv vesicles decreased respect to the stage 14. In contrast, in mutants for *exp*/*reb,* areas of the membrane without Kkv were detected, whereas in other regions Kkv was non-uniformly distributed and different intensities of the protein were visible (**Fig. 30 F**). In

an orthogonal view of the same images, it was possible to see how Kkv organization was more homogeneous in control **(Fig. 30 E')** than in mutant (**Fig. 30 F'**).

mummy (*mmy*) is a gene that encodes an enzyme involved in the synthesis of GlcNAc monomer. The nonsense mutation mmy^{H053} stops the production of the monomer and the embryos are chitin-less, so in this case, although Kkv protein is present, it has no substrate to produce polymers (Araújo *et al.*, 2005). To test the possibility that the functionality of Kkv protein is affecting its own distribution at the membrane, we analysed the apical distribution of Kkv in mmy^{H053} mutants. In this condition, we detected a massive presence of Kkv intracellularly, but the distribution at the apical membrane was still homogeneous (**Fig. 30 G-G'**).

In salivary glands of *yw* embryos, endogenous Kkv is present and Exp/Reb are absent. We compared control embryos with embryos overexpressing Reb in salivary glands. In this case, in *yw* embryos Kkv distribution was apical but nonuniform (**Fig. 30**Fig. **H**), instead when Reb was present the pattern appeared more homogeneous (**Fig. 30 I**).

Fig. 30. Kkv distribution at the tracheal apical membrane. Lateral views of the embryos, otherwise indicated differently, stained for Kkv (grey, red in G') and Armadillo to visualise the apical membrane of the cells (green in G). (**A-G**) Tracheal system, Dorsal Trunk. (**A**) In *yw* embryos at stage 14, Kkv is not uniformly distributed at the membrane and is not completely apical yet. (**B**) Embryos deficient for *exp*/*reb* at stage 14 are similar to the control. (**C**) In *yw* embryo at stage 16, Kkv is apical and it is distributed in stripes in a taenidial fold-manner. (**D**) In embryos deficient for *exp*/*reb* at stage 16, the shape of the tracheal tube is irregular because chitin is missing (Moussian *et al*., 2015), Kkv is still apical, but its distribution is irregular at the membrane. (**E**) In *yw* embryo at stage 15, Kkv is apical and homogeneous in distribution and in intensity; the image is a projection of 10 sections. (**E'**) The orthogonal view of E shows that Kkv distribution is mainly uniform. (**F**) In embryos deficient for *exp*/*reb* at stage 15, Kkv is apical but there are regions in which Kkv is absent (marked by a circumference) and the intensity of the signal is nonuniform; the image is a projection of 10 sections. (**F'**) The orthogonal view of F shows that Kkv distribution is nonuniform, there are region in which Kkv is absent (marked by a circumference). (**G-G'**) In embryos mutant for *mmy* at stage 15, Kkv is detected intracellularly but at the apical membrane Kkv appears distributed uniformly (marked by a circumference); the image is a projection of 10 sections. (**H-I**) Salivary glands. (**H**) In *yw* embryo at stage 15, Kkv is apical but it is nonuniformly distributed (Kkv absence marked by a circumference); the image is a projection of 10 sections. (**I**) In embryos overexpressing Reb in salivary gland at stage 15, Kkv is apical and it appears homogeneous at the membrane; the image is a projection of 10 sections. Scale bar 10µm.

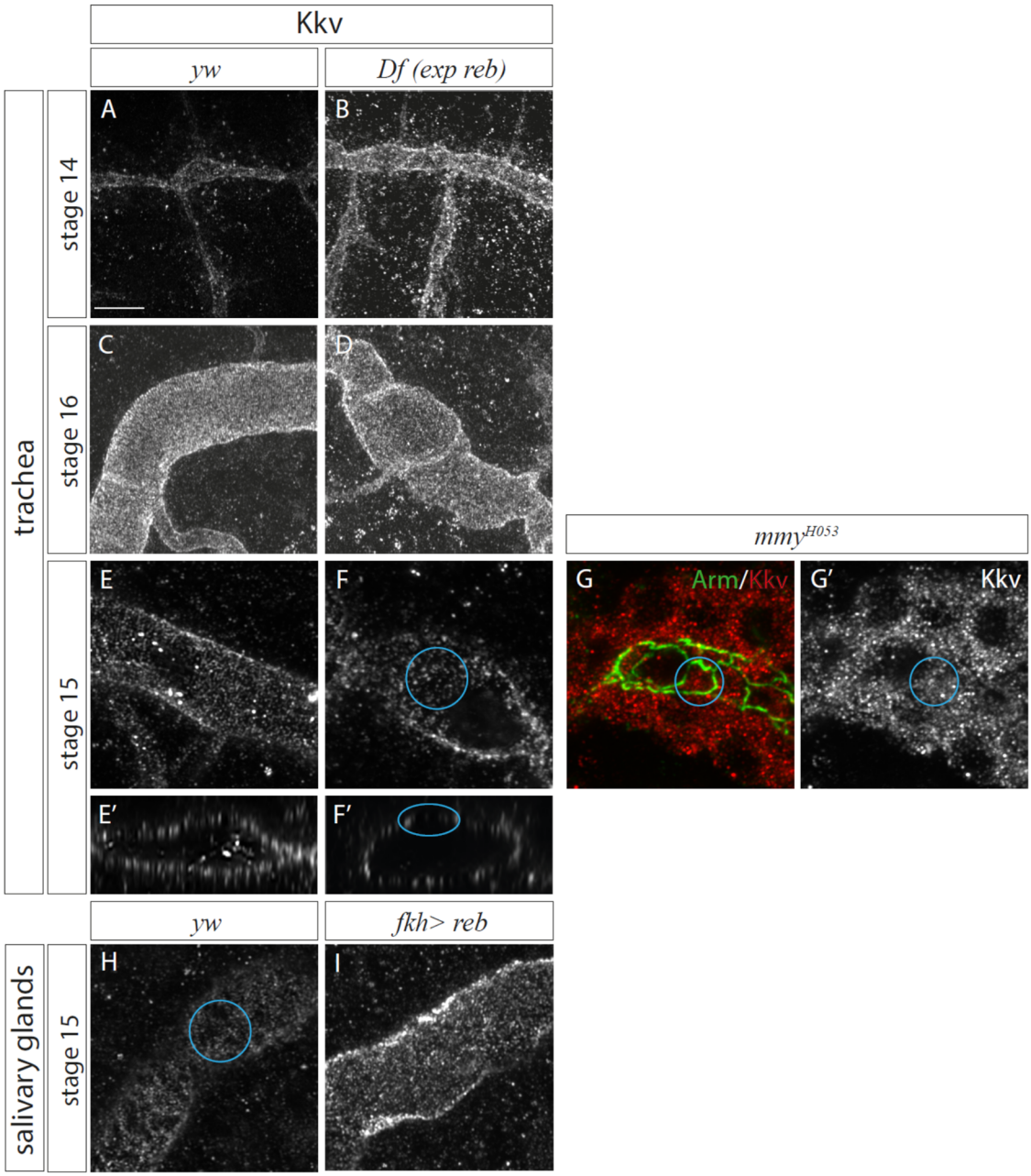

Hence, Kkv distribution at the apical membrane appears less regular when Exp and Reb are missing and Kkv functionality seems not a determinant of apical Kkv distribution.

To investigate the relation between Kkv and Exp/Reb, we analysed the trachea of wildtype embryos. Unfortunately, from the images that we obtained, it was difficult to determine a possible colocalisation between Reb and Kkv (**Fig. 31 A-C**). Thus, we decided to express Reb in salivary glands of third instar larvae because cells are bigger than embryonic cells. In general, Kkv and Reb patterns were complementary and Reb was interposed between Kkv (**Fig. 31 D-F**).

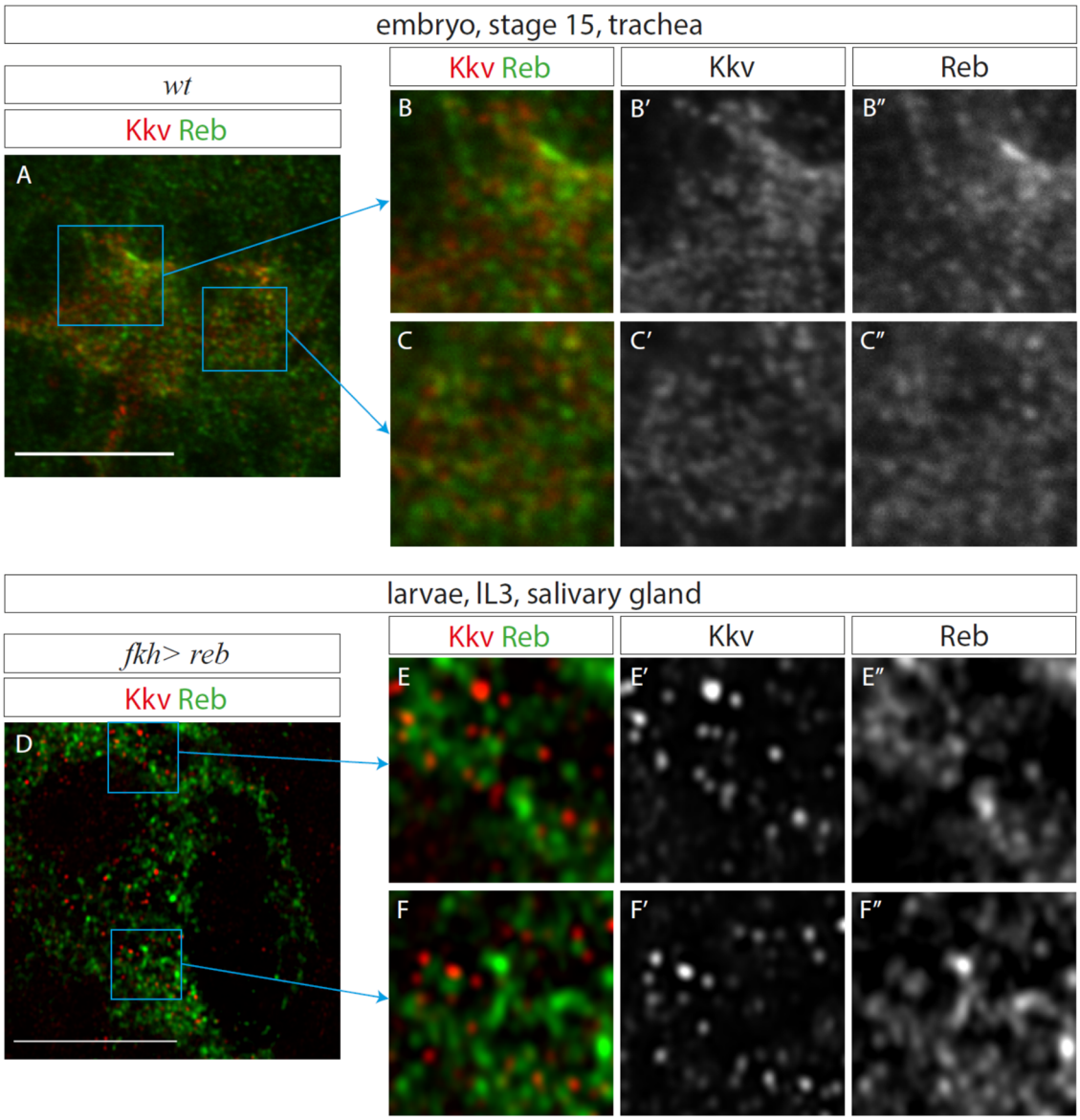

Fig. 31. Relation between Kkv and Reb. (**A-C**) Single section showing Reb and Kkv in a trachea of stage 15 embryo, stained for Kkv (red in A, B, C and grey in B', C') and Reb (green in A, B, C and grey in B'', C''); B-C are magnification of A. It is difficult to interpret the relation between Kkv and Reb. (**D-F**) Single section showing the overexpression of Reb in salivary gland of a third instar larvae, stained for Kkv (red in D, E, F and grey in E', F') and Reb (green in D, E, F and grey in E'', F''); E-F are magnification of D. Kkv and Reb appear mainly complimentary. Scale bar 10μm.

4.5 Analysis of chitin synthesis *in vitro*

Waste disposal, air pollution, and natural resources exhaustion have been recognized as the dominant cause of many environmental disasters. For these problems, it has been encouraged the use of organic products able to respect our habitat (Casadidio *et al.*, 2019). Presently, organic products are increasing their marketing power and social interest thanks to the high expectations of consumers towards ambient and human health (Tukker *et al.*, 2010; Liobikiene and Bernatoniene, 2016). Among biopolymers that are biodegradable and made from renewable raw materials, chitin and its deacetylated form, chitosan, are widely used in many sectors such as biomedical, biotechnology, water treatment, food, agriculture, veterinary, and cosmetics (Casadidio *et al.*, 2019). So far, the main commercial sources of chitin are crab and shrimp shells (Younes and Rinaudo, 2015). In this Thesis, we looked for new methods to synthesise chitin *in vitro*.

It has already been shown in our lab that the transfection of embryonic *Drosophila* S2 cells with Kkv promotes the formation of intracellular chitin particles, however no fibrillar chitin was observed. The co-transfection of Kkv with Exp, Reb or both did not lead to an increase of number of chitin particles. Interestingly, Kkv and Exp/Reb did not localise in the cell membrane region (Moussian *et al.*, 2015), likely because S2 cells are not polarised.

To further explore these preliminary results and advance in our endeavour of producing chitin *in vitro*, we decided to generate a new stable S2 cell line transfected with Reb-Cherry, Kkv and Exp-GFP, from now on, called RKE cells. As expected, RKE cells expressed the three proteins. In addition, we found that RKE cells contained intracellular chitin punctae and the proteins were not able to localise at the membrane (**Fig. 32 A**). We reasoned that to deposit chitin extracellularly these proteins should be at the membrane. To properly localise the proteins, we transfected RKE cells with Crumbs (Crb). Crb is an essential apical determinant that controls epithelial apicobasal polarity and is able to confer apical features to the membrane (Tepass and Tanentzapf, 2001). When we co-transfected RKE cells with Crb, we could detect Crb at the membrane of the cells. In these conditions, we were able to detect also Kkv at the membrane (**Fig. 32 B**), confirming that S2 cells need to be polarized to localise the chitin-producing proteins correctly. Interestingly, we found a few examples in which chitin was extruded to the extracellular

medium (**Fig. 32 C**), and in addition we observed that less chitin punctae were present inside the cells with respect to RKE cells without Crb (**Fig. 32 D**).

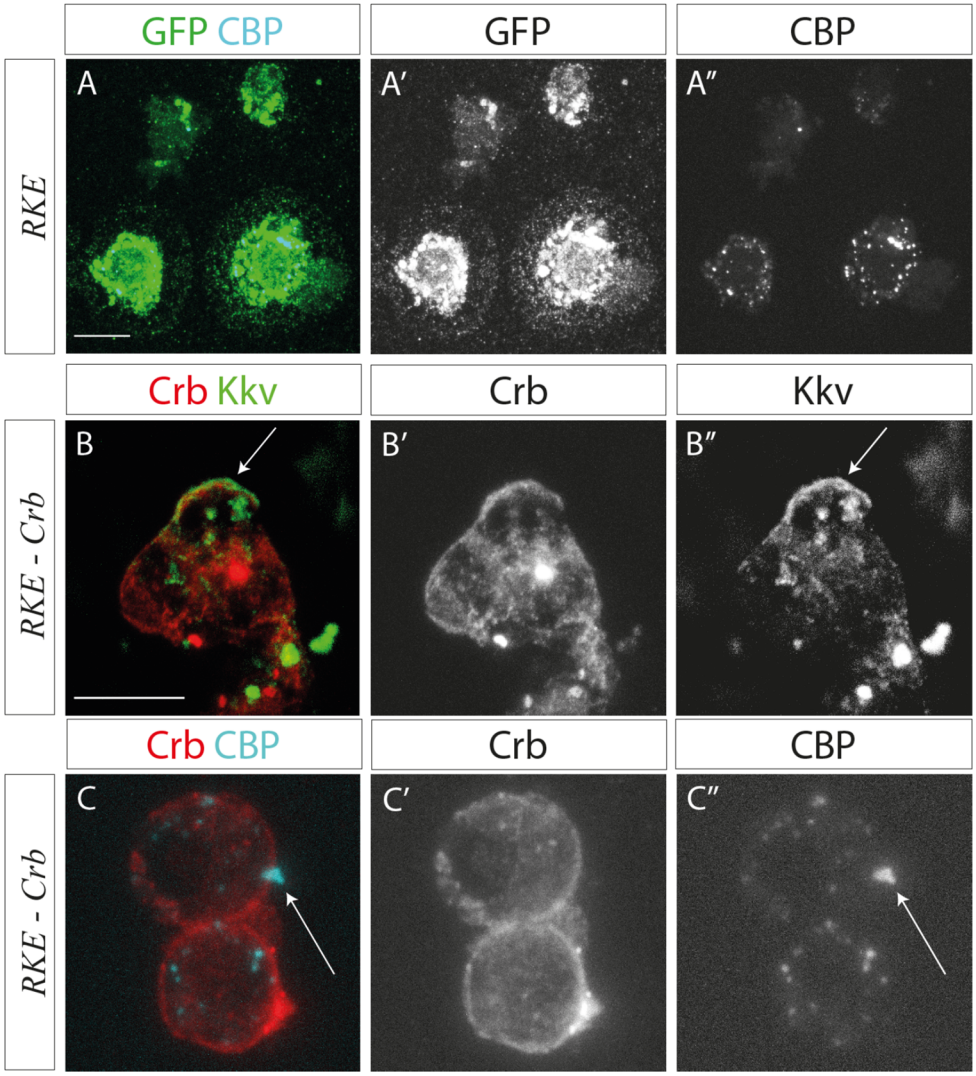

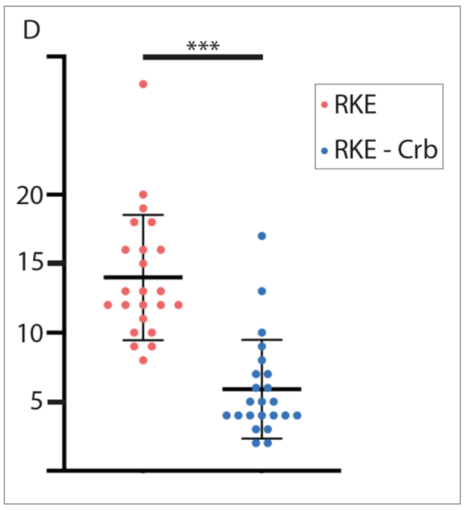

Fig. 32. Analysis of RKE cells. (**A**) RKE cells stained with GFP to visualise Exp-GFP (green, grey) and CBP to detect chitin (cyan and grey); Exp-GFP is not localised at the membrane and several intracellular chitin particles are present. (**B**) RKE cells transfected with Crb and stained for Kkv (green, grey) and Crb (red, grey); the arrow indicated Kkv localisation at the membrane. (**C**) In RKE cells transfected with Crb and stained for CBP (cyan, grey) and Crb (red, grey), few intracellular chitin particles are present, but extruding chitin is visible (indicated by an arrow). (**D**) Quantification of the number of chitin particles per cell in RKE cells (orange) and in RKE cells transfected with Crb (blue); n=23. Scale bar 10µm.

We speculated that most of the chitin was released to the extracellular space. To test our hypothesis and to detect the presence of chitin inside the cell or inside the culture medium, we decide to use a biochemical approach. We did a slotblot experiment comparing culture medium and cell lysate of different conditions: not transfected S2 cells (**Fig. 33 A-A'**), S2 cells transfected with Crb and Kkv (**Fig. 33 B-B'**), not transfected RKE cells (**Fig. 33 C-C'**) and RKE cells transfected with Crb (**Fig. 33 D-D'**). The membrane was revealed with CBP to detect chitin. Unfortunately, we were detecting signal also in not transfected S2 cells (**Fig. 33 A-A'**) that lack chitin (Moussian *et al.*, 2015) and no difference could be appreciated among the various conditions (Fig. 33). This was an indication that we could not distinguish between signal and background noise. Thus, this is not the appropriate technique to analyse the presence of chitin and other methods will be required.

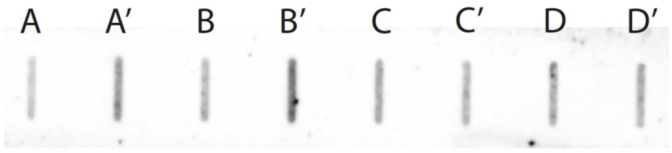

Fig. 33. Slotblot experiment. The membrane was incubated with CBP to detect chitin. (**A**) Culture medium and (**A'**) lysate of S2 cells. (**B**) Culture medium and (**B'**) lysate of S2 cells transfected with Crb and Kkv. (**C**) Culture medium and (**C'**) lysate of RKE cells. (**D**) Culture medium and (**D'**) lysate of RKE cells transfected with Crb. No difference is appreciated.

4.6 Analysis of Chitin Synthase 2

Drosophila melanogaster encodes two different chitin synthases: Krotzkopf verkehrt (Kkv) and Chitin Synthase 2 (ChS2). The first one produces chitin in the epidermis, the tracheae, the fore- and the hindgut; the second one is assumed to synthesise chitin in the midgut as the major component of the peritrophic matrix. The chitin marker CBP is able to bind chitin produced by Kkv, but it does not recognise chitin produced by ChS2. Both chitin synthases present several transmembrane domains, a conserved catalytic domain (QRRRW) and a conserved WGTRE motif. The main difference between the two proteins is the presence of a coiled coil domain at the C terminal to the WGTRE motif in Kkv (**Fig. 34 A, B, C**). This domain potentially mediates association to a yet unknown partner assisting chitin synthase localisation or activity (Moussian, 2013).

We wondered if the presence/absence of the coiled-coil domain is important to determine the specificities of the chitin synthases. To investigate the differences between Kkv and ChS2, we generated different transgenic lines. First, we generated a full length GFP-tagged ChS2 to determine its ability in chitin deposition. Then, we generated two different GFP-tagged chimeras to explore the possible functional role of the coiled-coil domain: one is composed by the N-terminal of ChS2 until the WGTRE motif and by the C-terminal of Kkv (generating a ChS2 with the coiled coil domain of Kkv, from now on GFPChS2-Kkv) (**Fig. 34 D**); the other one is composed by the N-terminal of Kkv until the WGTRE motif and by the C-terminal of ChS2 (generating a Kkv without its coiled coil domain, from now on GFPKkv-ChS2) (**Fig. 34 E**).

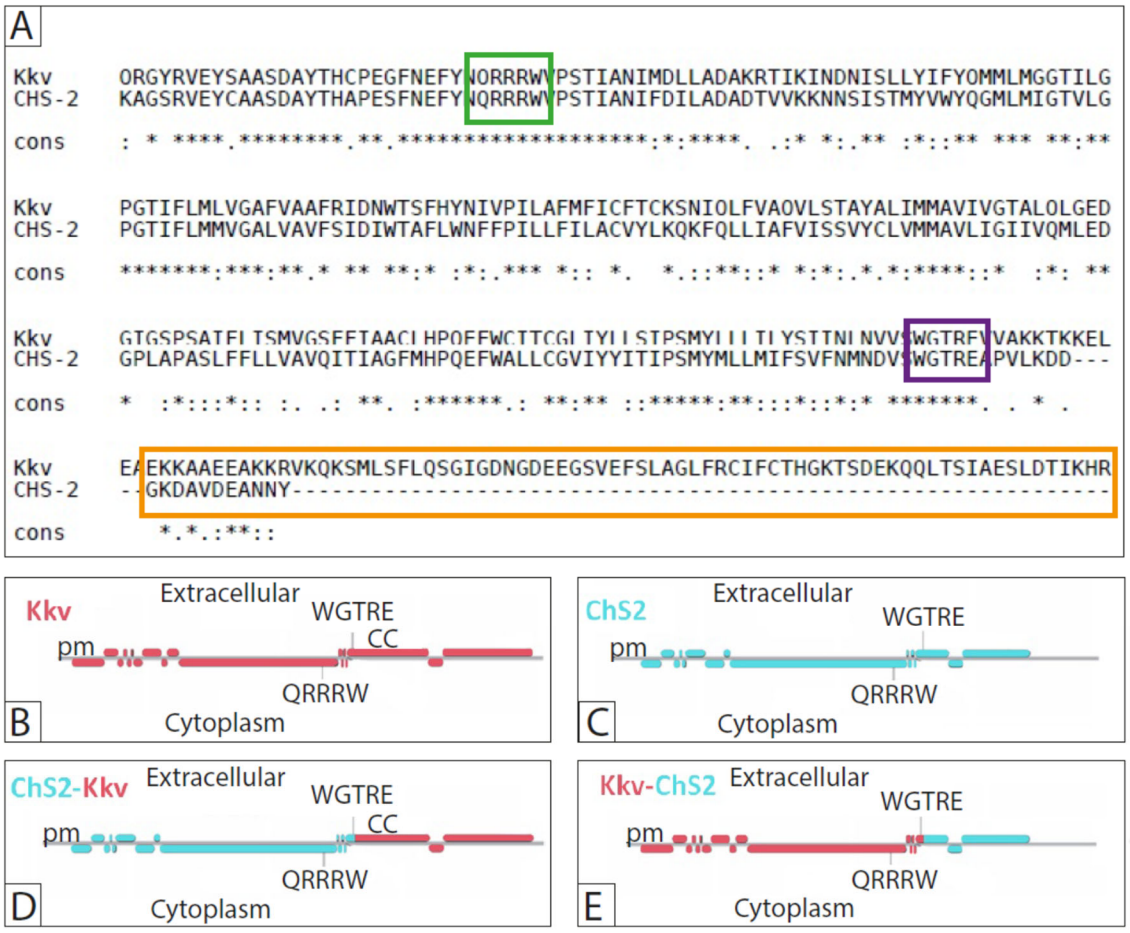

Fig. 34. Amino acids sequence alignment of Kkv and Chs2; structures of chitin synthases and the new chimeras (adapted from Moussian, 2013). (**A**) Partial amino acid sequence alignment of Kkv (amino acids 866-1165) and ChS2 (amino acids 836-1068). The chitin synthase Kkv presents several transmembrane domains, the catalytic domain QRRRW (green square), the conserved motif WGTRE (purple square) and a coiled coil domain (orange square). Chitin Synthase 2 differs mainly from Kkv for the absence of the coiled coil domain (Moussian, 2013). (**B**) Schematic representation of Kkv protein. (**C**) Schematic representation of ChS2 protein. (**D**) The chimera ChS2-Kkv is composed by the N-terminal part of ChS2 until the WGTRE motif and by the C-terminal part of Kkv starting from the coiled-coil domain. (**E**) The chimera Kkv-ChS2 comprises the N-terminal part of Kkv until the WGTRE motif and the C-terminal part of ChS2 right after the WGTRE motif.

4.6.1 ChS2 cannot deposit CBP-recognised chitin and Kkv needs all its domains to be functional

When we overexpressed GFP-ChS2 in the trachea of a wildtype embryo, no detectable effect was found and chitin was normally deposited in the lumen according to the spatio-temporal pattern (**Fig. 35 B**). Neither with GFP-ChS2-Kkv (**Fig. 35 C**) nor with GFP-Kkv-ChS2 (**Fig. 35 D**), we detected any defect in chitin deposition.

To determine if the new proteins could exert the function of Kkv, we assayed their rescuing capacity in a *kkv* mutant background. GFP-ChS2, GFP-ChS2-Kkv and GFP-Kkv-ChS2 could not rescue the absence of chitin produced by the absence of *kkv* (**Fig. 35 E, F, G**), like a wild type form of Kkv does, and the trachea was defective.

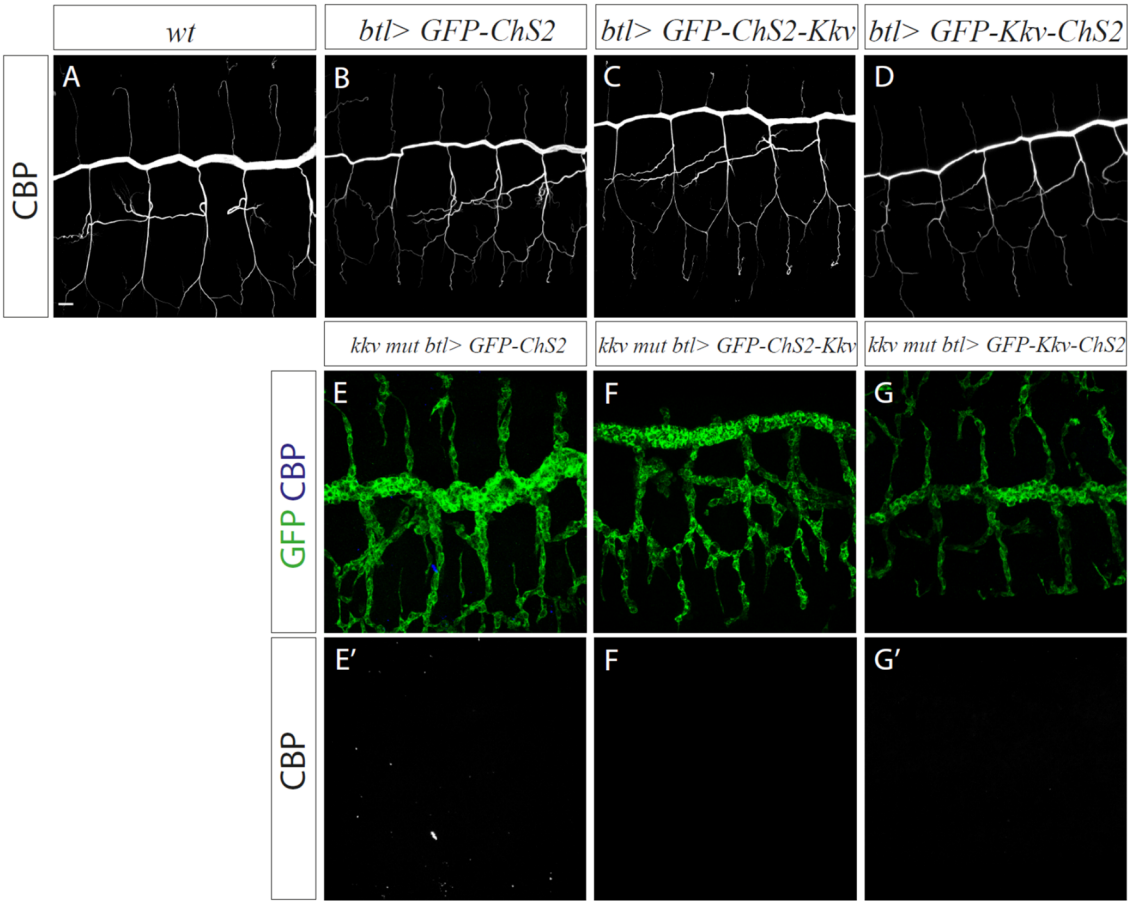

Fig. 35. Overexpression of the new constructs in a wild type and in a mutant background for *kkv*. Lateral views of the embryos at stage 15, stained for CBP to detect chitin (grey in A-D, blue in E-G) and GFP in green to detect ChS2 in E, ChS2-Kkv in F and Kkv-Chs2 in G. (**A-D**) The overexpression of the new constructs does not affect chitin deposition in trachea. (**A**) Wild type embryo. (**B**) Overexpression of GFP-ChS2. (**C**) Overexpression of GFP-ChS2-Kkv. (**D**) Overexpression of GFP-Kkv-ChS2. (**E**) GFP-ChS2 is not able to rescue the absence of chitin in a *kkv* mutant background. (**F**) GFP-ChS2-Kkv is not able to rescue the absence of chitin in a *kkv* mutant background. (**G**) GFP-Kkv-ChS2 is not able to rescue the absence of chitin in a *kkv* mutant background. Scale bar 10µm.

In a wild-type situation in the trachea, Kkv works together with Exp and Reb to deposit chitin. The over or misexpression of Exp/Reb in salivary gland is able to produce a small amount of chitin because Kkv is already expressed in this tissue (**Fig. 36 A-A'**). The concomitant overexpression of Exp/Reb and Kkv in the same tissue is able to deposit a bigger amount of chitin (**Fig. 36 B-B'**). When we co-expressed Reb and GFP-ChS2 in salivary gland, we obtained a similar phenotype to the overexpression of Reb alone indicating that the GFP-ChS2 and Reb are not working together to deposit chitin (**Fig. 36 C-C'**). The simultaneous overexpression of Reb with GFP-ChS2-Kkv (**Fig. 36 D-D'**) or with GFP-Kkv-ChS2 (**Fig. 36 E-E'**) was similar to the overexpression of Reb alone.

All together, these results indicate that ChS2 cannot deposit chitin recognised by CBP and that Kkv needs to be entire to be functional.

Fig. 36. Concomitant overexpression of Reb and the new UAS constructs in salivary glands. Lateral views of the embryos at stage 15, stained for CBP to detect chitin (red in A-E, grey in A'-E'), Reb (green in A) and GFP (green) to detect GFP-Kkv in B, GFP-ChS2 in C, GFP-ChS2-Kkv in D and GFP-Kkv-ChS2 in E. (**A**) The overexpression of Reb alone is able to trigger the deposition of ectopic chitin in the lumen. (**B**) The simultaneous overexpression of Reb and GFPKkv produces a bigger amount of ectopic chitin. (**C**) The simultaneous overexpression of Reb and GFP-ChS2 is similar to the overexpression of Reb alone. (**D**). The co-expression of Reb and GFP-ChS2-Kkv is similar to the overexpression of Reb alone. (**E**). A similar situation occurs for the co-expression of Reb and GFP-Kkv-ChS2. Scale bar 10µm.

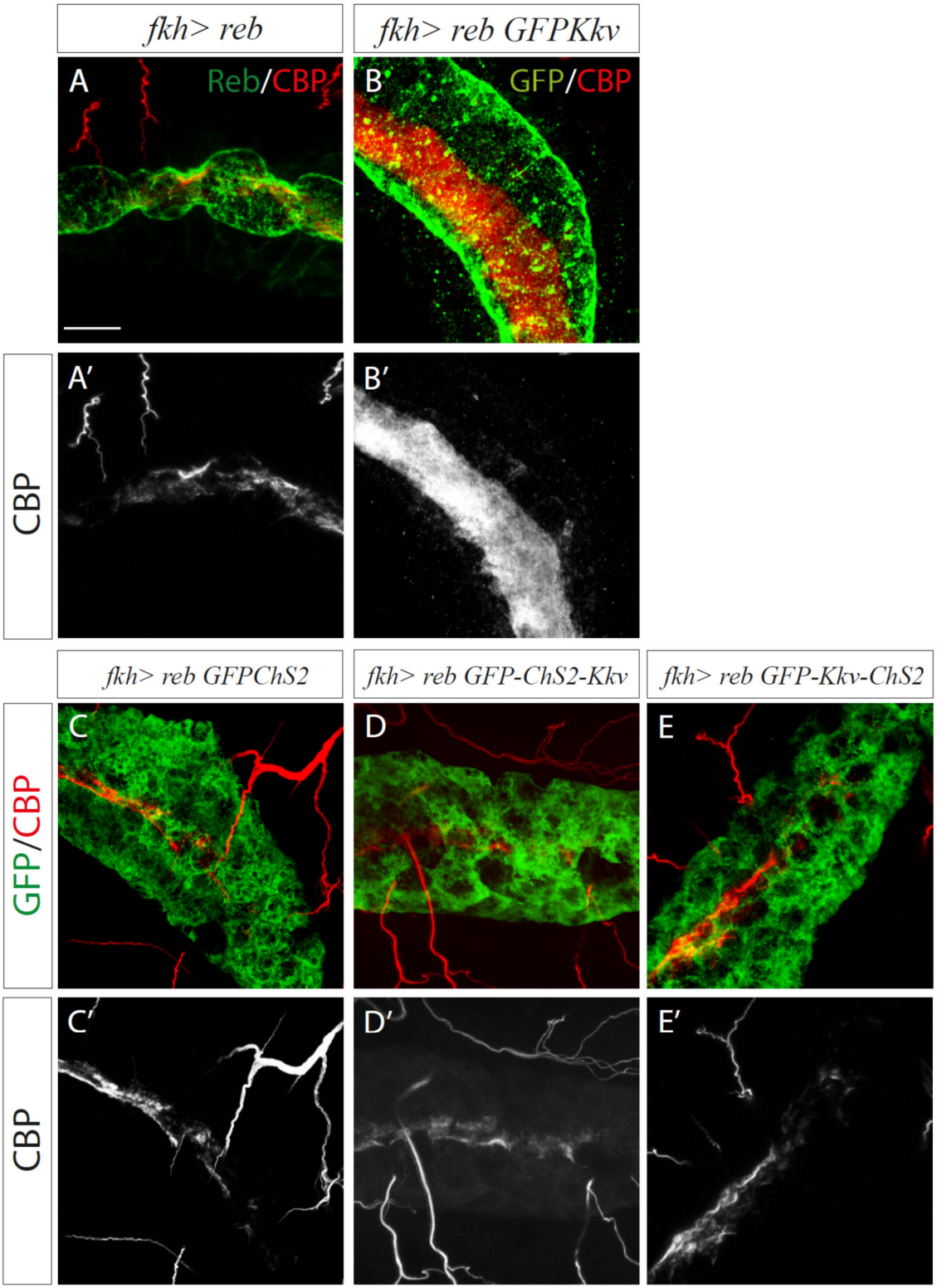
fkh> reb
fkh> reb GFPKkv
A
Reb/CBP
B'
GFP/CBP
A'
B'
CBP
fkh> reb GFPChS2
fkh> reb GFP-ChS2-Kkv
fkh> reb GFP-Kkv-ChS2
C
D
E
GFP/CBP
C'
D'
E'
CBP

4.6.2 Analysis of ChS2 localisation

In a wild-type background, the endogenous Kkv protein is present in the apical region of tracheal cells (**Fig. 37 A**). Instead, when we overexpressed GFP-ChS2 in the trachea, the protein accumulated mostly in the cytoplasm but it did not accumulate clearly in the apical region or at membrane, although some membrane accumulation is occasionally detected (**Fig. 37 B**). A similar situation occurred for the chimeras GFP-ChS2-Kkv (**Fig. 37 C**) and GFP-Kkv-ChS2 (**Fig. 37 D**). When we overexpressed GFP-ChS2 in the gut, a tissue where ChS2 should be expressed, the protein still localised in the cytoplasm.

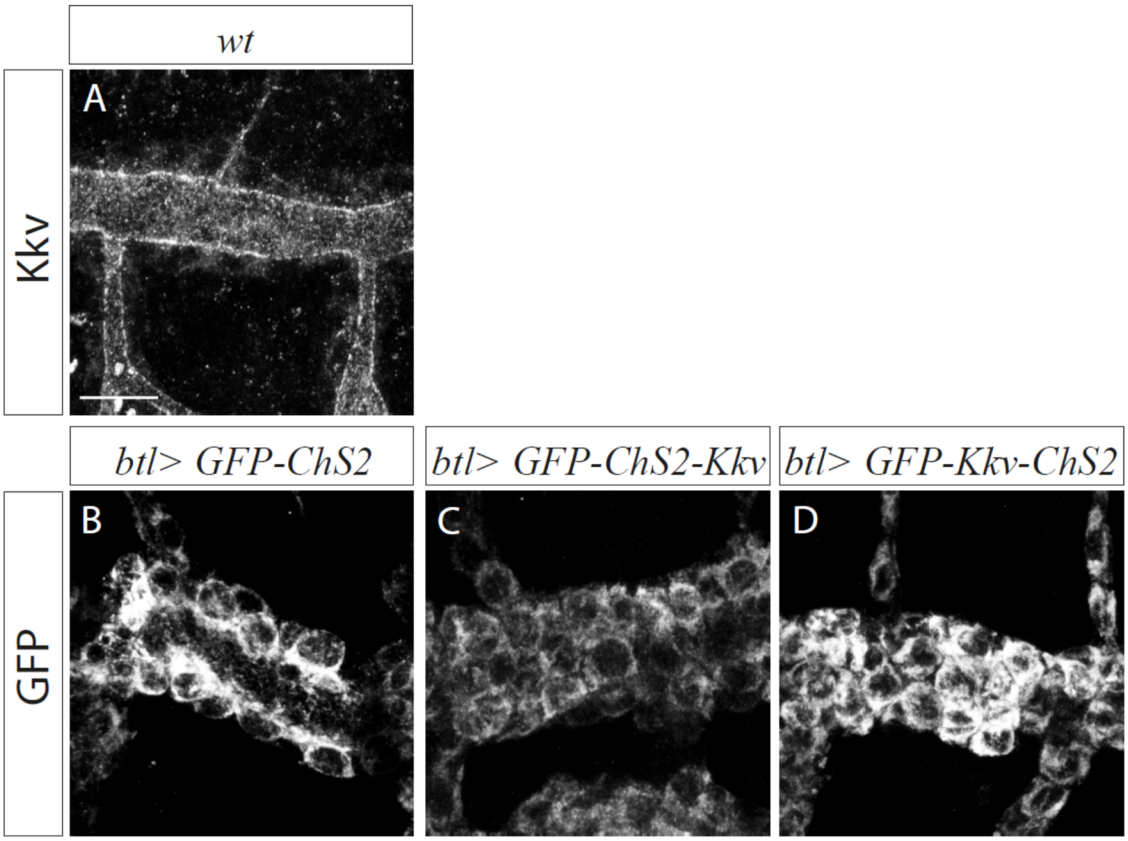

Fig. 37. Localisation of endogenous Kkv, GFP-ChS2, GFP-ChS2-KKv and GFP-Kkv-ChS2. Lateral views of the embryos at stage 15, stained for Kkv in A (grey) and GFP (grey) to detect GFP-ChS2 in B, GFP-ChS2-Kkv in C and GFP-Kkv-ChS2 in D. (**A**) In a wild-type condition, endogenous Kkv localises apically in the tracheal cells. (**B**) The overexpression of GFP-ChS2 does not produce any clear defect and the protein accumulates mostly in the cytoplasm. (**C**) The overexpression of the chimera GFP-ChS2-Kkv does not produce any clear effect and the protein accumulates in the cytoplasm. (**D**) A similar situation occurs with the overexpression of GFP-Kkv-ChS2. Scale bar 10µm.

The results suggested that ChS2 is not localised at the membrane, raising the issue on how it can deposit chitin in the Peritrophic Matrix. To confirm that the pattern we observed is real and it is not produced by the overexpression of the constructs, we decided to generate an antibody against ChS2. The antibody was able to recognise the overexpression of GFP-ChS2 in the trachea. When we used it to stain a wild type embryo, we noticed a pattern in the gut, but ChS2 was mainly localised in the cytoplasm (**Fig. 38**), confirming our observation. It was a surprising result if we consider that ChS2 has several transmembrane domains. More experiments are necessary to better characterize ChS2.

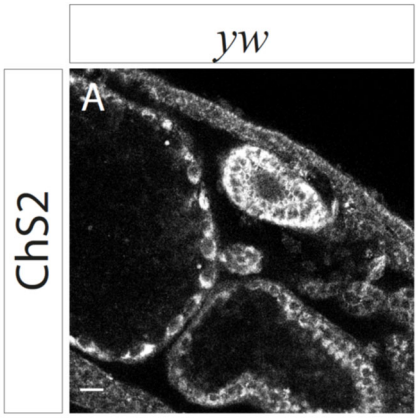

Fig. 38. Characterization of ChS2 antibody. Lateral views of an embryo at stage 15, stained for ChS2 (grey). A pattern in the gut is detectable but the protein is mainly in the cytoplasm. Scale bar 10µm.

5. Discussion

5. Discussion

The aim of this Thesis was to gain further insights into chitin synthesis and deposition in the apical extracellular matrices of *Drosophila melanogaster*. We investigated the molecular mechanisms of activity of Exp, Reb and Kkv through a structure-function analysis approach, we compared the molecular mechanisms of activity of the two chitin synthases (Kkv and ChS2) and we advanced in the production of chitin *in vitro*.

5.1 A structure-function analysis approach

The main approach used in this Thesis has been a structure-function analysis approach through the Gal4/UAS system (Brand and Perrimon, 1993) that permits the overexpression of a transgene in a spatio-temporal controlled manner.

In this work, we used two drivers: the *btlGal4* driver, that induces the expression of UAS transgenes in all the tracheal cells from early embryonic stages, and the *fkhGal4* driver, that permits the expression of UAS transgenes in salivary gland cells. Hence, we decided to generate UAS constructs of wild type and mutated proteins (for instance missing a specific domain) to perform a structure-function analysis. The Gal4/UAS system gave us the possibility to functionally test the new generated constructs, for example testing the capacity of the new proteins to rescue a loss of function phenotype or testing if they are necessary and sufficient to exert a specific function. The generation of UAS transgenes of proteins lacking a particular protein domain gave us the possibility to functionally test that specific domain.

However, the Gal4/UAS system is not perfect. This technique induces the production of a massive quantity of protein in all cells expressing the Gal4, preventing the possibility to obtain physiological and/or restricted expressions within the tissue. This could mask the endogenous requirements of different protein domains, as increased levels could bypass a lower protein efficiency.

To bypass this disadvantage, we considered the possibility to create transgenes of the proteins with their own promoter, but we discarded this idea when we realised that the nucleotide sequences of *kkv*, *exp* and *reb* are too big to work with. For future experiments, we believe that it will be useful to generate CRISPR mutant proteins to avoid UAS disadvantages.

5.2 Expansion and Rebuf

As indicated above, to investigate the molecular mechanism of activity of Exp and Reb we used a structure-function analysis approach. We started analysing the Nα-MH2 domain as it was the only recognisable domain present in these proteins (Iordanou *et al.*, 2014; Beich-Frandsen *et al.*, 2015; Moussian *et al.*, 2015). Moreover, we decided to look for highly conserved regions comparing the amino acids sequences of proteins homolog to Exp and Reb in other organisms and we found a highly conserved region not previously described in the literature, neither in Exp/Reb protein nor in any other protein, and we called it Conserved Motif.

5.2.1 Nα-MH2 domain of Exp and Reb is absolutely required to deposit extracellular chitin

Until the identification of Exp and Reb, the Nα-MH2 domain was found only in Smad proteins, that are involved in the TGF-β signaling pathway (Shi, 2001), but the participation of Exp/Reb in this pathway has been disproved in several works (Iordanou *et al.*, 2014; Beich-Frandsen *et al.*, 2015; Moussian *et al.*, 2015). In addition, structural data indicated clear differences between the MH2 domain in Smad proteins and the MH2 domain found in Exp protein, suggesting a possible different function (Beich-Frandsen *et al.*, 2015). Thus, we wanted to determine the role of this domain. In embryos lacking endogenous Exp/Reb proteins, chitin is not deposited in the lumen of tracheae or in the tracheal and epidermal cuticle, but the overexpression of the wildtype form of Exp/Reb reverts the phenotype (Moussian *et al.*, 2015). We observed that the overexpression of Exp/Reb lacking the Nα-MH2 domain ($Exp^{\Delta MH2}$, $Reb^{\Delta MH2}$) was not able to rescue the

absence of chitin in *exp/reb* mutants. However, Exp/Reb and Kkv were able to localise apically, indicating that the proteins reach their normal destination. Therefore, our results show that the Nα-MH2 domain is absolutely essential for the Exp/Reb function of extracellular chitin deposition, further suggesting a role we proposed for Exp and Reb in the extrusion of chitin to the extracellular compartment (Moussian *et al.*, 2015).

As we found that the Nα-MH2 domain is required for extracellular chitin deposition, we hypothesised that this domain alone could be sufficient to promote chitin deposition. Thus, we tested the ability of the Nα-MH2 domain alone to rescue the lack of chitin in *exp/reb* mutants and to promote chitin deposition when overexpressed with Kkv in the salivary glands. We found that Nα-MH2 domain alone could not perform these activities. Therefore, these results suggested that Nα-MH2 domain is not sufficient to promote chitin deposition and that other Exp/Reb domains may be involved. However, we observed that the Nα-MH2 domain alone is not localised apically. Because this minimal protein cannot localise to its normal apical domain, it is not possible to determine whether it is sufficient to deposit chitin. Further experiments directed to localise the Nα-MH2 domain at the apical domain would be needed to completely determine whether the Nα-MH2 domain is sufficient for chitin deposition. One possibility is to add to the N-terminal of Nα-MH2 domain a target sequence for myristoylation, it would permit to localise the protein to the apical plama membrane (Maurer-Stroh, Eisenhaber and Eisenhaber, 2002); another possibility is to add an anchor for glycosyl phospho inositol (GPI) lipid, in these conditions, the protein could anchor to the membrane (Mellman and Nelson, 2008).

5.2.2 Chitin particles and Kkv vesicles

The presence of intracellular Kkv vesicles and chitin particles has been described only during Kkv overexpression in absence of endogenous Exp/Reb, such as in salivary glands of wild type embryos and such as in trachea of embryo deficient for *exp*/*reb* (Moussian *et al.*, 2015). During the functional analysis of the Nα-MH2 domain of Exp and Reb, we found out that, in a wild type background, the co-expression of Kkv and $Exp^{\Delta MH2}$/$Reb^{\Delta MH2}$ produces many more chitin punctae and vesicles containing Kkv; we found the same strong phenotype also in absence of endogenous Exp/Reb. These results suggest that Exp/Reb proteins promote Kkv-dependent chitin synthesis and that the Nα-

MH2 domain is dispensable for chitin synthesis, but it is necessary for extracellular chitin deposition.

The simultaneous overexpression of wild type forms of Kkv and Exp or Reb induces the deposition of excessive chitin in trachea and salivary glands (Moussian *et al.*, 2015). In our conditions, we think that the inability of $Exp^{\Delta MH2}$ and $Reb^{\Delta MH2}$ to process and to deposit extra chitin synthesised by excessive Kkv activity induces the presence of intracellular chitin punctae. We speculate that the presence of Kkv vesicles and chitin particles could reflect the endogenous pathway of Kkv and chitin synthesis. From the analysis of the nature of Kkv vesicles and chitin particles, we found that Kkv, or Kkv complexes, are formed at the level of Golgi and then they are translocated to the apical plasma membrane, where chitin starts to be synthesised. Later, we speculate for an excess of protein at the membrane, Kkv is endocytosed together with the chitin fibre that could not be extruded. We observed that most Kkv vesicles correspond to endocytic vesicles, indicating that the protein is recycled after reaching the membrane. In line with this, it is worth to point out that we could not observe Kkv vesicles when Kkv does not reach the apical membrane (i.e. GFP-$Kkv^{\Delta WGTRE}$). Our results, in addition, suggest that most Kkv vesicles may be recycled back to the membrane, rather than degraded. However, we cannot exclude a certain degree ok Kkv degradation that we have not detected with our co-staining approach. Our analysis of live imaging in salivary glands also suggest the existence of Kkv vesicles containing chitin that eventually separate, suggesting that Kkv would synthesise short chitin fibres that could not be extruded, and eventually would be released in the cytoplasm. Unfortunately, we have not been able to determine the nature of chitin particles, and further analysis will be required to determine whether they correspond to chitin containing vesicles or whether they correspond to short fibres floating in the cytoplasm.

Remarkably, the trafficking of Kkv reminds the trafficking of the close related Cellulose Synthase: Cellulose Synthase Complexes (CSCs) assemble in Golgi and then CSCs are translocated from the Trans-Golgi Network to the plasma membrane; after the synthesis of cellulose, intact or degraded CSCs can be internalized through endocytosis and can be recycled back to the plasma membrane (Allen *et al.*, 2021). This would further suggest a high similarity between Chitin Synthases and Cellulose Synthases.

5.2.3 The conserved motif is dispensable for chitin synthesis and deposition

To carry on the structure-function analysis of Exp and Reb proteins, we did a comparison of amino acid sequences among proteins homolog to Exp and Reb. We identified a new highly conserved region that we called Conserved Motif (CM). This motif is not described in literature, neither in Exp/Reb proteins nor in any other protein.

We observed that Exp protein lacking the CM ($Exp^{\Delta CM}$) behaves as an endogenous form of Exp during chitin deposition: its overexpression induces earlier and stronger chitin deposition, $UASExp^{\Delta CM}$ is able to rescue the lack of chitin produced by the absence of *exp*/*reb* and its misexpression in the salivary gland is able to deposit ectopic chitin in the lumen. However, $Exp^{\Delta CM}$ localises mainly intracellularly with a bit of the protein at the membrane. Interestingly, $Exp^{\Delta MH2}$ is able to properly localise apically, in spite of being highly overexpressed with the Gal4/UAS system. This suggests that the CM is required for proper apical localisation. We speculate that the massive amount of protein produced by $UASExp^{\Delta CM}$ overexpression can mask the requirement of the CM domain for the proper localisation of Exp protein, and for this reason it is acting as a functional protein. It will be possible to validate our hypothesis generating a CRISPR mutant Exp protein lacking the CM. In line with a role of the CM in apical localisation, we find that UASMH2-Exp alone, which lacks the CM motif, does not localise apically. It will be also interesting to generate a Exp protein containing exclusively Nα-MH2 and CM and evaluate its localisation and activity.

From our data, we cannot unequivocally assign a role to the CM during chitin deposition, but such a highly conserved motif through evolution could be important for other unknown function(s) of Exp/Reb that were not analysed during this Thesis. The analysis of chitin deposition in the epidermal cuticle or in the tracheal cuticle should be investigated in detail to identify other possible functional requirements of this domain.

5.2.4 Physical interaction between Kkv and Exp/Reb?

It is still unknown how Exp and Reb work together with Kkv to deposit chitin, whether they form a complex or whether they interact indirectly. To investigate a possible physical interaction between Exp/Reb and Kkv, we performed several biochemical experiments, such as co-immunoprecipitation assays. Unfortunately, we were not able to detect Kkv

when we immunoprecipitated Reb and vice versa. These results do not completely exclude a physical interaction between Kkv and Exp/Reb because several aspects need to be taken in consideration during a co-immunoprecipitation experiment, for instance the binding of an antibody to the target can interfere in protein-protein interactions or the lysis buffer used to purify a protein can disrupt a protein complex. Hence, it is worth to repeat the experiments in other conditions, for example extracting the proteins in a less stringent lysis buffer. Future biochemical and/or proteomic approaches, like for instance proximity labelling techniques, could also help to determine possible physical interactions between these proteins or could help to discover new partners of Exp, Reb and Kkv. Nevertheless, our results so far do not point to a physical interaction or complex formation between Kkv and Exp/Reb. These results are in line with our cellular analysis of Exp/Reb and Kkv, where we do not find clear colocalisation of these proteins at the apical membrane.

5.3 Kkv

We were interested in analysing the function of specific domains in Kkv protein that we speculated could have a role in a direct or indirect interaction with Exp/Reb. In particular, through a structure-function analysis approach, we aimed to determine the role of WGTRE motif and the role of the coiled-coil domain of Kkv.

5.3.1 The conserved motif WGTRE is required for Kkv localisation

The conserved motif WGTRE is an essential domain for Kkv activity: it has been described that a point mutation changing the glycine into an aspartic acid gives rise to an inactive Kkv protein (Ostrowski *et al.*, 2002). The WGTRE motif has been suggested to be involved in oligomerisation or interactions with other factors (Zhu *et al.*, 2002; Moussian *et al.*, 2005; Van Leeuwen *et al.*, 2012); thus, we wanted to test if it could be involved in interactions with Exp/Reb. The mutant protein GFP-Kkv$^{\Delta WGTRE}$ is not able to rescue the absence of chitin provoked by *kkv*^{JB22} (a mutant form of *kkv* lacking all domains) and GFP-Kkv$^{\Delta WGTRE}$ is not able to work with Reb to produce extra chitin neither

in trachea nor in salivary glands. In addition, the overexpression of GFP-Kkv$^{\Delta WGTRE}$ does not lead to the formation of small chitin particles in salivary glands. All these results confirmed that Kkv without the WGTRE motif is not functional and that this motif is required for chitin synthesis and deposition.

Then, we analysed the subcellular accumulation of the mutant protein GFP-Kkv$^{\Delta WGTRE}$: the protein did not localise apically like a wild type Kkv does, instead we found a generalised pattern in the cytoplasm that corresponded to ER retention. The results strongly suggest a role for the WGTRE motif in Kkv trafficking indicating that Kkv localisation is important for Kkv function.

5.3.2 Is the SWG motif of Kkv a target of EH-domain containing proteins?

To further investigate the role of the WGTRE motif, we analysed the amino acid sequence alignment among proteins homolog to Kkv. We found that an S residue before the WGTRE motif is highly conserved, revealing the presence of an SWG motif. The SWG motif has been described to be a target for proteins containing a EH domain, usually involved in endocytosis, vesicle transport and signal transduction (Paoluzi *et al.*, 1998). We reasoned that the role of EH-domain containing proteins in vesicle transport could explain our result of the retention of GFP-Kkv$^{\Delta WGTRE}$ in the ER. However, the downregulation of the known EH-domain containing proteins of *Drosophila* did not affect Kkv localisation or chitin deposition. Null conditions for these proteins and analysis of redundancy between them should be tested before discarding the hypothesis that SWG motif of Kkv is a target of EH- domain containing proteins. At the moment, we don't know how the absence of the WGTRE motif produce the retention of Kkv in ER, if the protein does not pass a quality control or if the (S)WGTRE sequence is a signal for the transport to the exocytic pathway.

5.3.3 The coiled coil domain is dispensable for Kkv activity

The main difference between class A and class B chitin synthases (respectively, Kkv and ChS2 in *Drosophila melanogaster*) is the presence of a coiled-coil domain in class A enzymes, contributing to the specificity of epidermal chitin synthases. The coiled-coil domain could mediate oligomerisation of ChS complexes or could mediate an association

to a yet unknown partner through protein-protein interactions, assisting chitin synthase localisation or activity (Merzendorfer, 2006; Moussian, 2013; Adler, 2019).

Our results indicated that the coiled-coil domain is dispensable for Kkv localisation as the mutant protein localised apically. In trachea, the overexpression of GFP-Kkv$^{\Delta CC}$ did not produce any detectable defect and it was able to rescue the absence of chitin in a *kkv^{IB22}* background. In salivary gland, the overexpression of GFP-Kkv$^{\Delta CC}$ was able to produce chitin vesicles as the overexpression of wild type Kkv does and it was able to work together with Reb to deposit chitin. All together our data indicated that the mutant protein is functional and that the coiled-coil domain is not necessary for Kkv function.

However, we found a situation in which GFP-Kkv$^{\Delta CC}$ behaved differently from the wild type protein. While the tracheal co-expression of Reb and GFP-Kkv leads to advanced chitin deposition and abnormal tube morphogenesis, the concomitant overexpression of Reb and GFP-Kkv$^{\Delta CC}$ resulted in normal chitin deposition and tube formation. This is an intriguing behaviour, because the sole overexpression of Reb in an otherwise wild type condition produce a dominant effect. Therefore, the result suggested that GFP-Kkv$^{\Delta CC}$ is acting to decrease Kkv general activity. We propose two possibilities that could explain our results. In our first hypothesis, we suggest that GFP-Kkv$^{\Delta CC}$ is less efficient that GFP-Kkv to deposit chitin. Because overexpression would load the apical domain of this less efficient protein, the excess of Rebuf would act in concert with it but would not be able to produce increased chitin. Nevertheless, in mutant conditions for *kkv*, this less efficient protein would be functional enough to produce chitin. In our second hypothesis, we propose a model based on a presumptive oligomerisation of Kkv units. We propose that Kkv$^{\Delta CC}$ pure oligomers and Kkv^{WT} oligomers would be fully functional, whereas Kkv$^{\Delta CC}$-Kkv^{WT} would not be, maybe due to conformational issues. In a mutant background for *kkv^{IB22}*, only Kkv$^{\Delta CC}$ oligomers would be present. In contrast, in a wild type background, many Kkv$^{\Delta CC}$- Kkv^{WT} inactive oligomers would form, which would not be able to lead to increased chitin deposition. In support of this hypothesis it has been proposed that ChSs may work as oligomers, forming complexes to produce chitin (Maue *et al.*, 2009; Moussian, 2013; Sacristan *et al.*, 2013; Gohlke *et al.*, 2017). A combination of both hypothesis could also explain the results with Kkv$^{\Delta CC}$. Generating CRISPR mutants lacking the coiled-coil domain should help to avoid the effects of overexpression and to determine whether any of our hypotheses are correct.

5.3.4 Exp/Reb are necessary for the regulation of Kkv distribution at the membrane

The analysis of Kkv and Exp/Reb at the apical membrane, with super-resolution microscopy, suggests that Exp/Reb could have a role in the regulation of the distribution of Kkv, or Kkv complexes, at the apical membrane. In absence of Exp/Reb, for instance in salivary glands or in trachea at early stages or in embryo deficient for *exp*/*reb*, Kkv presents a non-uniform pattern in terms of intensity and distribution. Instead, in presence of Exp/Reb, either in ectopic expression of the proteins in salivary glands or in wild type situation at later stages in the trachea, we detected a uniform and homogeneous pattern of Kkv. We can speculate that the pattern of Kkv is affected when the protein is not working or when the morphology of the trachea is compromised. We disproved these hypotheses analysing the pattern of the protein in *mmy* mutants: in this condition, Kkv and Exp/Reb are present but the substrate of chitin is missing and it cannot be polymerised, resulting in phenotypes of chitin-less trachea; however, Kkv, or Kkv complexes, show a homogenous distribution at the membrane. Hence, all together our data indicated the importance of Exp/Reb in the regulation of Kkv distribution at the apical membrane, suggesting a role in the organization of Kkv, or Kkv complexes, at the membrane.

It would be interesting to determine if the Nα-MH2 domain or the Conserved Motif of Exp/Reb have a role in this newly identified function of the proteins. To do so, we will analyse the distribution of Kkv at the membrane in the presence of mutant Exp/Reb proteins.

To analyse the conformational organisation of Kkv and to detect possible rosette complexes at the membrane, we may need to reach a significant higher resolution than that offered by optical microscopy. In fact, the rosettes of Cellulose Synthases were discovered only through electron microscopy analysis (Haigler and Roberts, 2019). It will be important to implement serial-EM or FIB-SEM tomography in our tissue analysis.

5.3.5 Reb and Kkv pattern are complementary

The newly identified role of Exp/Reb in the distribution of Kkv at the membrane led us to investigate in more detail the relation between Kkv and Exp/Reb. The analysis of images analysing the trachea did not help us to clarify this issue, so we decided to use

salivary glands of third instar larvae because the cells are bigger than embryonic cells. In general, Kkv and Reb patterns were complementary and Reb was interposed between Kkv rather than colocalising with it. This result suggests that the interaction between Kkv and Exp/Reb is indirect rather than direct, which is in line with our co-immunoprecipitation assay, where Kkv is not able to immunoprecipitate Reb and vice versa. Future biochemical and/or proteomic approaches, like for instance proximity labelling techniques could help us to confirm this conclusion, and to determine common partners of Kkv and Exp/Reb involved in chitin machinery complexes. We can speculate that Exp/Reb provide the proper density and distribution of Kkv complexes at the apical membrane to obtain the correct structure of chitin microfibrils. Exp/Reb could interact with unknown protein(s) that marks specific site at the plasma membrane and Kkv could occupy the unmarked spaces.

5.4 Chitin synthesis *in vitro*

Currently, organic products are increasing their marketing power and social interest thanks to the high expectations of consumers towards ambient and human health (Tukker *et al.*, 2010; Liobikiene and Bernatoniene, 2016). A product needs to satisfy precise characteristics to be classified as "green": it must be biodegradable, biodynamic, ecological and natural (Cervellon *et al.*, 2011). A strategy that favours sustainable consumption, minimizing ambient impact, is to raise awareness of purchasing products based on biopolymers from renewable resources. Among biopolymers that are biodegradable and made from renewable raw materials, chitin and its deacetylated form, chitosan, are widely used in many sectors such as biomedical, biotechnology, water treatment, food, agriculture, veterinary, and cosmetics (Casadidio *et al.*, 2019). Due to the diversity of sources of chitin and their state of organization in the solid state, the quality of commercial chitin available is not uniform and causes many difficulties and high cost during transformation and chemical modification (Rinaudo, 2006). So far, the main commercial sources of chitin are crab and shrimp shells. Chitin isolation from shellfish requires the removal of the two major constituents of the shell: proteins, by deproteinization, and inorganic calcium carbonate, by demineralization, together with

small amounts of pigments and lipids. In some cases, an additional step of decolorization is applied to remove residual pigments. Owing to differences in the ultrastructure of the original material, all these treatments must be adapted to initial chitin source to produce, first, a high-quality chitin and, after partial deacetylation, chitosan. Many methods have been proposed and used over the years to prepare pure chitin; however, no standard method has been adopted (Younes and Rinaudo, 2015). These synthetic methods are very risky and have many disadvantages due to high temperature and high concentration of acid and alkali solutions. In addition, the production of chitin and chitosan by chemical process has different industrial drawbacks such as high energy consumption, long handling times, greater solvent wasted, high environmental pollution, high production of waste, and difficulty in recovering waste products such as pigment and proteins (Casadidio *et al.*, 2019). As an alternative to the chemical procedures, we believe that the synthesis of chitin *in vitro* can represent a more ecological, efficient and "green" method.

5.4.1 Progresses in chitin synthesis *in vitro*

In this work we tried to obtain chitin *in vitro*. To do so, we generated a new stable S2 cell line expressing Exp, Reb and Kkv. The cells expressed the three proteins, but they were not able to localise apically and many particles of chitin were present intracellularly. We succeeded to localise apically the proteins transfecting the new cell line with the apical determinant Crumbs. This result indicates that the cells need to be polarised to correctly localise the chitin machinery. In polarised S2 cells, we found that fewer chitin particles were present intracellularly as compared to unpolarised RKE cells, and we even found a few examples in which chitin was extruded. We speculated that most of the chitin was released to the extracellular space. Unfortunately, with the technique we used, we were not able to confirm the presence of chitin neither in the cell lysate nor in the culture medium. Other methods will be required to analyse the presence of chitin in cell lysates or in the culture medium. For instance, we can purify chitin from the media and from cell lysate by affinity chromatography using a chitin binding domain.

The ability of polarised RKE cells to extrude chitin in the extracellular space can be given either by the correct localisation of Kkv protein at the membrane or by Exp/Reb activity or by both. To analyse this point it will be important to quantify intracellular chitin

punctae in polarised cells transfected only with Kkv and compare it with polarised RKE cells.

In spite of the fact that we have not completed our objective to synthesise chitin *in vitro*, our work represents a progress towards this process and we consider that it is worth to pursue in this direction to finally obtain chitin *in vitro*.

5.5 Comparing Chitin Synthase 2 and Kkv

Drosophila melanogaster encodes two different chitin synthases: Krotzkopf verkehrt (Kkv) and Chitin Synthase 2 (ChS2). The first one produces chitin in the epidermis, the tracheae, the fore- and the hindgut; the second one is assumed to synthesize chitin in the midgut as the major component of the peritrophic matrix. The chitin marker CBP is able to bind chitin produced by Kkv, but it does not recognise chitin produced by ChS2. Both chitin synthases possess several transmembrane domains, a conserved catalytic domain (QRRRW) and a conserved WGTRE motif. The main difference between the two proteins is the presence of a coiled coil domain at the C terminal to the WGTRE motif in Kkv. This domain potentially mediates association to yet unknown partners assisting chitin synthase localisation or activity (Moussian, 2013).

We proved that ChS2 is not able to exert Kkv functions in trachea as it is not able to rescue the defects provoked by the absence of *kkv*. We demonstrated that Kkv protein needs to be entire to exert its functions, in fact protein chimeras formed by the N-term of Kkv and the C-term of ChS2 and vice versa could not rescue the phenotypes provoked by the absence of *kkv*. Moreover, ChS2 and the new chimeras were not able to work together with Reb to induce chitin deposition in the salivary gland.

Remarkably, ChS2 and the chimeras were not able to localise at the membrane like Kkv does, and they were largely found in the cytoplasm. The staining of wild type embryos with a new antibody against ChS2 showed that the endogenous ChS2 does not localise at the membrane at embryonic stages. This was surprising considering that it is accepted in the field that the nascent chitin, while it is polymerized by ChS, is translocated across the plasma membrane and released into the extracellular space through the pore formed by

the transmembrane helices of the ChS (Merzendorfer, 2006). The biosynthesis of the peritrophic matrix occurs in response to feeding and development of the insects (Terra, 2001). This raises the possibility that ChS2 will only localise apically and become active at larval stages when the animals feed. We, therefore, will need to perform the analysis of ChS2 localisation and function at larval stages. Nevertheless, our results indicate that, in contrast to Kkv, ChS2 is not intrinsically able to localise at the apical membrane even when it is expressed in polarised tissues. Indeed, Chs2 and the new chimeras cannot localise at the membrane despite their homology with Kkv in key domains such as the catalytic domain, the WGTRE motif and several transmembrane domain. Finally, we can confirm that Kkv protein needs to be intact to reach and properly localise at the membrane.

6. Conclusions

6. Conclusions

1. Nα-MH2 domain is essential for Exp/Reb function and for chitin deposition to the extracellular compartment but it is dispensable for chitin synthesis.

2. Nα-MH2 is dispensable for the localisation of Exp, Reb and Kkv.

3. Nα-MH2 domain is not able to localise apically, but it promotes Kkv-dependent chitin synthesis.

4. Exp and Reb promote Kkv-dependent chitin synthesis.

5. The conserved motif of Exp/Reb is dispensable for chitin synthesis and deposition.

6. Kkv (or Kkv complex) is formed in Golgi and then translocated to the membrane.

7. Kkv is mainly recycled in chitin-producing tissues.

8. The conserved motif WGTRE is required for Kkv function and localisation.

9. Kkv localisation is important for Kkv function.

10. The coiled coil domain is dispensable for Kkv activity and localisation.

11. Exp/Reb are necessary for the regulation of Kkv distribution at the membrane.

12. Reb and Kkv pattern are complementary.

13. S2 cells need to be polarised to properly localise chitin machinery.

14. ChS2 cannot exert Kkv function.

15. Epithelial chitin deposition requires all the domains of Kkv.

7. Bibliography

7. Bibliography

Adler, P. N. (2019) 'The localization of chitin synthase mediates the patterned deposition of chitin in developing Drosophila bristles', *BioRxiv*.

Affolter, M. and Caussinus, E. (2008) 'Tracheal branching morphogenesis in Drosophila: New insights into cell behaviour and organ architecture', *Development*, 135(12), pp. 2055–2064. doi: 10.1242/dev.014498.

Allen, H. *et al.* (2021) 'A historical perspective on the regulation of cellulose biosynthesis', *Carbohydrate Polymers*, 252, p. 117022. doi: 10.1016/j.carbpol.2020.117022.

Arakane, Y. *et al.* (2005) 'The Tribolium chitin synthase genes TcCHS1 and TcCHS2 are specialized for synthesis of epidermal cuticle and midgut peritrophic matrix.', *Insect molecular biology*, 14(5), pp. 453–463. doi: 10.1111/j.1365-2583.2005.00576.x.

Arakane, Y. *et al.* (2008) 'Chitin synthases are required for survival, fecundity and egg hatch in the red flour beetle, Tribolium castaneum.', *Insect biochemistry and molecular biology*, 38(10), pp. 959–962. doi: 10.1016/j.ibmb.2008.07.006.

Araújo, S. J. *et al.* (2005) 'mummy/cystic encodes an enzyme required for chitin and glycan synthesis, involved in trachea, embryonic cuticle and CNS development - Analysis of its role in Drosophila tracheal morphogenesis', *Developmental Biology*, 288(1), pp. 179–193. doi: 10.1016/j.ydbio.2005.09.031.

Araújo, S. J., Cela, C. and Llimargas, M. (2007) 'Tramtrack regulates different morphogenetic events during Drosophila tracheal development.', *Development (Cambridge, England)*, 134(20), pp. 3665–3676. doi: 10.1242/dev.007328.

Barbehenn, R. V and Stannard, J. (2004) 'Antioxidant defense of the midgut epithelium by the peritrophic envelope in caterpillars.', *Journal of insect physiology*, 50(9), pp. 783–790. doi: 10.1016/j.jinsphys.2004.05.012.

Beich-Frandsen, M. *et al.* (2015) 'Structure of the N-terminal domain of the protein Expansion: An "Expansion" to the Smad MH2 fold', *Acta Crystallographica Section D:*

Biological Crystallography, 71, pp. 844–853. doi: 10.1107/S1399004715001443.

Bellen, H. J. *et al.* (2004) 'The BDGP gene disruption project: single transposon insertions associated with 40% of Drosophila genes.', *Genetics*, 167(2), pp. 761–781. doi: 10.1534/genetics.104.026427.

Bhattacharyya, S. and Pucadyil, T. J. (2020) 'Cellular functions and intrinsic attributes of the ATP-binding Eps15 homology domain-containing proteins', *Protein Science*, 29(6), pp. 1321–1330. doi: 10.1002/pro.3860.

Bi, Y. *et al.* (2015) 'Insights into the structure and function of membrane-integrated processive glycosyltransferases', *Current Opinion in Structural Biology*, 34, pp. 78–86. doi: 10.1016/j.sbi.2015.07.008.

Bolognesi, R. *et al.* (2001) 'The peritrophic membrane of Spodoptera frugiperda: secretion of peritrophins and role in immobilization and recycling digestive enzymes.', *Archives of insect biochemistry and physiology*, 47(2), pp. 62–75. doi: 10.1002/arch.1037.

Bolognesi, R., Terra, W. R. and Ferreira, C. (2008) 'Peritrophic membrane role in enhancing digestive efficiency. Theoretical and experimental models.', *Journal of insect physiology*, 54(10–11), pp. 1413–1422. doi: 10.1016/j.jinsphys.2008.08.002.

Braconnot, H. (1811) 'Sur la nature des champignons', *Annales de chimie ou recueil de mémoires concernant la chimie et les arts qui en dépendent et spécialement la pharmacie*, 79, pp. 265–304.

Brand, A. H. and Perrimon, N. (1993) 'Targeted gene expression as a means of altering cell fates and generating dominant phenotypes', *Development*, 118(2), pp. 401–415. doi: 10.1242/dev.118.2.401.

Brunner, E. *et al.* (2009) 'Chitin-based scaffolds are an integral part of the skeleton of the marine demosponge Ianthella basta', *Journal of Structural Biology*, 168(3), pp. 539–547. doi: 10.1016/j.jsb.2009.06.018.

Casadidio, C. *et al.* (2019) 'Chitin and chitosans: Characteristics, eco-friendly processes, and applications in cosmetic science', *Marine Drugs*, 17(6). doi: 10.3390/md17060369.

Cervellon, M. C., Rinaldi, M. J. and Wernerfelt, A. S. (2011) 'How green is green? Consumers' understanding of green cosmetics and their certifications', in *In Proceedings*

of the 10th International Marketing Trends Conference. Paris, France, pp. 20–21.

Chandran, R. R. *et al.* (2018) 'Rebuff regulates apical luminal matrix to control tube size in Drosophila trachea', *Biology Open*, 7(9), pp. 1–9. doi: 10.1242/bio.036848.

Coutinho, P. M. *et al.* (2003) 'An evolving hierarchical family classification for glycosyltransferases.', *Journal of molecular biology*, 328(2), pp. 307–317. doi: 10.1016/s0022-2836(03)00307-3.

Crini, G., Badot, P. M. and Guibal, E. (2007) 'Chitine et chitosane – Du biopolymère à l'application', *Presse universitaire de Franche-Comté*.

Devine, W. P. *et al.* (2005) 'Requirement for chitin biosynthesis in epithelial tube morphogenesis', *Proceedings of the National Academy of Sciences of the United States of America*, 102(47), pp. 17014–17019. doi: 10.1073/pnas.0506676102.

Dong, B. and Hayashi, S. (2015) 'Shaping of biological tubes by mechanical interaction of cell and extracellular matrix', *Current Opinion in Genetics and Development*, 32, pp. 129–134. doi: 10.1016/j.gde.2015.02.009.

Ehrlich, H. *et al.* (2007) 'First evidence of the presence of chitin in skeletons of marine sponges. Part II. Glass sponges (Hexactinellida: Porifera)', *Journal of Experimental Zoology Part B: Molecular and Developmental Evolution*, 308(4), pp. 473–483. doi: 10.1002/jez.b.21174.

Fränkel, S. and Kelly, A. (1901) 'Beiträge zur Constitution des Chitins', *Monatsh Chem*, 23(2), pp. 123–132.

Fujimuro, M., Sawada, H. and Yokosawa, H. (1994) 'Production and characterization of monoclonal antibodies specific to multi-ubiquitin chains of polyubiquitinated proteins', 349, pp. 173–180.

Glazer, L. and Shilo, B. Z. (1991) 'The Drosophila FGF-R homolog is expressed in the embryonic tracheal system and appears to be required for directed tracheal cell extension.', *Genes & development*, 5(4), pp. 697–705. doi: 10.1101/gad.5.4.697.

Gohlke, S., Muthukrishnan, S. and Merzendorfer, H. (2017) 'In Vitro and In Vivo Studies on the Structural Organization of Chs3 from Saccharomyces cerevisiae.', *International journal of molecular sciences*, 18(4). doi: 10.3390/ijms18040702.

Gonell, H. W. (1926) ‘Rontgenographische Studien an Chitin’, *Hoppe-Seyler’s Zeitschrift fuer Physiologische Chemie Berlin*, 152, pp. 18–30.

González, M. *et al.* (2011) ‘Generation of stable Drosophila cell lines using multicistronic vectors’, *Scientific Reports*, 1. doi: 10.1038/srep00075.

Haigler, C. H. and Roberts, A. W. (2019) ‘Structure/function relationships in the rosette cellulose synthesis complex illuminated by an evolutionary perspective’, *Cellulose*, 26(1), pp. 227–247. doi: 10.1007/s10570-018-2157-9.

Hayashi, S. and Kondo, T. (2018) ‘Development and function of the drosophila tracheal system’, *Genetics*, 209(2), pp. 367–380. doi: 10.1534/genetics.117.300167.

Hegedus, D. *et al.* (2009) ‘New insights into peritrophic matrix synthesis, architecture, and function.’, *Annual review of entomology*, 54, pp. 285–302. doi: 10.1146/annurev.ento.54.110807.090559.

Heldin, C. H., Miyazono, K. and ten Dijke, P. (1997) ‘TGF-beta signalling from cell membrane to nucleus through SMAD proteins.’, *Nature*, 390(6659), pp. 465–471. doi: 10.1038/37284.

Henderson, K. D. and Andrew, D. J. (2000) ‘Regulation and function of Scr, exd, and hth in the Drosophila salivary gland.’, *Developmental biology*, 217(2), pp. 362–374. doi: 10.1006/dbio.1999.9560.

Iordanou, E. *et al.* (2014) ‘The novel Smad protein Expansion regulates the receptor tyrosine kinase pathway to control Drosophila tracheal tube size’, *Developmental Biology*, 393(1), pp. 93–108. doi: 10.1016/j.ydbio.2014.06.016.

Jennings, B. H. (2011) ‘Drosophila-a versatile model in biology & medicine’, *Materials Today*, 14(5), pp. 190–195. doi: 10.1016/S1369-7021(11)70113-4.

Jürgens, G. *et al.* (1984) ‘Mutations affecting the pattern of the larval cuticle inDrosophila melanogaster : II. Zygotic loci on the third chromosome.’, *Wilhelm Roux’s archives of developmental biology*, 193(5), pp. 283–295. doi: 10.1007/BF00848157.

Kelkenberg, M. *et al.* (2015) ‘Chitin is a necessary component to maintain the barrier function of the peritrophic matrix in the insect midgut.’, *Insect biochemistry and molecular biology*, 56, pp. 21–28. doi: 10.1016/j.ibmb.2014.11.005.

Kerman, B. E., Cheshire, A. M. and Andrew, D. J. (2006) 'From fate to function: the Drosophila trachea and salivary gland as models for tubulogenesis', *Differentiation*, 74(7), pp. 326–348. doi: 10.1111/j.1432-0436.2006.00095.x.From.

Klämbt, C., Glazer, L. and Shilo, B. Z. (1992) 'breathless, a Drosophila FGF receptor homolog, is essential for migration of tracheal and specific midline glial cells.', *Genes & development*, 6(9), pp. 1668–1678. doi: 10.1101/gad.6.9.1668.

Ledderhose, G. (1876) 'Über salzsaures Glucosamin', *Berichte der deutschen chemischen Gesellschaft*, pp. 1200–1201.

Van Leeuwen, T. *et al.* (2012) 'Population bulk segregant mapping uncovers resistance mutations and the mode of action of a chitin synthesis inhibitor in arthropods', *Proceedings of the National Academy of Sciences of the United States of America*, 109(12), pp. 4407–4412. doi: 10.1073/pnas.1200068109.

Lehane, M. J. (1997) 'Peritrophic matrix structure and function.', *Annual review of entomology*, 42, pp. 525–550. doi: 10.1146/annurev.ento.42.1.525.

Letizia, A. *et al.* (2013) 'A functional role of the extracellular domain of Crumbs in cell architecture and apicobasal polarity.', *Journal of cell science*, 126, pp. 2157–63. doi: 10.1242/jcs.122382.

Liobikiene, G. and Bernatoniene, J. (2016) 'Theory of planned behavior approach to understand the green purchasing behavior in the EU: A cross-cultural study', *Ecological Economics*, 125, pp. 38–46.

Liu, X. *et al.* (2019) 'Biosynthesis , modifications and degradation of chitin in the formation and turnover of peritrophic matrix in insects', *Journal of Insect Physiology*, 114, pp. 109–115. doi: 10.1016/j.jinsphys.2019.03.006.

Liu, X., Zhang, J. and Zhu, K. Y. (2019) 'Chitin in arthropods: Biosynthesis, modification, and metabolism', in *Targeting Chitin-containing Organisms*, pp. 169–207. doi: 10.1007/978-981-13-7318-3_9.

Loganathan, R., Cheng, Y. L. and Andrew, D. J. (2016) 'Organogenesis of the Drosophila respiratory system', in *Organogenetic Gene Networks*, pp. 151–211.

Loganathan, R., Little, C. D. and Rongish, B. J. (2020) 'Extracellular matrix dynamics in tubulogenesis', *Cellular Signalling*, 72(December 2019), p. 109619. doi:

10.1016/j.cellsig.2020.109619.

Lotmar, W. and Picken, L. E. R. (1950) ‘A new crystallographic modification of chitin and its distribution’, *Experientia*, 6(2), pp. 58–59.

Luschnig, S. *et al.* (2006) ‘serpentine and vermiform encode matrix proteins with chitin binding and deacetylation domains that limit tracheal tube length in Drosophila.’, *Current biology : CB*, 16(2), pp. 186–194. doi: 10.1016/j.cub.2005.11.072.

Manning, G. and Krasnow, M. A. (1993) ‘Development of the Drosophila tracheal system’, in Bate, M. and Arias, M. (eds) *The Development of Drosophila melanogaster*. Cold Spring Harbor Laboratory Press, pp. 609–686.

Maruyama, R. and Andrew, D. J. (2012) ‘Drosophila as a model for epithelial tube formation.’, *Developmental Dynamics*, 241(1), pp. 119–135.

Matusek, T. *et al.* (2006) ‘The Drosophila formin DAAM regulates the tracheal cuticle pattern through organizing the actin cytoskeleton.’, *Development (Cambridge, England)*, 133(5), pp. 957–966. doi: 10.1242/dev.02266.

Maue, L., Meissner, D. and Merzendorfer, H. (2009) ‘Purification of an active, oligomeric chitin synthase complex from the midgut of the tobacco hornworm.’, *Insect biochemistry and molecular biology*, 39(9), pp. 654–659. doi: 10.1016/j.ibmb.2009.06.005.

Merzendorfer, H. (2006) ‘Insect chitin synthases: A review’, *Journal of Comparative Physiology B: Biochemical, Systemic, and Environmental Physiology*, 176(1), pp. 1–15. doi: 10.1007/s00360-005-0005-3.

Merzendorfer, H. and Zimoch, L. (2003) ‘Chitin metabolism in insects: Structure, function and regulation of chitin synthases and chitinases’, *Journal of Experimental Biology*, 206(24), pp. 4393–4412. doi: 10.1242/jeb.00709.

Meyer, K. H. and Pankow, G. (1935) ‘Sur la constitution et la structure de la chitine’, *Helv Chim Acta 18*, 18(1), pp. 589–598.

Moussian, B. *et al.* (2005) ‘Involvement of chitin in exoskeleton morphogenesis in Drosophila melanogaster’, *Journal of Morphology*, 264(1), pp. 117–130. doi: 10.1002/jmor.10324.

Moussian, B. *et al.* (2006) ‘Drosophila Knickkopf and Retroactive are needed for

epithelial tube growth and cuticle differentiation through their specific requirement for chitin filament organization.', *Development (Cambridge, England)*, 133(1), pp. 163–171. doi: 10.1242/dev.02177.

Moussian, B. (2013) 'The apical plasma membrane of chitin-synthesizing epithelia', *Insect Science*, 20(2), pp. 139–146. doi: 10.1111/j.1744-7917.2012.01549.x.

Moussian, B. *et al.* (2015) 'Deciphering the Genetic Programme Triggering Timely and Spatially-Regulated Chitin Deposition', *PLoS Genetics*, 11(1), pp. 1–24. doi: 10.1371/journal.pgen.1004939.

Moussian, B. (2019) 'Chitin : Structure, Chemistry and Biology', in *Targeting Chitin-containing Organisms*. Springer Singapore, pp. 5–18. doi: 10.1007/978-981-13-7318-3.

Muthukrishnan, S. *et al.* (2012) *Chitin Metabolism in Insects*, *Insect Molecular Biology and Biochemistry*. doi: 10.1016/B978-0-12-384747-8.10007-8.

Muthukrishnan, S. *et al.* (2019) 'Chitin organizing and modifying enzymes and proteins involved in remodeling of the insect cuticle', in *Targeting Chitin-containing Organisms*. Springer Singapore, pp. 83–114. doi: 10.1007/978-981-13-7318-3_5.

Odier, A. (1823) 'Mémoires sur la composition chimique des parties cornées des insectes', *Mémoires de la Societé d'Histoire Naturelle de Paris*, 1, pp. 29–42.

Ostrowski, S., Dierick, H. A. and Bejsovec, A. (2002) 'Genetic control of cuticle formation during embryonic development of Drosophila melanogaster', *Genetics*, 161(1), pp. 171–182. doi: 10.1093/genetics/161.1.171.

Öztürk-Çolak, A. *et al.* (2016) 'A feedback mechanism converts individual cell features into a supracellular ECM structure in drosophila trachea', *eLife*, 5(FEBRUARY2016), pp. 1–21. doi: 10.7554/eLife.09373.

Öztürk-Çolak, A., Moussian, B. and Araújo, S. J. (2016) 'Drosophila chitinous aECM and its cellular interactions during tracheal development', *Developmental Dynamics*, 245(3), pp. 259–267. doi: 10.1002/dvdy.24356.

Paoluzi, S. *et al.* (1998) 'Recognition specificity of individual EH domains of mammals and yeast', *EMBO Journal*, 17(22), pp. 6541–6550. doi: 10.1093/emboj/17.22.6541.

Peters, W. (1972) 'Occurrence of chitin in Mollusca', *Comparat Biochem Physiol B*,

41(3), pp. 541–550.

Peters, W. (1992) ‘Peritrophic membranes’, *Zoophysiology*, 30.

Qin, B., Lam, S. S. W. and Lin, K. (1999) ‘Crystal structure of a transcriptionally active Smad4 fragment’, *Structure*, 7, pp. 1493–1503.

Ramos, A., Mahowald, A. and Jacobs-Lorena, M. (1994) ‘Peritrophic matrix of the black fly Simulium vittatum: formation, structure, and analysis of its protein components.’, *The Journal of experimental zoology*, 268(4), pp. 269–281. doi: 10.1002/jez.1402680403.

Ribeiro, C., Neumann, M. and Affolter, M. (2004) ‘Genetic control of cell intercalation during tracheal morphogenesis in Drosophila.’, *Current biology : CB*, 14(24), pp. 2197–2207. doi: 10.1016/j.cub.2004.11.056.

Rinaudo, M. (2006) ‘Chitin and chitosan: Properties and applications’, *Progress in Polymer Science (Oxford)*, 31(7), pp. 603–632. doi: 10.1016/j.progpolymsci.2006.06.001.

Rotstein, B. *et al.* (2011) ‘Tramtrack is genetically upstream of genes controlling tracheal tube size in Drosophila’, *PLoS ONE*, 6(12). doi: 10.1371/journal.pone.0028985.

Rudall, K. M. (1963) ‘The chitin/protein complexes of insect cuticles’, *Treherne & Wiggles-worth*, 1, pp. 257–313.

Sacristan, C. *et al.* (2013) ‘Oligomerization of the chitin synthase Chs3 is monitored at the Golgi and affects its endocytic recycling.’, *Molecular microbiology*, 90(2), pp. 252–266. doi: 10.1111/mmi.12360.

Samakovlis, C. *et al.* (1996) ‘Development of the Drosophila tracheal system occurs by a series of morphologically distinct but genetically coupled branching events’, *Development*, 122(5), pp. 1395–1407. doi: 10.1242/dev.122.5.1395.

Santolini, E. *et al.* (1999) ‘The EH network’, *Experimental Cell Research*, 253(1), pp. 186–209. doi: 10.1006/excr.1999.4694.

Schindelin, J. *et al.* (2012) ‘Fiji: an open-source platform for biological-image analysis.’, *Nature methods*, 9(7), pp. 676–682. doi: 10.1038/nmeth.2019.

Schottenfeld, J., Song, Y. and Ghabrial, A. S. (2010) ‘Tube continued: morphogenesis of the Drosophila tracheal system’, *Current Opinion in Cell Biology*, 22(5), pp. 633–639.

doi: 10.1016/j.ceb.2010.07.016.Tube.

Semino, C. E. *et al.* (1996) 'Homologs of the Xenopus developmental gene DG42 are present in zebrafish and mouse and are involved in the synthesis of nod-like chitin oligosaccharides during early embryogenesis', *Proceedings of the National Academy of Sciences of the United States of America*, 93(10), pp. 4548–4553. doi: 10.1073/pnas.93.10.4548.

Semino, C. E. and Allende, M. L. (2000) 'Chitin oligosaccharides as candidate patterning agents in zebrafish embryogenesis', *International Journal of Developmental Biology*, 44(2), pp. 183–193. doi: 10.1387/ijdb.10794076.

Shi, Y. (2001) 'Structural insights on Smad function in TGFbeta signaling.', *BioEssays : news and reviews in molecular, cellular and developmental biology*, 23(3), pp. 223–232. doi: 10.1002/1521-1878(200103)23:3<223::AID-BIES1032>3.0.CO;2-U.

Shiga, Y., Tanaka-Matakatsu, M. and Hayashi, S. (1996) 'A nuclear GFP/β-galactosidase fusion protein as a marker for morphogenesis in living Drosophila', *Developmental, Growth & Differentiation*, 38(1), pp. 99–106.

Shishido, E. *et al.* (1993) 'Two FGF-receptor homologues of Drosophila: one is expressed in mesodermal primordium in early embryos.', *Development*, 117, pp. 751–761.

Silva, C. M. and Terra, W. R. (1995) 'An α-glucosidase from perimicrovillar membranes of Dysdercus peruvianus (Hemiptera: Pyrrhocoridae) midgut cells. Purification and properties', *Insect biochemistry and molecular biology*, 25, pp. 487–494.

Sobala, L. F. *et al.* (2016) 'Correction: ChtVis-tomato, a genetic reporter for in vivo visualization of chitin deposition in drosophila (Development, (2015) 142, (3974-3981))', *Development (Cambridge)*, 143(19), p. 3638. doi: 10.1242/dev.143826.

Städeler, G. (1859) 'Untersuchungen über das Fibroin, Spongin und Chitin, nebst Bemerkungen über den thierischen Schleim', *Justus Liebig Annalen der Chemie*, 111(1), pp. 12–28.

Sutherland, D., Samakovlis, C. and Krasnow, M. A. (1996) 'branchless encodes a Drosophila FGF homolog that controls tracheal cell migration and the pattern of branching.', *Cell*, 87(6), pp. 1091–1101. doi: 10.1016/s0092-8674(00)81803-6.

Swanson, L. E. and Beitel, G. J. (2006) 'Tubulogenesis: An Inside Job: New work shows

that a dynamic and highly patterned apical extracellular matrix regulates epithelial cell shape and tube size from within the lumen of the Drosophila tracheal system.', *Current Biology*, 24(16(2)), pp. R51–R53.

Tang, W. J. *et al.* (2015) 'Chitin is endogenously produced in vertebrates', *Current Biology*, 25(7), pp. 897–900. doi: 10.1016/j.cub.2015.01.058.Chitin.

Tepass, U. and Tanentzapf, G. (2001) 'Epithelial Cell Polarity and Cell Junctions in Drosophila', *Annu. Rev. Gent.*, (35), pp. 747–84.

Terra, W. R. (2001) 'The origin and functions of the insect peritrophic membrane and peritrophic gel.', *Archives of insect biochemistry and physiology*, 47(2), pp. 47–61. doi: 10.1002/arch.1036.

Tonning, A. *et al.* (2005) 'A transient luminal chitinous matrix is required to model epithelial tube diameter in the Drosophila trachea', *Developmental Cell*, 9(3), pp. 423–430. doi: 10.1016/j.devcel.2005.07.012.

Tsai, Y. C. and Weissman, A. M. (2010) 'The Unfolded Protein Response, Degradation from the Endoplasmic Reticulum, and Cancer', *Genes & Cancer*, 1(7), pp. 764–778. doi: 10.1177/1947601910383011.

Tsarouhas, V. *et al.* (2007) 'Sequential Pulses of Apical Epithelial Secretion and Endocytosis Drive Airway Maturation in Drosophila', *Developmental Cell*, 13(2), pp. 214–225. doi: 10.1016/j.devcel.2007.06.008.

Tsuneizumi, K. *et al.* (1997) 'Daughters against dpp modulates dpp organizing activity in Drosophila wing development.', *Nature*, 389(6651), pp. 627–631. doi: 10.1038/39362.

Tukker, A. *et al.* (2010) 'Sustainable Consumption and Production', *Journal of Industrial Ecology*, 14(1), pp. 1–3.

Uv, A. E., Cantera, R. and Samakovlis, C. (2003) 'Drosophila tracheal morphogenesis: Intricate cellular solutions to basic plumbing problems.', *Trends in Cell Biology*, 13(6), pp. 301–309.

Wang, S. *et al.* (2006) 'Septate-junction-dependent luminal deposition of chitin deacetylases restricts tube elongation in the Drosophila trachea.', *Current biology : CB*, 16(2), pp. 180–185. doi: 10.1016/j.cub.2005.11.074.

Wharton, D. (1980) ‘Nematode egg-shells’, *Parasitology*, 81(2), pp. 447–463.

Wigglesworth, V. B. (1972) *The Principles of Insect Physiology*.

Wu, J. *et al.* (2002) ‘Structural Mechanism of Smad4 Recognition by the Nuclear Oncoprotein Ski : Insights on Ski-Mediated Repression of TGF- □ Signaling’, 111, pp. 357–367.

Younes, I. and Rinaudo, M. (2015) ‘Chitin and chitosan preparation from marine sources. Structure, properties and applications’, *Marine Drugs*, 13(3), pp. 1133–1174. doi: 10.3390/md13031133.

Zhang, Jianzhen *et al.* (2010) ‘Silencing of two alternative splicing-derived mRNA variants of chitin synthase 1 gene by RNAi is lethal to the oriental migratory locust, Locusta migratoria manilensis (Meyen).’, *Insect biochemistry and molecular biology*, 40(11), pp. 824–833. doi: 10.1016/j.ibmb.2010.08.001.

Zhang, L. and Ward, R. E. I. (2009) ‘uninflatable encodes a novel ectodermal apical surface protein required for tracheal inflation in Drosophila.’, *Developmental biology*, 336(2), pp. 201–212. doi: 10.1016/j.ydbio.2009.09.040.

Zhang, Y. *et al.* (2005) ‘The chitin synthase genes chs-1 and chs-2 are essential for C. elegans development and responsible for chitin deposition in the eggshell and pharynx, respectively’, *Developmental Biology*, 285(2), pp. 330–339. doi: 10.1016/j.ydbio.2005.06.037.

Zhu, K. Y. *et al.* (2016) ‘Biosynthesis, Turnover, and Functions of Chitin in Insects’, *Annual Review of Entomology*, 61(1), pp. 177–196. doi: 10.1146/annurev-ento-010715-023933.

Zhu, Y. C. *et al.* (2002) ‘Sequence of a cDNA and expression of the gene encoding a putative epidermal chitin synthase of Manduca sexta’, *Insect Biochemistry and Molecular Biology*, 32(11), pp. 1497–1506. doi: 10.1016/S0965-1748(02)00070-X.

Zimoch, L. and Merzendorfer, H. (2002) ‘Immunolocalization of chitin synthase in the tobacco hornworm.’, *Cell and tissue research*, 308(2), pp. 287–297. doi: 10.1007/s00441-002-0546-7.

8. Appendices

8. Appendices

8.1 List of abbreviations

ab	Antibody
aECM	Apical extracellular matrix
btl	*breathless*
CBP	Chitin Binding Probe
CCV	Clathrin-Coated Vesicles
Chr	Chromosome
ChS	Chitin Synthase
ChS2	*Chitin Synthase 2*
CM	Conserved Motif
CME	Clathrin-Mediated Endocytosis
Co-IP	Co-immunoprecipitation
crb	*crumbs*
CSC	Cellulose Synthase Complex
DB	Dorsal Branch
DT	Dorsal Trunk
EE	Early Endosome
EH	Eps15 Homology
ER	Endoplasmic Reticulum
exp	*expansion*
$Exp^{\Delta CM}$	Expansion lacking the Conserved Motif
$Exp^{\Delta MH2}$	Expansion lacking the Nα-MH2 domain
FG	Foregut
Fig.	Figure
fkh	*forkhead*
GB	Ganglionic Branch
GFP	Green Fluorescent Protein

GlcNAc	N-acetyl-D-glucosamine
GTF2	Family 2 of glycosyltransferases
HG	Hindgut
IP	Immunoprecipitation
kkv	*krotzkopf verkehrt*
$Kkv^{\Delta CC}$	Kkv lacking the Coiled-coil Domain
$Kkv^{\Delta WGTRE}$	Kkv lacking the WGTRE Conserved Motif
LT	Lateral Trunk
MASC	Microtubule Associated Cellulose Synthase Complex
MG	Midgut
MH2	Mad Homology domain 2
mmy	*mummy*
MT	Malpighian Tubules
MVB	Multi Vesicular Bodies
PM	Peritrophic Matrix
reb	*rebuf*
$Reb^{\Delta MH2}$	Rebuf lacking the Nα-MH2 domain
RKE cells	S2 cells line transfected with Reb-Cherry, Kkv and Exp-GFP
S2 cells	Schneider 2 cells
SmaCC	Small Cellulose Synthase Complex
SV	Secretory Vesicles
TC	Transverse Connective
TGN	Trans Golgi Network
TMS	Trans-Membrane Segment
VB	Visceral Branch
wt	wild type

8.2 List of figures

8.3 Resumen en castellano

La quitina es el componente principal de la matriz extracelular apical de tejidos ectodérmicos y de la matriz peritrófica de insectos; en *Drosophila*, está sintetizada por Kkv y ChS2. Kkv no es suficiente para depositar quitina, las proteínas Expansion (Exp) y Rebuf (Reb) son también necesarias para este proceso. Kkv y Exp/Reb constituyen el programa genético mínimo necesario y suficiente para la deposición de quitina.

Los objetivos de este trabajo han sido investigar los mecanismos moleculares de Exp, Reb y Kkv a través de un análisis de estructura-función, producir quitina extracelular en cultivo celular e investigar cómo las diferencias entre Kkv y ChS2 se correlacionan con la deposición de quitina y con el requisito funcional de Exp/Reb.

El dominio Nα-MH2 de Exp y Reb es necesario para la deposición extracelular de quitina. Con la comparación de proteínas homólogas a Exp, encontramos una nueva región conservada que no está involucrada en la deposición de quitina, pero es relevante para la localización de Exp/Reb. Las proteínas Exp/Reb parecen regular la distribución de Kkv en la membrana apical. Kkv se ensambla al nivel de Golgi, se traslada a la membrana y comienza la síntesis de quitina. Posteriormente, Kkv se endocita y se recicla. El motivo WGTRE de Kkv está involucrado en la localización de la proteína y la localización de la proteína es importante para su función. El dominio coiled-coil de Kkv es prescindible para su actividad.

Es posible sintetizar quitina *in vitro* en cultivo celular de células S2 transfectadas con Kkv y Exp/Reb, pero las proteínas no están localizada en la membrana y la quitina está presente en vesículas intracelulares. Las células deben estar polarizadas para localizar las proteínas y estas tienen menos vesículas de quitina que las células no polarizadas con la misma actividad. Especulamos que la mayoría de las vesículas de quitina se extruyen al compartimento extracelular.

ChS2 no puede ejercer la función de Kkv y, en el embrión, no se localiza en la membrana. Finalmente, ChS2 no actúa con Exp y Reb para depositar quitina.